UNIVERSITÀ DEGLI STUDI DI MILANO

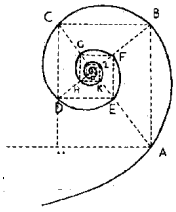

SCUOLA DI DOTTORATO IN MEDICINA MOLECOLARE

Curriculum di Oncologia molecolare

CICLO XXVIII

Anno Accademico 2014/2015

TESI DI DOTTORATO DI RICERCA

Settore scientifico disciplinare Patologia generale MED04

Mechanisms of drug-escape and relapse in multiple myeloma: interplay between ADAR1 and NOTCH in aberrant RNA editing

Dottorando: Elisa LAZZARI

Matricola N° R10151

TUTORE: Prof.ssa Raffaella CHIARAMONTE

CO-TUTORE: Prof.ssa Catriona JAMIESON

DIRETTORE DEL DOTTORATO: Ch.mo Prof.Mario CLERICI

ABSTRACT

Multiple myeloma (MM) is a plasma cell malignancy that accounts for more than 10% of all blood cancers. Despite a wide variety of available lines of treatment, virtually all patients experience cycles of remission/relapse or become unresponsive to treatment. A growing body of evidence highlights the contribution of clonal heterogeneity to disease progression and resistance to therapy. In recent years the importance of post-transcriptional regulatory mechanisms (such as RNA editing) in cancer has emerged. RNA editing is particularly intriguing as a potential source of genetic diversity, as can affect several mRNA features, including stability, localization, nuclear retention, and alternative splicing. In mammals, most RNA editing is carried out by Adenosine Deaminases acting on dsRNA (ADAR) that catalyze the hydrolytic deamination of adenosines (A) to inosines (I). In particular, ADAR1 has been associated with disease progression and cancer stem cell maintenance in both solid tumors and hematopoietic malignancies. The central aim of this work was to investigate ADAR1 as a mechanism of clonal heterogeneity and drug resistance in MM. We postulated that ADAR1-dependent aberrant A-to-I RNA editing in MM cells could drive transcriptome "reprogramming" in MM tumor cells, thus contributing to disease relapse and drug resistance. We also sought to identify cell-intrinsic and microenvironment-derived mechanisms that promote aberrant ADAR1-mediated RNA editing. We hypothesized that BM inflammatory signals, promoted by MM deregulated pathways such as Notch, sustain ADAR1-mediated reprogramming. We observed significantly increased ADAR1 expression in plasma cell leukemia (PCL), the advanced, highly drug-resistant stage of MM, and detected aberrant RNA editing in GLI1 and APOBEC3D transcripts by a novel RNA editing site-specific qPCR assay (RESSqPCR) that we developed. Furthermore, we established successful MM xenografts by intrahepatic transplantation of ADAR1-enriched PCL samples, thus providing a robust new in vivo model and platform for testing new therapeutic strategies aimed at treating drug-resistant forms of MM. We showed that continuous in vitro exposure to the anti-MM agent and immunomodulatory drug (IMiD), lenalidomide, induced ADAR1 expression and widespread aberrant RNA editing activity in MM cells, coupled with increased self-renewal capacity and a cancer stem cell phenotype. Furthermore, we observed that pro-inflammatory IL-6 promoted RNA editing, suggesting that MM-associated microenvironmental factors may play a key role in triggering ADAR1-associated malignant transcriptome recoding. Notably, IL-6 production from human BM stromal cells and from MM cells can be inhibited by silencing the overexpressed Notch ligands Jagged1 and Jagged2 in MM cells. In keeping with these findings, ADAR1 overexpression and deregulated RNA editing represents a unique source of RNA and protein diversity, and may endow survival advantages to MM cells in selective environments, such as the BM niche or under the pressure of chemotherapy. This work therefore identifies ADAR1 as a potential new diagnostic and therapeutic target in MM, and inhibition of this pathway, or its regulators and editing substrates, could provide a dynamic avenue to prevent disease relapse and disease progression and achieve long-term survival.

SOMMARIO

Il Mieloma Multiplo (MM) è un tumore delle plasma cellule che rappresenta più del 10% dei tumori del sangue. Nonostante gli approcci terapeutici disponibili, quasi tutti i pazienti affrontano cicli di remissione/ricaduta e/o sviluppano resistenza farmacologica. Un numero crescente di osservazioni sottolinea il contributo dell'eterogeneità clonale nella progressione tumorale e nella refrattarietà alla terapia. Negli ultimi anni l'importanza dei meccanismi di regolazione post-trascrizionale (come l'RNA editing), è emersa in oncologia. L'RNA editing è particolarmente interessante come potenziale fonte di diversità genetica, poichè può influenzare diverse caratteristiche dell'mRNA, compreso stabilità, localizzazione, retenzione nucleare e splicing alternativo. Nei mammiferi la maggior parte dell'RNA editing avviene ad opera delle adenosina-deaminasi che agiscono sull'RNA a doppio filamento (ADAR), enzimi che catalizzano la deaminazione delle adenosine in inosine. In particolare, ADAR1 è stato associato alla progressione tumorale e al mantenimento delle cellule tumorali staminali in tumori solidi ed ematologici. Lo scopo principale di questa tesi è stato quello di investigare ADAR1 come meccansimo di supporto all'eterogeneità clonale e alla farmaco-resistenza nel MM. Abbiamo ipotizzato infatti che la deregolazione dell'RNA editing dipendente da ADAR1 possa portare alla "riprogrammazione" del trascrittoma delle cellule di MM, contribuendo alla ricaduta. Inoltre, abbiamo cercato di identificare meccamismi intrinseci e derivanti dal microambinete che potessero promuovere la deregolazione dell'RNA editing mediata da ADAR1. Abbiamo ipotizzato che segnali infiammatori nel midollo osseo, indotti da pathyway deregolati come quello di Notch, sostengano la riprogrammazione ADAR1-mediata. Abbiamo osservato un significativo aumento dell'espressione di ADAR1 in campioni di leucemia delle plasma cellule (PCL), la fase avanzata e altamente resistente alla terapia del MM, e rilevato aberrante RNA editing negli trascrittidi GLI1 e APOBEC3D, grazie ad un nuovo metodo per quantificare RNA editing in siti specifici da noi sviluppato (RESSqPCR). Inoltre, abbiamo xenotrapiantato con successo cellule di PCL, esprimenti alti livelli di ADAR1, tramite inienzione intraepatica, così fornendo un robusto e innovativo modello in vivo e piattaforma per testare nuove strategie terapeutiche finalizzate a trattare le forme refrattarie di MM. Abbiamo mostrato come l'esposizione prolungata in vitro al farmaco immunomodulatorio (IMiD) anti-MM lenalidomide induce l'espressione di ADAR1 e deregolata attività di RNA editing nelle cellule di MM, accompagnate da aumentata capacità di auto-rinnovamento e da un fenotipo tipico delle cellule tumorali staminali. Inoltre abbbiamo osservato che la stimolazione con interleuchina pro-infiammatoria 6 (IL-6) promuove l'RNA editing, suggerendo come fattori microambientali associati al MM possano giocare un ruolo nell'innescare la riprogrammazione maligna associata ad ADAR1. Di particolare rilevanza, la produzione di IL-6 da parte delle cellule midollari stromali e delle cellule di MM può essere inibita dal silenziamento dei ligandi di Notch Jagged1 e Jagged2, overespressi dalle cellule di MM. In linea con questi risultati, l'overespressione di ADAR1 e il deregolato RNA editing rappresentano una eccezionale fonte di diversità a livello trascrizionale e proteico, e portebbero avvantaggiare la sopravvivenza delle cellule di MM in ambienti selettivi, rappresentati dalla nichia midollare o dalla pressione selettiva della chemioterapia. Questo lavoro di conseguenza identifica ADAR1 come potenziale nuovo target diagnostico e terapeutico nel MM; l'inibizione di questo pathway, o dei

suoi regolatori e dei target soggetti ad editing, potrebbe fornire un approccio dinamico per prevenire ricadute, l'avanzamento della patologia e raggiungere la sopravvivenza a lungo termine dei pazienti.

INDEX

Introduction

1. Multiple Myeloma

Multiple myeloma is a neoplastic plasma-cell disorder that is characterized by clonal proliferation of malignant plasma cells (PCs) in the bone marrow (BM) microenvironment, monoclonal protein in the blood or urine and associated organ dysfunction. It belongs to a group of related *paraproteinaemias*, namely diseases that produce an immunoglobulin from a single clone that is present at high levels in the serum. They include multiple myeloma (MM), monoclonal gammopathy of undetermined significance (MGUS) and Waldenstrom's macroglobulinaemia (WM).

MM accounts for 1% of all cancers and 13% of all hematologic cancers [1]. In Western countries the annual incidence is 5.6 cases per 100.000 persons [2], and the median age at diagnosis is about 65 years [3]. The disease is slightly more common in men than in women and is twice as common in African-Americans compared to Caucasians [4]. Almost all patient with MM evolve from the asymptomatic premalignant stage of MGUS, which affects at least 3% of adults older than 50 years [4]. Moreover, in some cases, MM arises from another asymptomatic but more advanced premalignant stage, referred as smoldering multiple myeloma (SMM). The risk to progress from SMM to MM is 10% per year in the first 5 years, 3% per year for the next 5 years and 1% per year for the last 10 years, reaching a cumulative probability of progression of 75% at 15 years [5]. Tumor cells then can accumulate further cytogenetic and molecular alterations that contribute to disease progression to secondary plasma cell leukemia (PCL), the leukemic transformation of end-stage MM [6].

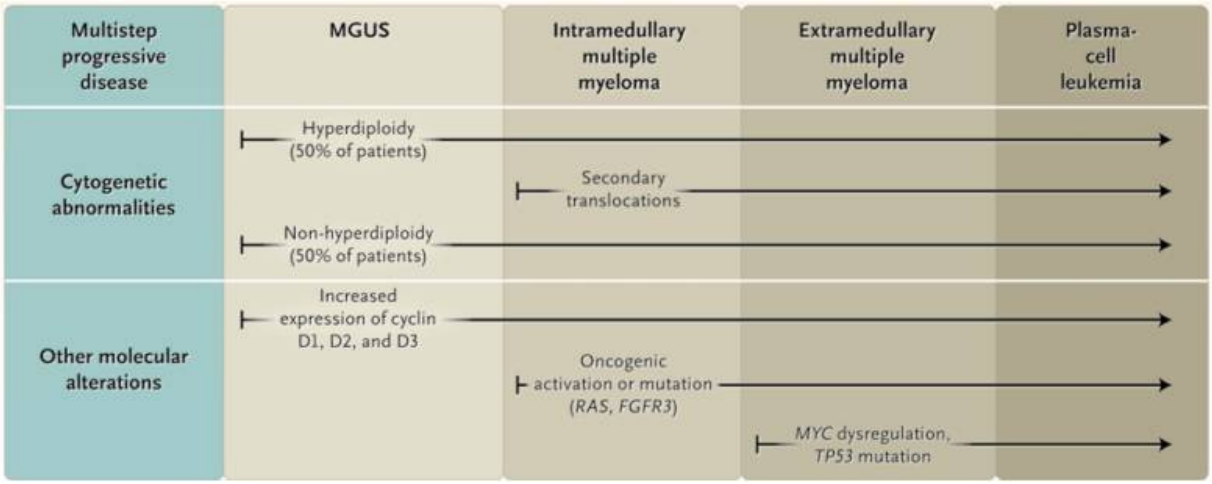

Figure 1.1: Multistep pathogenesis of Multiple Myeloma (adapted from [2]). Early chromosomal abnormalities are shared by plasma cells in MM and in MGUS. Secondary translocations and mutations involving MYC, RAS and TP53 play a role in tumor progression and drug resistance. Moreover, abnormal interactions between plasma cells and bone marrow are hallmarks of disease progression.

1.1 Diagnosis

The diagnosis of MM requires at least 10% or more clonal plasma cells on bone marrow examination or a biopsy-proven plasmacytoma and evidence of end-organ damage, such as hypercalcemia, renal insufficiency, anemia and bone lesions that are felt to be related to the underlying plasma cell disorder. Moreover, the presence of 60% or more clonal plasma cells in the marrow should also be considered as myeloma, regardless of the presence/absence of end-organ damage [7]. When MM is clinically suspected, patients should be tested for the presence monoclonal proteins (M proteins) through a series of tests, such as serum protein electrophoresis, serum immunofixation and serum-free light chain (FLC) assay [1]. However, approximately 2% of patients with MM have non-secretory disease and no evidence of M protein on any of the mentioned assays [8]. Three main staging systems have been developed during the years, namely Durie&Salmon system, the International Staging System (ISS) [9] and the latest Mayo Stratification of Myeloma and Risk-Adapted Therapy (mSMART) guidelines [10]. All the three systems split the patients in three risk categories, termed as stage I, II and III by Durie&Salmon and ISS classifications, while low, standard and high-risk by mSMART classification. While the previous staging systems evaluated mainly blood parameters such as hemoglobin, M proteins, calcium, albumin, creatinine and β2-microglobulin, mSMART guidelines introduced molecular cytogenetic markers to assess disease aggressiveness, taking into consideration hyperdiploidy and several recurrent chromosomal aberrations. Patients with standard-risk have a median overall survival (OS) of 6-7 years, while those with high-risk disease have a median OS of less than 2-3 years, despite therapy (autologous stem-cell transplantation) [11]. Risk stratification also helps to design specific risk-adapted therapeutic

regimens that will be discussed more accurately in the following paragraphs.

1.2 Pathogenesis

As MM is a tumor of antibody-producing PCs, it is fundamental to understand how B cells develop. During the early B cell differentiation in the BM, the variable (V), diversity (D) and joining (J) gene segments of the immunoglobulin (Ig) genes are rearranged to generate the primary Ig repertoire. Ig heavy chain gene *(IGH)* rearrangement precedes Ig light chain, and D_H to J_H joining precedes V_H to DJ_H joining. The assembly of a functional IgH-IgL complex on the cell surfaces (the so-called pre B-cell receptor, BCR), allows B cells to escape apoptosis and exit the BM environment and move to secondary lymphoid organs. In the lymph node virgin B cells reach the germinal center (GC), where cells expressing a functional BCR undergo affinity maturation in response to antigen-presenting cells (APCs). This process requires the *IGH* locus to undergo somatic hypermutation (SHM), to produce highly specific and avid antibodies, and class switch recombination (CSR), namely the mechanism that changes the IgM isotype to IgG-, IgA- or IgE-generating antibodies with different functional characteristics. If illegitimate CSR occurs in the GC, the cell can still undergo maturation to a memory B cell, and it may exit the lymph node with an acquired ability to survive and proliferate as a consequence of oncogene deregulation. The acquired survival/proliferative ability would allow this premalignant clone of PCs to accumulate secondary hits, which will eventually occur in and deregulate critical genes, leading to emergence of a malignant myeloma clone in the BM. The malignant PCs observed in MM are localized to the BM in the earlier stages of the disease and most closely resemble long-lived PCs. These cells have undergone antigen selection outside the BM, as demonstrated by their isotype-

switched and somatically hypermutated Ig genes. Myeloma cells have significantly lower rates of Ig secretion compared with normal PCs; therefore it appears that critical tumor transformation events take place after or do not interfere with most of the normal B-cell differentiation process, leading to long-lived PCs [12],[13]. Moreover, a critical feature shared by MGUS and MM is an extremely low rate of proliferation [14][15], usually with no more than a small percentage of cycling cells until advanced stage disease. This suggest the existence of a malignant, self-renewing precursor cell as a result of oncogenic transformation and selection, but the phenotype and features of this population have not yet been fully elucidated, as discussed in the next paragraphs.

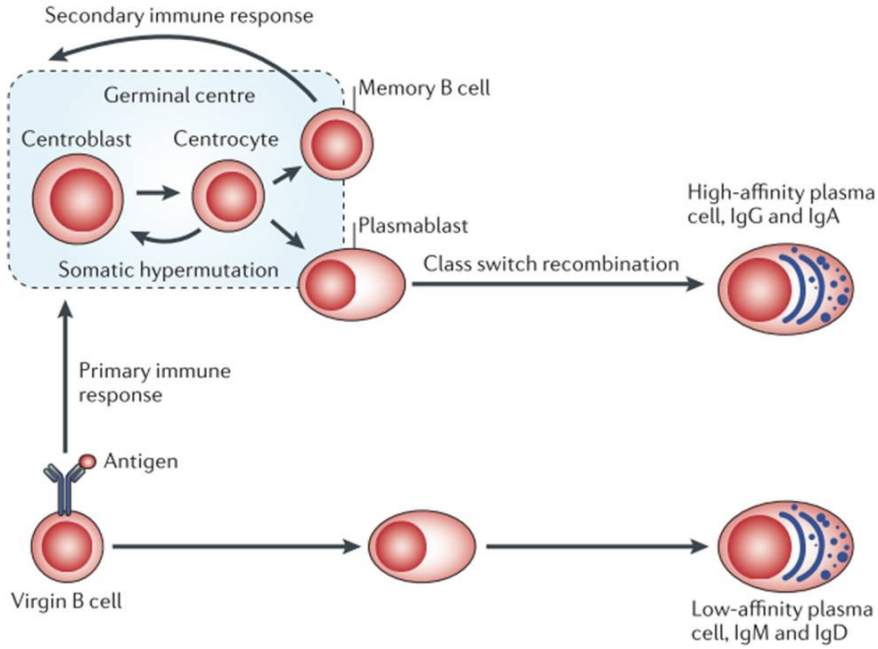

Figure 1.2: The B cell development (adapted from [16]). In the germinal center, affinity maturation occurs through somatic hypermutation and antigen selection. Subsequently, class switch recombination leads to the development of immunoglobulin (Ig) isotypes. After this, the plasmablast migrates to the BM were it becomes a long-lived plasma cell that produces antibody. The machinery necessary to generate these physiological DNA rearrangements can malfunction, leading to malignant change.

1.3 Genetic alterations

Myeloma is thought to evolve most commonly from the asymptomatic stage of MGUS through a multistep process that involves both genetic and epigenetic changes.

Karyotypes normally seen in this disease are extremely complex; indeed, while most blood cancer present with single chromosomal translocations, MM cells from newly diagnosed have an average of seven different abnormalities in chromosome number and/or structure and the karyotypic complexity is thought to increase during tumor progression [17].

Genomic instability is intrinsic to B lymphoid cells; thus it is not surprising that a primary event in many B cell tumors is the translocation of an oncogene near one of the potent Ig enhancers. MM is a paradigmatic case as well, indeed primary translocation involving the immunoglobulin heavy chain locus (*IGH*) are present in 50% of MGUS tumors, 60% of intramedullary and 70-80% of PCL tumors. Ig kappa translocations are less frequent, they are present only in 17% of intramedullary MM, whereas Ig lambda translocation are very rare [18].

Primary translocations are mediated mainly by errors in the IgH switch recombination, while sometimes by errors in SHM during PC generation in GC. As B-cell DNA- modification mechanisms seem to be inactive in normal and neoplastic PCs, secondary translocations must be mediated by other mechanisms [19]. Five partner oncogenes commonly placed under the control of the Ig loci are: cyclin D1 (*CCND1*) on chromosome 11q13, *CCND3* on 6p21, fibroblast growth factor receptor 3 (*FGFR3*) and multiple myeloma SET domain (*MMSET*) [20],[21] on 4p16, *c-MAF* (16q23) and *MAFB* (20q11). Together, the combined prevalence of these five IgH translocation partners is about 40% in MM, with approximately 15% 11q13, 3% 6p21, 15% 4p16, 5% 16q23 and 2% 20q11 [22].

While primary translocations involve B-cell-specific mechanisms and are frequently already present in MGUS, secondary translocations happen later in disease progression. These events are often non reciprocal and can involve more than two different chromosomes. c-*MYC* (8q24) is typically deregulated by such events, and its rearrangements correlate with the severity of the disease [23]. *MYC* translocations are absent or rare in MGUS, but occur in 15% of MM tumors, 45% of advanced tumors and 90% of human myeloma cell lines (HMCL) [22].

Another common mutation that increases in frequency with disease stage is the monoallelic loss of 13q, which occurs in approximately 60% of MM. Nearly half of MM tumors are hyperdiploid (HRD; 48-75 chromosomes) and often have multiple trisomies. Non HRD tumors (<48 or >75 chromosomes) are associated to a poorer prognosis than HRD tumors [24].

Moreover, activating mutations of *NRAS* or *KRAS2,* mutations in *TP53* and the inactivation of cyclin-dependent kinase inhibitors CDKN2A and CDKN2C are other secondary late-onset mutations implicated in disease progression [18],[19].

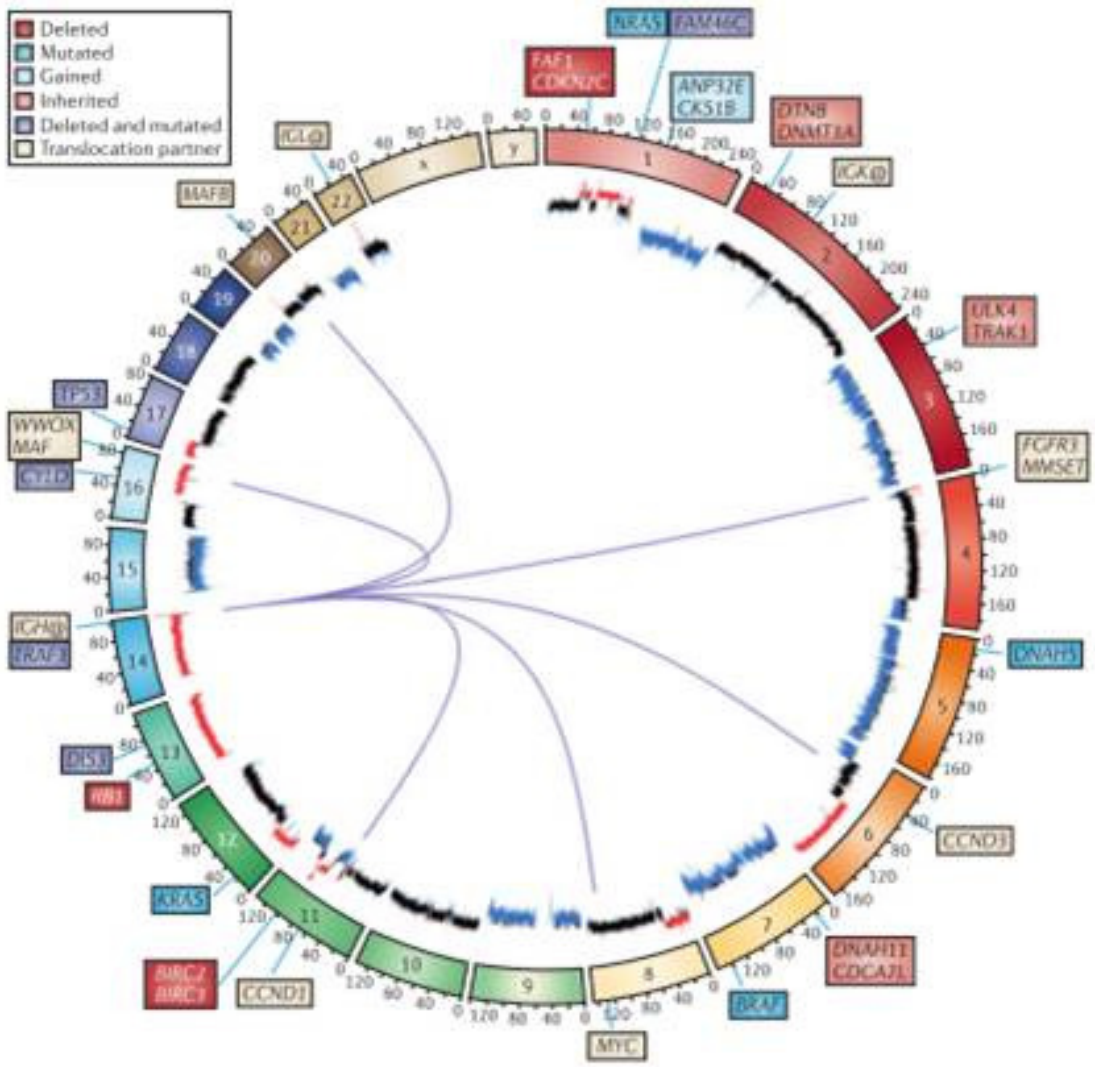

Figure 1.2: The key genetic changes in MM genome (adapted from [16]). The Circos plot shows the key translocations, copy number abnormalities and mutation in MM. Chromosome are arranged around the circle starting from chr.1 (brown) and continuing clockwise. IgH translocations (IGH@) are presented as lines emerging from chr.14 to their partner chromosomes. Copy number data is presented on the inside of the circle, while deletions and/or mutations are labeled outside of the circle.

1.3.1 Low versus high risk MM

The advent of new technologies, such as interphase fluorescence *in situ* (FISH), comparative genomic hybridization and gene-expression profiling (GEP) have provided the necessary tools to stratify MM patients in deeper detail. The combination of the International Staging System (ISS), based on serum albumin and beta-2 microglobulin, with genetics helped to segregate patients in three risk groups. Accordingly to the International Myeloma Working Group (IMWG) high-risk patients with either ISS stage II or III and the presence of either t(4;14), and/or 17p13 deletion have a median overall survival of about 2 years, whereas low-risk patients with ISS stage I or II and absence of these high-risk genetics have 5-and 10-year overall survival rates of 70% and 51%, respectively [25]. Recent prognostic models include several other genetic lesions. For example, according to the Medical Research Council Myeloma IX trial, patients can be classified in three genetic risk groups as follows: a favorable risk group with no adverse FISH lesions, an intermediate group with one adverse genetic lesion involving the immunoglobulin heavy chain gene (IGH) –t(4;14), t(4;16), t(14;20), 17p deletion, or 1q gain, and a high-risk group with more than one adverse genetic lesion [26].

A particularly interesting high-risk mutation is represented by 1q21 gain. In recent years, several independent groups pointed out its importance in disease progression and prognosis [27]–[29]. Amplifications in 1q21 are very common, 30-45% of MM patients harbor +1q21, and its frequency increases in relapsed MM [28],[29]. Moreover, +1q21 were found to co-segregate with other IGH-involving translocations, thus lowering overall survival to 1 year [26]. Such strong association with adverse prognosis stresses the importance of clearly correlate 1q21 mutations with overexpressed genes on 1q, in order to identify new therapeutic targets. Chromosomal gains of 1q21 region can occur in the form if

isochromosome, duplications or jumping translocations [30],[31]. One of the genes located at 1q21 is CKS1B: it codes for an accessory protein to the E3 ligase SCF-Skp2, which induces degradation of the CDK inhibitor $p27^{Kip1}$ by ubiquitination. Elevated expression of CKS1B may lead to inappropriate degradation of p27, which regulates Cdk2-cyclin E activity and G1/S cell cycle transition [32]. CKS1B expression increases with 1q21 amplification and elevated levels are associated with more proliferative MM [29],[34]. CKS1B overexpression may be from increased copy number of 1q21, however, other genes located in this region have been associated with poor prognosis and/or drug resistance in MM, including IL-6 receptor (IL-6R), Bcl-2 family member Myeloid Cell Leukemia 1 (MCL-1)[35],[36], and other not yet identified genes could play a critical role in MM progression. Furthermore, most of the studies so far focused on isolated bulk tumor cells, defined as syndecan-1 (CD138) expressing-plasma cells, while still little is known about 1q overexpressed genes in the context of myeloma cancer stem cells.

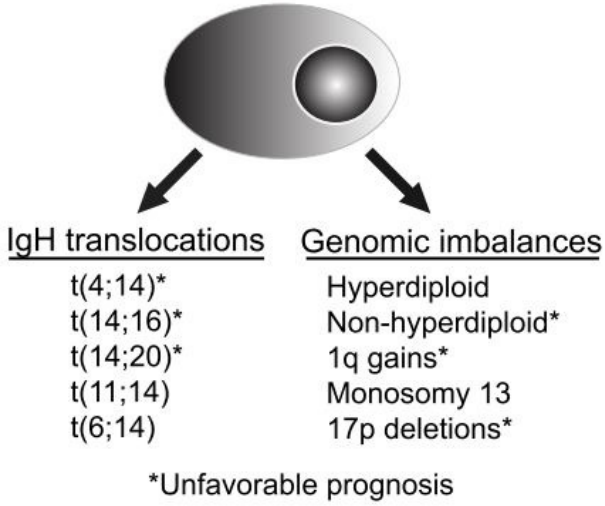

Figure 1.4: Genetic classifications of MM (adapted from [37]**).** The most common high-risk genetic features are t(4;14), del17p and gain 1q21. Detection of these chromosomal abnormalities is achieved by FISH on CD138-selected BM cells or in clonally restricted plasma cells stained for cytoplasmic light chain immunoglobulin.

1.4 Current therapies

Initial treatment for newly diagnosed MM depends on eligibility for autologous stem cell transplant (ASCT) and risk-stratification. If the patient is younger than 70 years ASCT is taken into consideration, while for persons older than 70 years, or younger patients in whom transplantation is not feasible, chemotherapy is the initial treatment of choice. Moreover, based on risk-stratification, is preferred to achieve complete remission (CR) in high-risk patient, while standard and low-risk patients have similar overall survival regardless of whether CR is achieved [38].

ASCT is applicable to more than half of MM patients and has very low mortally rates (1-2%) [39], but this approach has some pitfalls: on one hand post-transplantation CR rate is between 30-35% despite large doses of chemotherapy and/or radiation [40] and on the other hand ASCT could be contaminated by myeloma cells and/or myeloma cancer stem cells.

Typically patients are treated with two to four cycles of induction therapy in order to harvest CD34 positive hematopoietic stem cells (HSCs). After harvest, patients can immediately undergo ASCT or resume induction therapy delaying the transplant until first relapse [41].

Initial treatments include combination regimens with two/three different kind of drugs, such as recently introduced immunomodulatory agents (IMiDs), proteasome inhibitors, and classical chemotherapeutics like alkylating agents and corticosteroids. While IMiDs and proteasome inhibitors will be discussed in further detail in the next paragraphs, I will provide here a brief description about alkylating agents and corticosteroids.

The most common alkylating drug used in MM is melphalan, which acts adding an alkyl group to DNA, inducing DNA damage and duplication arrest. It is commonly used at low doses in combination with prednisone and/or bortezomib, or in high doses as part of the condition regimen for ASCT. As any alkylating agent, this drug cannot distinguish healthy cells from tumor cells, therefore is associated with severe side effects, such as myelosuppression and gastrointestinal effects.

Dexamethasone and prednisone are corticosteroids commonly used in MM therapy: Beside their anti-inflammatory properties, they can also induce apoptosis in MM cells, by activation of death-inducing genes and by repression of transcription factor activity [42]. Dexamethasone was shown to synergize with thalidomide and lenalidomide, prolonging time to progression and overall survival [43]; notably its activity as single agent was shown to be reduced by IL-6 [44].

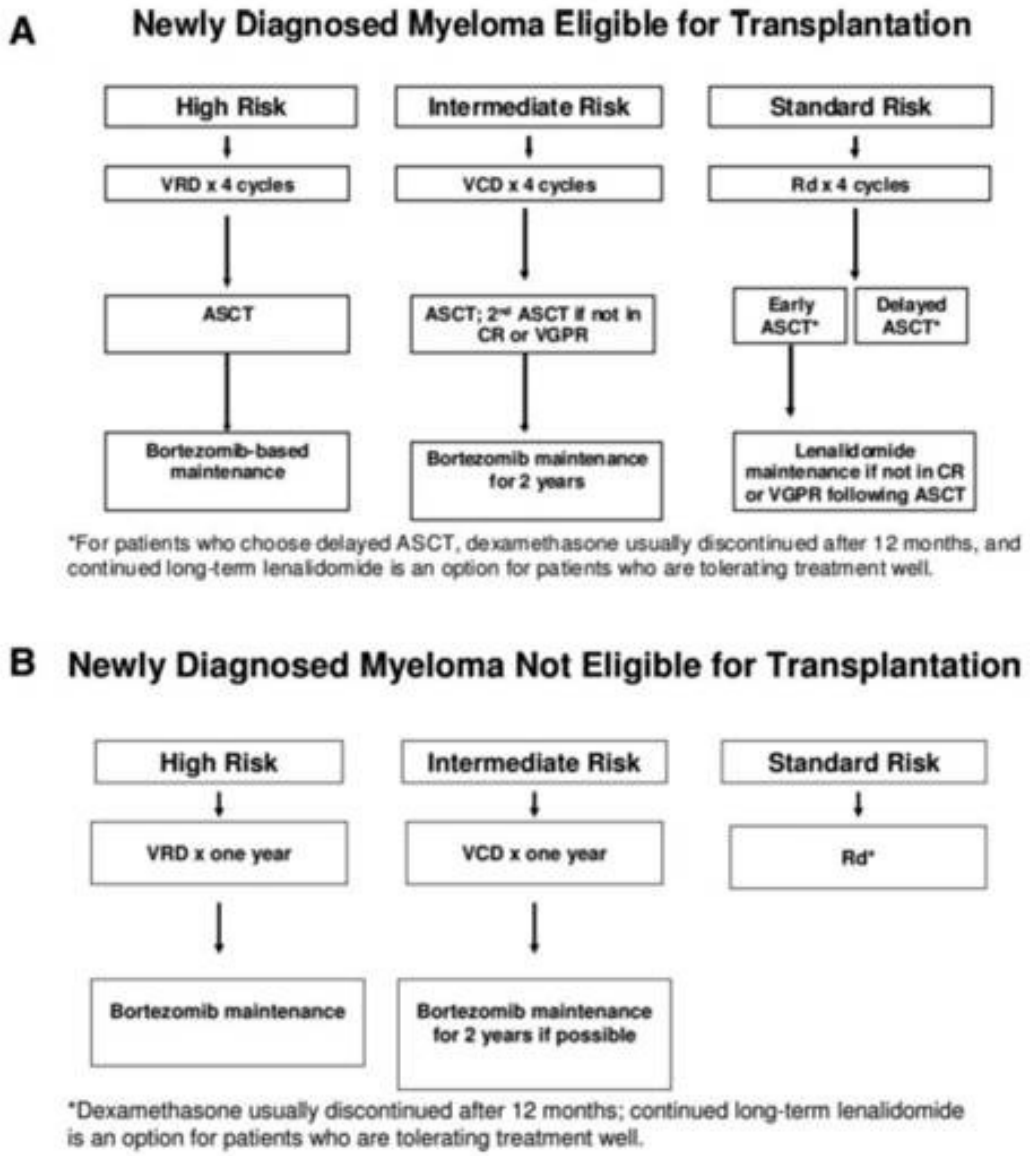

Figure 1.5: Treatment approaches of newly diagnosed myeloma patients (adapted from [1]). Abbreviations: ASCT, autologous stem-cell transplantation; CR, complete response; Dex, dexamethasone; Rd, lenalidomide plus low-dose dexamethasone; VCD, bortezomib, cyclophosphamide, dexamethasone; VGPR, very good partial response; VRD, bortezomib, lenalidomide, dexamethasone**.**

1.4.1 Proteasome Inhibitors

Bortezomib is a first-in-class proteasome inhibitor, it targets the 26S proteasome, a multicatalytic proteinase complex involved in degradation of cyclin and cyclin-dependent kinase inhibitor (CKI) proteins, thereby regulating cell-cycle progression.

Bortezomib inhibits NF-κB activation and nuclear translocation by protecting from 26S degradation its inhibitor IκBα, a protein that is constitutively bound to cytosolic NF-κB. Degradation of IκBα by proteasome activates NF-κB , which in turn up-regulates the transcription of pro-survival proteins, modulates MM cell-adhesion-induced cytokine transcription and secretion in BM stromal cells (BMSC), decreases apoptosis susceptibility, influences the expression of adhesion molecules on BMSCs/MM cells and their related binding, and induces drug resistance in myeloma cells [45].
Bortezomib can also induce myeloma cell apoptosis through caspase-8 and -9 activation, inhibits IL-6 and BMSC–MM cell adherence-induced p42/p44 MAPK phosphorylation and proliferation in MM cells. Adverse effects include lymhopenia, neuropathy, thrombocytopenia and anemia [41]. Second generation proteasome inhibitors, i.e. carfilzomib, have been recently approved for relapsed patients in order to overcome bortezomib resistance.

1.4.2 Immunomodulatory drugs

Immunomodulatory drugs (IMiDs) are a group of compounds analogue to thalidomide, derivative of glutamic acid with anti-angiogenic and anti-inflammatory properties. The two leading IMiDs compounds are lenalidomide (commercial name Revlimid) and pomalidomide (Actimid); first tested in clinical trial in MM in 1999 and then expanded for other conditions, i.e. low-risk myelodysplastic syndrome [46].

Thalidomide (α-N-phthalimido-glutaramide) is a synthetic derivative of glutamic acid, which was unfortunately famous for causing birth defects when used as antiemetic in pregnancy in the late '50s and early 60's. After its withdrawal from markets, it was subsequently found to be effective in the treatment of erythema nodosum leprosum, a cutaneous complication of leprosy and its efficacy was proved to be related to TNFα expression inhibition. Thalidomide was also found to have anti-angiogenic and immunomodulatory properties, including T-cell stimulation [47]–[49]. Lenalidomide and pomalidomide were then developed in order to achieve TNFα inhibition with less toxicity compared to thalidomide. These features helped resurrect thalidomide as potential anti-cancer treatment. In MM patients, immune surveillance against tumor antigens is impaired, including antibody responses, impaired antigen-presenting cells and dysfunction of NK, T and B cells [50].

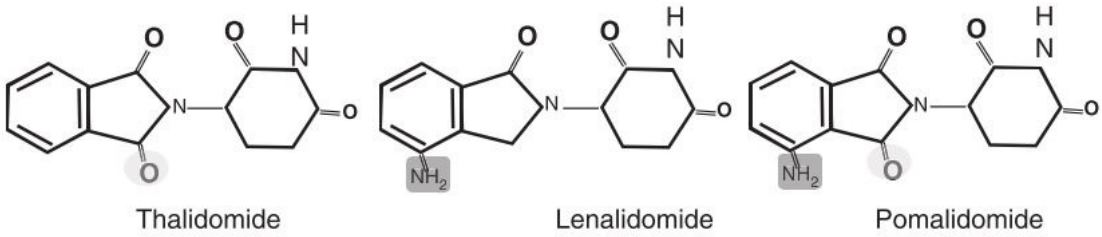

Figure 1.6: Chemical structure of thalidomide and its analogues, lenalidomide and pomalidomide (adapted from [50] **).** Lenalidomide and pomalidomide were derived by adding an amino group to the fourth carbon of the phthaloyl ring of thalidomide.

IMiDs can induce proliferation and enhance cytokine production, i.e. IL-2 and IFNγ in partially activated CD3+ T cells [51], increase dendritic cell-induced NK T cell expansion and NK T IFNγ secretion [52], increase NK cell proliferation and enhance antibody-dependent cellular cytotoxicity (ADCC) [53]. Outside the context of MM, other immunomodulatory effects include downregulation of TNFα production in LPS-stimulated monocytes [54], therefore IMiDs activity may vary in a disease/cell type-specific context. Furthermore, IMiDs have a major role in disrupting MM-BM protective interactions: they were found able to abrogate VEGF and βFGF secretion in *in vitro* MM-BMSCs co-cultures (from both cell types) [55] and to inhibit the expression of cyclo-oxigenase (COX)-2, which synthesize pro-inflammatory prostaglandins. Lastly, IMiDs also exert direct anti-proliferative effects on myeloma cells via inhibition of the cyclin-dependent kinase pathway, activation of Fas-mediated cell death and downregulation of anti-apoptotic proteins. In HMCL lenalidomide induced the expression of cyclin-dependent kinase inhibitor p21, thus leading to a G1 cell cycle arrest. Lenalidomide activity was thought to be dependent on Interferon Regulatory Factor (IRF) 4 inhibition: IRF4 is a transcription factor required for the generation of immunoglobulin-secreting plasma cells, which is often upregulated in MM in coordination with upregulation of MYC [56]. Lenalidomide treatment induces a downregulation of IRF4 mRNA and protein levels [57]. However, how lenalidomide would inhibit IRF4 was not fully elucidated. Preclinical studies identified an E3 ligase protein, cereblon (CRBN) as the direct molecular target of IMiDs. CRBN is a component of the cullin ring E3 ubiquitin complex, that contains DNA damage-binding protein 1 (DDB1), cullin (Cul) 4a and regulator of cullins (Roc) 1 [58]. *In vitro* long-term selection for lenalidomide resistance is accompanied by a reduction in CRBN [59]; very interestingly CRBN does not appear to be frequently mutated in MM patients [60],[61], thus suggesting that transcriptional or post-transcriptional factors may influence IMiDs

responsiveness. Recently two independent groups found that lenalidomide-bound CRBN acquires the ability to target for proteasomal degradation two lymphoid transcription factors, Ikaros family zinc finger protein IKZF1 and IKZF3, essential transcription factors in myeloma [62],[63]. IMiDs are used both for newly diagnosed as well as relapsed patients, in combination with other agents, i.e. dexamethasone and/or bortezomib. Side effects include neutropenia, deep vein thrombosis, infections and increased secondary tumors [64]

1.4.3 Risk-adapted regimens

Standard-risk patients can be treated with lenalidomide plus low-dose dexamethasone (Rd) or a bortezomib-containing triplet, such as bortezomib-cyclophosphamide-dexamethasone (Velcade-Cyclo-Dex). Standard and high-risk patients require a bortezomib-based triplet regimen, such as VCD, bortezomib-thalidomide-dex (VTD) or bortezomib-lenalidomide-dex (VRD). In patients with newly diagnosed MM not eligible for transplant, initial therapies include the previously mentioned and melphalan-based regimens, which are falling out of favor due to concerns about stem cell damage. Unfortunately, almost all MM patients face relapse and/or become refractory to treatment, with a remission period shortening with each regimen [65]. The median OS for relapsed/refractory MM is around 5-9 months. Treatment for these patients include doxorubicin (topoisomerase inhibitor), carfilzomib (a novel proteasome inhibitor) and pomalidomide, as single/combination agents [41]. Furthermore novel agents such as monoclonal antibody (Mab)-based therapies and histone deacetylase inhibitors are under pre-clinical and clinical evaluation [66],[67].

2 The Bone Marrow niche

The bone marrow (BM) microenvironment consists of cellular and non-cellular elements. Cell components include HSCs, progenitor cells, immune cells, erythrocytes, BM fibroblast-like stromal cells (BMSCs), vascular endothelial cells, osteoclasts (OCs) and osteoblasts (OBs). The non-cellular elements are represented by extracellular matrix (ECM) proteins, such as fibronectin, collagen, laminin and osteopontin. The direct interaction of MM cells with BM microenvironment cells activate signaling pathway mediating growth, survival, drug resistance and the migration of MM cells [68], as well as osteoclastogenesis [69] angiogenesis [70] and secretion of several soluble factors, such as interleukin 6 (IL-6) [71], vascular endothelial growth factor (VEGF) [72], stromal cell-derived factor 1 (SDF-1) [73] and insulin-like growth factor (IGF1) [74]. Both homotypic and heterotypic adhesion of MM cells to either BMSCs or ECM are mediated through several adhesion molecules, i.e. CD44, very late antigen 4 (VLA-4, also known as integrin α4β1), VLA-5 (α5β1), intracellular adhesion molecule (ICAM-1), NCAM, syndecan 1 (CD138) and MPC-1. Furthermore, several developmentally conserved signaling pathways have emerged as important signaling circuits for tumor bulk and cancer stem cells, including Notch, Wingless-type (Wnt) and Sonic hedgehog (Shh), thus contributing in the creation of a niche that balances signals of differentiation and self renewal [75].

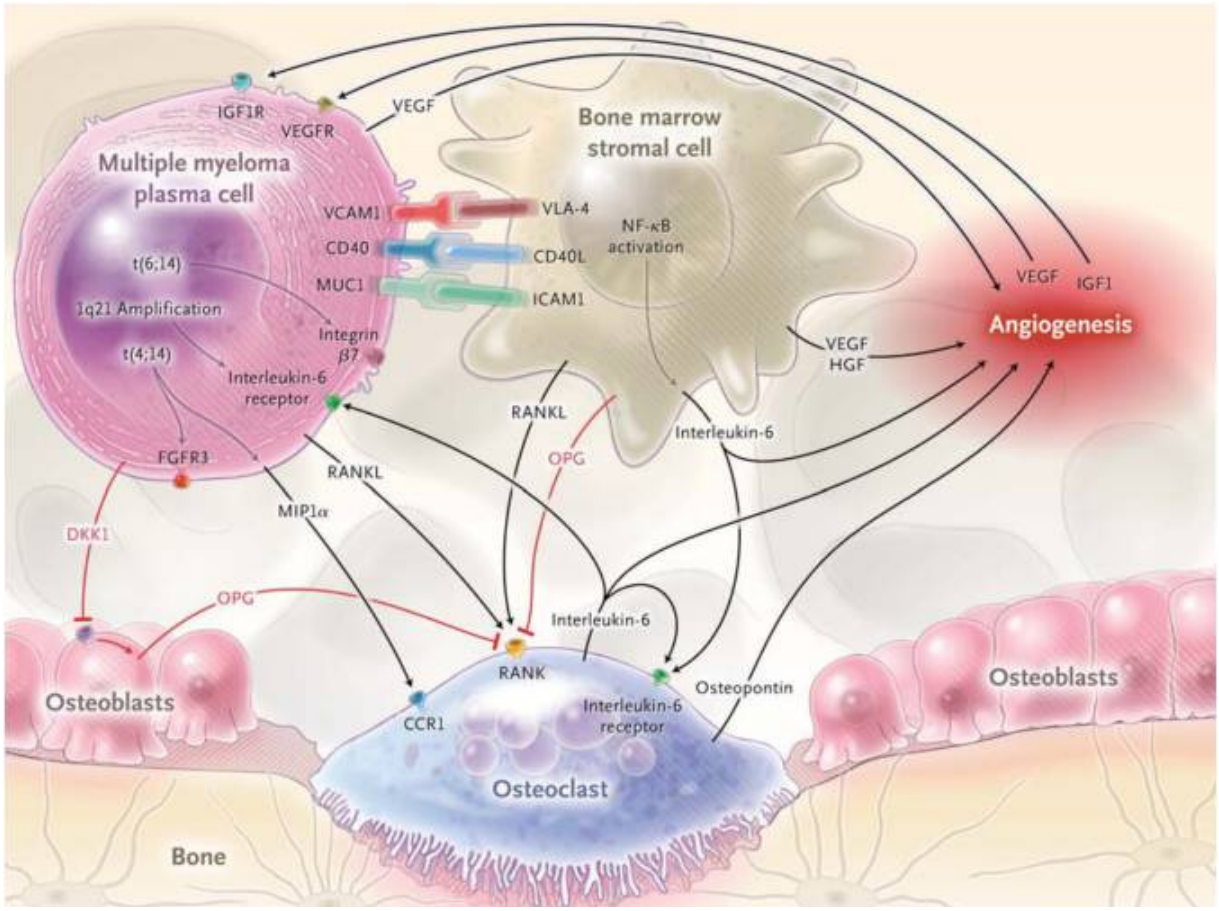

Figure 2.1: Interactions between tumor plasma cells and the BM in MM (adapted from [2]). Interactions are mediated by cell-adhesion molecules such as VCAM1 and integrin VLA-4. Cell-cell contact increases the production of growth factors IL-6 and VEGF. Chromosomal abnormalities can cause overproduction of cytokines receptors, such as IL-6 receptor (1q21).

2.1 Pro-inflammatory signals in MM BM

Since MM mainly progresses in the BM, signals from this microenvironment play a critical role in maintaining plasma cell growth, survival, migration, drug resistance and angiogenesis. Reciprocal interactions between PCs and BM cells are mediated by an array of cytokines and receptors. PCs in the BM secrete tumor necrosis factor-α (TNFα), transforming growth factor-β (TGF-β), VEGF, angiopoietin-1, FGF-2 and matrix metalloproteases (MMPs). Moreover, the cell-cell interactions mediated by adhesion molecules between PCs and BM cell trigger transcription and secretion by the latter of cytokines, such as IL-6, VEGF, SDF-1 (CXCL12), Hepatocyte growth factor-scatter factor (HGF-SF) and IGF-1[70],[73],[76]–[79].

One of the most important cytokines in myeloma is IL-6: in the 90's IL-6 was shown to induce *in vitro* growth of freshly isolated MM cells, which expressed IL-6 receptor (IL-6R). In the same decade, many studies showed that BMSCs are the major source of IL-6 and that, virtually all human MM-derived cell lines express IL-6R mRNA [71],[80],[81]. Notably, several MM cell lines have also been described to produce IL-6, thus leading to hypothesize also an autocrine signaling pathway.

Various soluble factors have been shown to mediate IL-6 secretion by BMSCs or MM cells, e.g. IL-1α, IL-1β, TNFα and VEGF. In MM, VEGF is expressed and secreted by tumor cells as well as BMSCs. It induces proliferation through Raf-1-MEK-extracellular-signal-regulated protein kinase (ERK) pathway, it triggers migration of human MM cells through a protein kinase C (PKC)-dependent cascade [72] and it stimulates the expression of IL-6 by microvascular endothelial cells and BMSCs [77].

IL-6 is not only important for myeloma cell proliferation but also plays a critical role in OC development. Bone lesions are a hallmark of myeloma, leading to hypercalcemia, bone pain and increased risk of fractures. Myeloma growth is associated with increased numbers of OCs and

suppression of osteoblastogenesis in areas adjacent to tumor foci. OCs play an active role, cooperating with MM cells to produce VEGF, osteopontin and stimulating BM niche cells to secrete IL-6 [82],[83].

Another potent mediator of inflammation and bone resorption expressed by BMSCs and PCs from myeloma patients is TNFα. Several studies confirmed a central role for this cytokine in the growth and survival of MM cells in the BM milieu, given that TNFα induces proliferation expression of ICAM-1, VCAM-1 and VLA-4 and MAPK/ERK activation in MM cells, and on the other hand IL-6 secretion, NF-κB activation and expression of ICAM-1 and VCAM-1 in BMSCs [84].

2.2. Relapsed and refractory MM

In spite of current efficient therapies drug resistance (DR) is a major concern in MM. During the past years many studies were focused on the mechanisms underlying DR, and several factors appear to contribute to this process, including cytogenetic and epigenetic alterations, deregulated signaling in the BM niche and MM cancer stem cells maintenance. As discussed previously, MM has a high level of genomic instability, indeed patients who relapse or become refractory to therapy carrying any high-risk marker may be referred as intrinsically drug-resistant.

In the following paragraphs we will discuss more extensively microenvironment-induced and cancer stem cell-dependent drug resistance.

2.2.1 BM-dependent drug resistance

The contribution of BM niche components such as BMSCs and extracellular ECM proteins is critical in MM pathogenesis. The mechanisms of MM drug-resistance due to BM niche effects can be grouped in soluble factor-mediated DR (SFM-DR) and in cell-adhesion-mediated DR (CAM-DR). SFM-DR can be highly ascribed to IL-6, but also other cytokines, including Insulin-like Growth Factor (IGF) 1 [85] and TGF-β (Hideshima et al., 2007) have been implicated in drug-resistance.

MM cells exhibit preferred adhesion to several ECM constituents, including laminin, collagens and fibronectin (FN), *via* β1 integrin-mediated adhesion.

Adhesion molecules are responsible for the development of MM cells resistance to front-line chemotherapeutic drugs.

CAM-DR to doxorubicin, melphalan, bortezomib and mitoxantrone has been induced *in vitro* through adhesion to fibronectin (FN) or BMSCs, which is mostly mediated by VLA-4 [86]–[88], and by other integrins, i.e. β7 [89].

2.2.2 Myeloma Cancer Stem Cells

The high relapse rates in MM led researcher to investigate the hypothesis of a quiescent, tumor-initiating cancer stem cell population within the bulk of malignant plasma cells. In the early 90's studies on the B cell repertoire in MM patients led to believe that clonotypic B cells were represented by a proportion of circulating CD19+ B cells since these peripheral blood B cells shared the same IgH rearrangements of BM plasma cells. Scientific literature on myeloma cancer stem cells (CSC) is highly conflicting. On one hand, a convincing amount of data supports the fact that tumor-initiating cells expressing syndecan-1 on their surface (CD138+) (CD138+/CD19-/CD38+/CD45low in primary human samples) have increased clonogenic ability *in vitro*, are able to propagate in immunocompromised mice and in syngenic immunocompentent mouse model of MM (5T33) [90]–[92]. On the other hand, several groups confirm Matsui's studies, which identified CD138- (CD138-, CD19+ and CD20+) as myeloma putative CSCs. His work suggests that MM cells contain a rare subpopulation which is clonotypic, drug resistant and expressing memory B cell-like phenotypic markers (CD138-/CD19+/CD20+/CD27+). CD138- cells appear to have clonogenic potential, are able to propagate MM tumor in NOD/SCID mice, are drug-resistant and enriched in a side population (SP) with high ALDH1 activity and drug-efflux pump [93]–[97].

2.3. Notch pathway alterations in MM

Normal stem-cell fate is controlled by several developmental conserved pathways, such as Sonic hedgehog (SHH), Wingless-type (Wnt) and Notch [98]. Notch is an evolutionary conserved pathway that regulates stem cell fate and self-renewal, both in physiological and malignant contexts[99],[100]. Notch receptors are single pass type I transmembrane proteins that are evolutionary conserved. Four paralogs exist in mammals, namely *NOTCH1, NOTCH2, NOTCH3* and *NOTCH4*, which display both redundant and unique functions. The mature form of Notch on the cell surface is a large heterodimer, held together by non-covalent calcium-dependent interactions through the heterodimerization domain (HD). Most Notch ligands are themselves type I transmembrane proteins. They can be grouped based on the presence or absence of a cysteine-rich domain in Jagged/Serrate or Delta, respectively. Mammals display five Notch ligands, *JAGGED1-2* and *DELTA-like -1,-3,-4* (*DLL-1*, *DLL-3*; *DLL-4*).

It is well established that Notch activation occurs in a ligand-dependent fashion and it involves a series of proteolytic events that culminate with a cleavage within the transmembrane domain mediated by γ-secretase, a multi-component protease complex [101],[102]. This cascade of proteolytic activation releases the NICD (Notch IntraCellular Domain), which is able to translocate in the nucleus, where it binds to CLS (CBF-1/Suppressor of Hairless/Lag1) proteins, through RAM and ANK domains. In absence of activation by Notch, CSL acts as a transcriptional repressor. Upon NICD binding, co-repressor complexes are removed and CSL is converted into a transcriptional activator by SKIP (Ski-interacting protein). Additional engagement of co-activator Mastermind-like 1 (MAML1), histone acetyltransferases p300, PCAF and GCN5 might occur through the ANK domain [103].

Given that Notch receptor can only signal once after proteolytic-activation, regulation of either ligand or receptor availability at the cell surface are tightly regulated. DSL ligand endocytosis is triggered by monoubiquitination mediated by the E3 ubiquitin ligases Neuralized (which preferentially recognizes Delta ligands) and Mindbomb (which recognizes Serrate/Jagged). Endocytosis of the Notch receptor is controlled in time and space by Numb, a conserved membrane-associated protein that acts upstream of the γ-secretase cleavage, to block Notch signaling in daughters of a asymmetric dividing cells. Moreover, several E3 ubiquitin ligases, e.g. Deltex, API/Itch and Su(dx), can control Notch receptor trafficking either towards lysosomal degradation or recycling [104].

At the nuclear level, during the transcriptional activation process, NICD is phosphorylated on its PEST domain by the CDK8 kinase and targeted for proteasomal degradation by the E3 ubiquitin ligase Fbw7Sel10 [105].

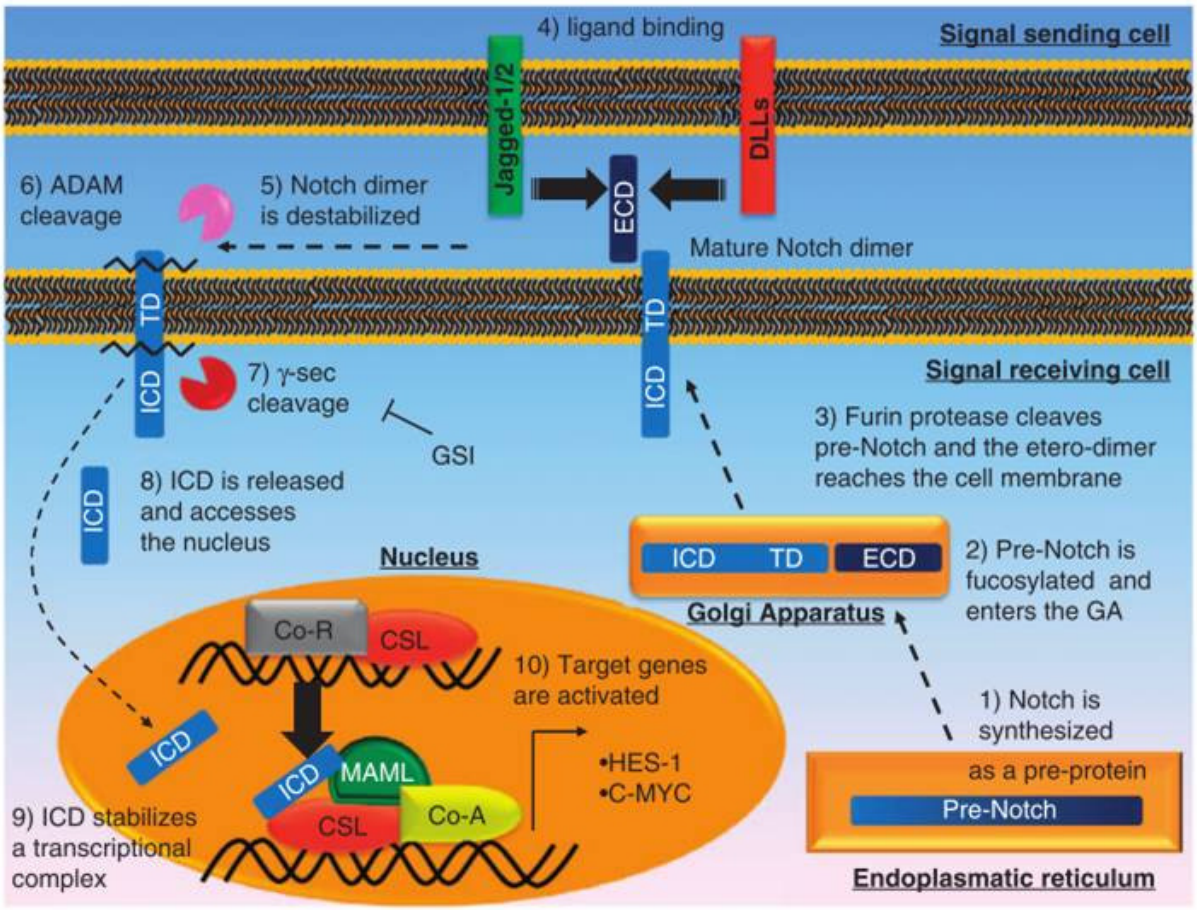

Figure 2.2: The Notch pathway (adapted from [100]). Notch receptors are single-pass, hetero-dimeric proteins consisting of two peptides: one extracellular (extracellular domain (ECD)) and one intracellular, the latter containing a transmembrane domain (TD) and an intracellular domain (ICD). The ECD blocks Notch activation, unless it binds the ligands (Jagged or DLLs) expressed by an adjacent cell (4). Such interaction disrupts the hetero-dimer conformation (5), allowing the ADAM (a disintegrin and metallo- proteinase domain) proteinase to cut the TD-ICD extracellularly (6). Immediately after that, the g-secretase complex cuts the TD-ICD (7) releasing the ICD, which translocates to the cell nucleus (8). This third proteolytic processing is inhibited by gamma secretase inhibitors (GSI). Here, the ICD interacts with the CSL DNA-binding proteins (from CBF1/RBP-J in vertebrates), converting CSL from a transcriptional repressor to an activator (9) by displacing corepressors (Co-R) and recruiting histone acetyltransferases and co-activators, such as mastermind- like proteins (MAML). Notch targets genes, such as HES-1 and C-MYC, are then activated.

MM cells express Notch-1, -2 and-3 receptors and their ligands, leading to homotypic interactions. Among ligands, Jagged-2 is overexpressed in MM and MGUS patients, and its levels of expression increase with the stage of the disease. Moreover, *in vitro* interaction between stromal cells and MM cells that overexpressed Jagged-2 can increase secretion of IL-6, VEGF and IGF-1 by the stromal cells [106]–[109]. Notch ligands are also expressed by stromal cells and macrophages, which can activate Notch in MM cells thorough heterotypic interactions [110].

Noteworthy, Notch signaling promotes β1 integrins activation and the expression and function of several chemokine receptors involved in MM [111],[112], thus contributing to BM-dependent drug resistance [113],[114].

In the last few years the importance of Notch signaling in bone remodeling has emerged. Indeed Notch overexpression blocks the maturation of OB precursors by opposing canonical Wnt/ β-catenin signaling [115]. On the other side, myeloma can drive osteoclastogenesis by activating Notch signaling in tumor cells and OCs, through RANKL secretion and direct interactions.

3. RNA editing

In the mid-80's the term RNA editing was coined to describe a novel phenomenon in which uridine (U) residues in protozoa mitochondrial RNA molecules were inserted and deleted. Since then, the term has been used to describe many cellular processes of enzymatic post-transcriptional RNA modification. The main types of RNA editing are deletion/insertion of one or multiple C or U residues, or the substitution of one base by another [116]. In highly developed eukaryotic cells it commonly happens with the hydrolytic deamination of either C-to-U or A-to-I bases [117],[118]. In mammals the most prevalent form of RNA editing is the deamination at the C6 position of adenosine that is subsequently converted into an inosine (A-to-I). Inosine behaves like guanosine with respect to its base-pairing properties and translational potential. As a result, any A-to-I modification within RNA has the same consequence as an A-to-G mutation. The enzymes responsible for this conversion are the Adenosine Deaminase Acting on RNA (ADAR) family of editases that catalyze A-to-I editing in structured or double stranded RNAs.

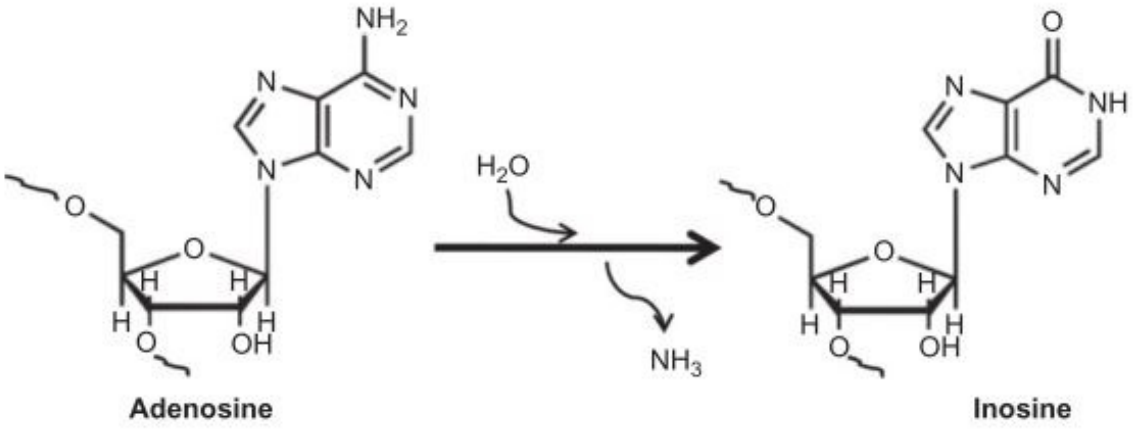

Figure 3.1: Mechanism of adenosine to inosine modification catalyzed by ADAR proteins (adapted from [119]).

3.1 A-to-I editing effects

The functional consequences of specific RNA editing events depend on where within the RNA molecule the modification takes place. An edited base within a translated exon may result in a non synonymous codon change that will lead to a single aminoacid substitution in the resulting protein. Alternatively, a change that involves a pre-mRNA splice site may create or destroy a consensus slicing signal as well as miRNA biogenesis could be affected by site-selective editing events. Furthermore, A-to-I changes may influence the folding properties of a RNA molecule, its half life, transport and interaction with other nucleic acids or proteins.

Until recently only a very small number of proteins with aminoacid substitutions caused by A-to-I editing were known, but thanks to improved bioinformatics analysis and deep sequencing approaches, new evidences support the notion that hundreds of gens undergo recoding editing resulting in aminoacid substitution [120]. However, the experimental validation of predicted editing sites is tricky because of RNA editing regulation in space, time and cell-specific context, as well as by the fact that only a small subset of transcripts from a given gene may undergo editing, thus representing a low frequency event.

By far the most widespread activity of A-to-I editing affects repetitive elements within primate transcripts, in particular Alu-type retrotransposon sequences (Kim et al. 2004; Athanasiadis et al. 2004). Alu sequences are transcribed by RNA polymerase III and encode for not functional protein. More than one million copies of Alu elements are interspersed in the human genome and had no obvious function, but were thought to be implicated in creation of new exons and donation of new regulatory elements. Alu elements can form structures in which one Alu in the (+) sense of orientation base pairs with another Alu sequence that is in the opposite (-) orientation. Alu sequences are not uniformly distributed in the human

genome, but rather are more frequent in GC-rich and gene-rich regions [121]. Considering the high sequence similarity between Alu elements, such highly base-paired double stranded RNA structures are very likely targets for RNA editing enzymes. Alu editing may be responsible for the significant differences between inosine levels detected in mRNAs compared to the few edited transcripts identified so far [123]. Most Alu repeats are located in introns and non-translated exons (UTRs). The outcome of editing events in such regions is not immediately predictable. Several mechanisms have been recently described: on one hand, Alu-edited RNA can be sequestered in the nucleus by a protein complex with particular affinity for inosine in RNA molecules[124], while other studies suggest that other Alu-edited transcripts are exported and associate with polysomes despite being edited [125],[126].

Non-coding RNAs represent others potential RNA editing targets, considering that miRNAs go through a base-paired intermediate as part of their maturation process. miRNAs are constituted by 20-22 nuculeotide long single stranded RNA molecules regulating the translation of target mRNAs. The primary transcripts of miRNA genes, called pri-miRNAs, are generated by RNA polymerase II as long transcript containing an hairpin structure. Then pri-miRNAs are processed within the nucleus through cleavage by the RNAse III Drosha into 70-100 nucleotide (nt) pre-miRNA. Pre-miRNA are exported to the cytoplasm and further processed into a short 22-25 nt RNA duplex by the RNAse III Dicer. The resulting single stranded mature miRNA from one of the two strands is incorporated into a functional complex, named RNA-induced silencing complex (RISC), ready to target complementary mRNAs. A-to-I editing events can affect the ability of Drosha and Dicer to bind and cleave pri and/or pre-miRNAs [127]. Hyperedited transcripts are specifically recognized by the RNAse III Tudor-SN (part of the RISC), leading to their degradation. Editing changes have also been described to downregulate the downstream processing of the pri-

or pre-miRNA, thus repressing miRNA biogenesis (Yang et al. 2006). If the base alteration occurs within the sequence of the mature miRNA then editing is able to alter the miRNA target spectrum [129].

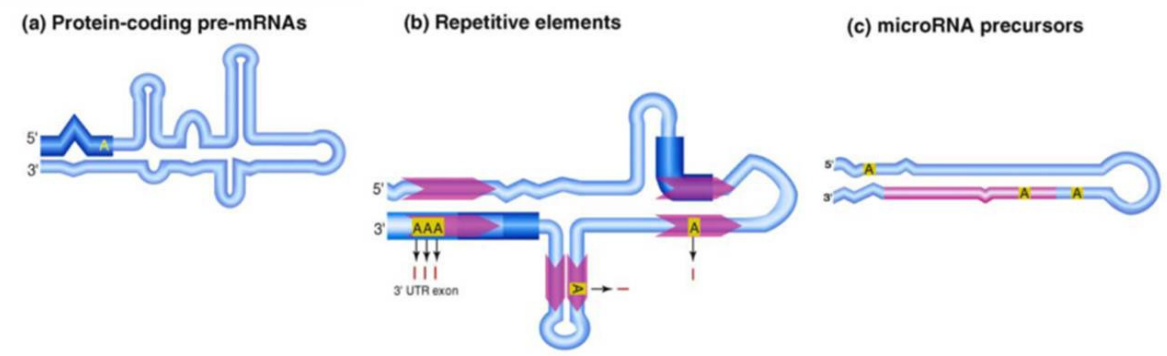

Figure 3.2: Illustration of the three major types of A-to-I RNA editing targets and their fates (adapted from [118]). (a) The pre-mRNA editing of protein-coding genes with a composite RNA secondary structure leads to highly site-selective recoding if it affects a non-synonymous codon site. (b) Pairs of repetitive elements, such as primate Alus located in coding or non-coding exons or introns, can generate RNA secondary structures targeted by the RNA editing machinery. (c) The characteristic secondary structure of pre-miRNAs is a frequent target of ADARs.

3.2 Adenosine Deaminases Acting on RNA: ADARS

ADARs were originally identified in *Xenopus laevis* eggs and embryos as dsRNA unwinding enzymes, and shortly after it was discovered that this family encodes for dsRNA-specific adenosine deaminases [130]. In humans the ADAR family is composed of three highly conserved members, ADAR1 (chromosome 1), ADAR2 (chromosome 21) and ADAR3 (chromosome 10). They share common domains, namely double-stranded RNA-binding domains (dsRBD) and the catalytic adenosine deaminase domain. ADAR1 and ADAR2 are the only ones with confirmed deaminase activity, while ADAR3 apparently lacks of function, despite its conserved functional domains.

One to three repeats of the dsRBD, forming a highly conserved α-β- β- β- α configuration structure, are present among ADARs. The dsRBD makes direct contact with the dsRNA [131] and it is required for dsRNA binding [132]. The C-terminal region contains the catalytic domain, consisting of amino acid residues that are conserved in other deaminases, including the cytidine deaminases APOBEC1, involved in the C-to-U mRNA editing mechanism [133],[134]. By crystallography, histidine H394, glutamic acid E396 and other two cystein residues C451 and C516 were indentified to be involved in the coordination of a zinc atom and in the formation of the catalytic center [135].

On the other hand, other structural features are unique to particular ADAR members. For example, ADAR1 contains two additional Z-DNA binding domains, Zα and Zβ [136], that have still unclear functional significance.

Notably, ADAR1 maps on chromosome 1q21, a genomic location involved in high-risk myeloma, and exists in two different isoforms: the constitutively and ubiquitously expressed ADAR1 p110 and the inducible ADAR1 p150 [137]–[139]. ADAR1 p150 is under an interferon (IFN)-inducible promoter and contains the Z-DNA binding domain Zα and a unique nuclear export

signal, not present in p110. Therefore, while p110 is usually only found in the nucleus, p150 can localize to both nucleus and cytoplasm [136],[138],[140],[141]. ADAR1 p150 has also been showed to be induced by other inflammatory signals, such as TNFα [142].

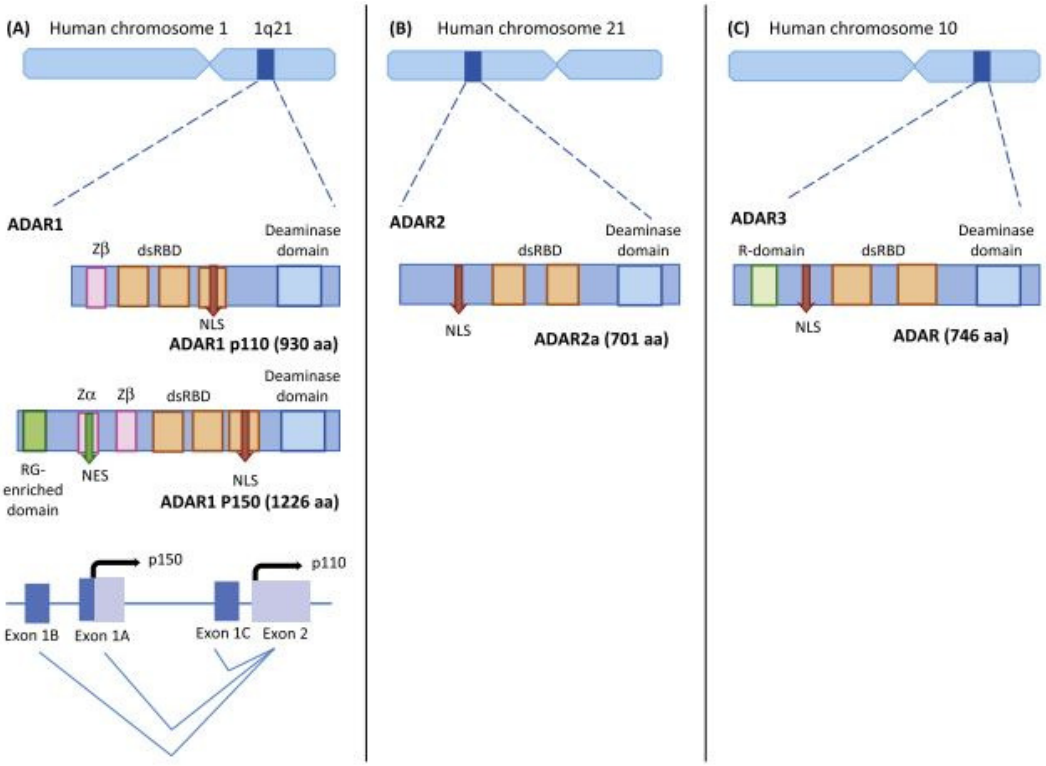

Figure 3.3: The ADAR family of editases (adapted from [127]). (A) ADAR1 maps to chr.1q21 and can be expressed in two isoforms, p110 and p150. ADAR1 p150 is expressed from an IFN-inducible promoter using a translational start-site in exon 1A, located after the IFN-inducible promoter. ADAR1 p110 is generated from mRNA using either exon 1b or exon 1C that follow a constitutive promoter. Exons 1B and 1C do not contain any translational start-sites, and ADAR1 p110 is produced from a start codon located in exon 2. Exon 1A, exon 1B and exon1C are spliced to exon 2 at the same junction. (B) ADAR2 maps to chromosome 21 and, although several different transcript variants have been identified, only one protein product has been confirmed. (C) ADAR3 maps to the short arm of chromosome 10. Although it has a deaminase domain, no editing activity has been reported for this family member.

3.3 ADAR1 in cancer

A growing body of evidence shows that A-to-I editing is an important contributor in tumors, occurring both in hematological and solid malignancies. The levels of editing in tumors can be either increased or decreased. For example, A-to-I editing in Alu repeats in the glutamate receptor subunit 2 (GluA2) has been linked to glioma progression. In this context, the decrease in editing correlated with the grade of malignancy [143],[144]. In other solid tumors, especially in epithelial tissues, disease progression has been associated with increased editing: in hepatocellular carcinoma and in esophageal squamous cell carcinoma, A-to-I editing led to a single amino acid substitution in antizyme inhibitor (AZIN) 1, thus increasing tumor invasiveness and tumorigenic potential [145],[146]. Notably, increased editing was associated with ADAR1 upregulation. Beside solid tumors, aberrant ADAR1-dependent RNA editing has been observed also in hematological malignancies, such as acute myeloid leukemia (AML) [147] and chronic myeloid leukemia (CML). In particular, in CML RNA editing was linked to therapy resistant leukemia stem cell generation. Indeed, the progression from chronic to blast crisis phase was associated with an increased expression of inflammation-responsive ADAR1 p150 and of IFNγ pathway gene expression in malignant progenitor cells[148].

Aim of the work

Multiple myeloma (MM) is the second most common hematological malignancy after leukemia, affecting a significant percentage of the aging population. Autologous stem cell transplant is still considered the best therapeutic option, which is highly limited by the average patient's age. Both transplant-eligible and ineligible patients face high dose chemotherapy, painful adverse effects and the almost 100% chance of relapse and/or drug unresponsiveness. Myeloma therapy is extremely expensive, averaging several thousands of dollars per month for a single therapy cycle; therefore it is crucial to determine the best therapeutic regimen according to patient-specific risk factors. The mutation patterns of MM are complex, and more similar to those found in epithelial tumors and the blast phase of chronic myelogenous leukemia than to those in other hematopoietic tumors. In these cancers, the contribution of post-transcriptional mechanisms such as RNA editing have recently emerged as a key factor in cancer progression, especially in the context of protective niches such as the BM microenvironment. This study aimed to investigate post-transcriptional niche-responsive drug escape mechanisms that could drive MM progression and emergence of malignant clones refractory to therapy. In particular, we investigated the Adenosine Deaminase Acting on RNA (ADAR1) RNA editing enzyme as mechanism of drug resistance and a novel therapeutic target. We postulated that ADAR1-dependent aberrant A-to-I RNA editing in MM cells could drive transcriptome "reprogramming" in MM tumor cells, thus contributing to disease relapse and drug resistance. Moreover, we evaluated whether BM inflammatory signals promoted by deregulated cell survival pathways in MM cells, such as aberrant Notch activation, sustain ADAR1-mediated reprogramming.

Materials and methods

Primary sample processing

MM patient samples and normal age-matched control bone marrow (BM) samples were obtained from consenting patients in accordance with Institutional Review Board approved protocols at University of California-San Diego (UCSD). Peripheral blood (PB) or BM samples were processed by Ficoll density centrifugation in a SepMate conical tube (StemCell Technologies). Viable total mononuclear cells (TMNC) were collected for further analyses and stored in liquid nitrogen. Purified plasma cell leukemia samples were a kind gift by Dr. Mark Minden, University of Toronto.

Cell lines and culture conditions

NCI-H929 cells (ATCC) were grown in RMPI-1640 Glutamax medium (Life Technologies) supplemented with 10% FBS and 0.05 mM β-mercaptoethanol. OPM2 and U266 (from Dr.C.Carlo Stella, University of Milano, Italy) cells were maintained in complete RPMI-1640 medium supplemented with 10% V/V FBS, 2mM L-glutamine, 100U/mL penicillin and 100µg/mL streptomycin. Human bone-marrow derived stromal cell line HS5 (from Dr. E. Ferrero, University of Milan) and murine stromal cell line NIH3T3 (ATCC) were grown in DMEM medium supplemented with 10% V/V FBS, 2mM L-glutamine, 100U/mL penicillin and 100µg/mL streptomycin.

All cell lines were maintained in T-25 or T-75 culture flasks and were cultured at dilutions of 1:3-1:6 every 2-4 days.

To generate lenalidomide-resistant NCI-H929 cells, cells were treated twice a week with fresh lenalidomide (AvaChem Scientific) at a final concentration of 1µM. Lenalidomide-treated and vehicle-treated control cells were sub-cultured for up to 10 weeks at the optimal concentration of $5x10^5$ cells/mL (log phase). Once the proliferation of cells was no longer inhibited by lenalidomide at 1 µM (10 weeks), as determined by Trypan

Blue viability, lenalidomide treatment was scaled up to 10 μM, as previously described.

In IL-6 exogenous stimulation experiments, NCI-H929 wild type cells were plated at $0.3x10^6$ cells/ml, then IL-6 (R&D Systems) was added to the complete growth media at 0-5-10-20ng/ml. Cells were collected for further analysis after 24h/48h of incubation.

In order to discriminate stromal cells from OPM2 and U266 cells in co-culture experiments, HS5 cells were transduced with a GFP-expressing lentiviral vector. GFP+ HS5 were selected by puromycin and maintained in cultured as described for parental cell line.

Nucleic acid isolation, reverse transcription and quantitativePCR

Cell lines (0.5-2 x 10^6 cells) or primary purified TMNCs (50-$10x10^4$ cells) were harvested in lysis buffer (Qiagen). RNA was purified using RNeasy extraction kits with a DNase (Qiagen) incubation step to digest any trace genomic DNA present. For RNA extraction from cell line lysates, samples were extracted using RNeasy mini columns, and for primary cells, samples were lysed and extracted using RNeasy micro columns. Immediately prior to reverse transcription of RNA samples, nucleic acid concentrations were quantified on a NanoDrop 2000 spectrophotometer (Thermo Scientific).For standard qPCR analysis of relative mRNA expression levels, cDNA was synthesized using 50 ng - 1 μg of template RNA in 20-40 μL reaction volumes using the First-Strand SuperScript III Reverse Transcriptase Supermix (Life Technologies) followed by incubation with RNase H according to the manufacturer's protocol. All cDNA products were stored at -20°C.

Primers were synthesized by ValueGene (San Diego, CA) and diluted to 10 μM working dilutions in DNase/RNase-free water. qPCR was performed in duplicate using cDNA (1-2 μL reverse transcription product per reaction) on an iCycler (Bio-Rad) using SYBR GreenER Super Mix (Life Technologies)

in 25-μL volume reactions containing 0.2 μM of each forward and reverse primer. Cycling conditions were as follows: 50°C for 2 minutes, then 95°C for 8 minutes and 30 seconds, followed by 40 cycles of 95°C for 15 seconds and 60°C for 60 seconds. Melting curve analysis was performed on each plate according to the manufacturer's instructions. For standard qPCR, HPRT mRNA transcript levels were used to normalize Ct values obtained for each gene, and relative expression levels were calculated using the 2^{-ddCt} method. To ensure validity of results, only Ct values <35 were used in gene expression analyses. All primer sets were tested in a no-template control (NTC) reaction containing only water instead of cDNA, and all gave Ct values >35 in NTC reactions. For all experiments, assays were repeated at least three times using separate RNA extracts and cDNA preparations.

RESSqPCR

RESSq-PCR assay primer design was carried out for specific cancer and stem cell-associated loci. For this assays, allele-specific primers were designed using Primer1, generating two outer and two inner primers for each editing site with melting temperatures ranging from 60-68°C. The forward (FW) outer and reverse (REV) outer primers flank the editing site and can be used for Sanger sequencing validation of each editing site, and also as a qPCR positive control to ensure that the editing region is detectable in cDNA. The 3' ends of the FW inner and REV inner primers match either the WT A or edited G nucleotide, and include an additional mismatch two nucleotides upstream of the 3' primer end to enhance allelic discrimination. All RESSq-PCR primer sequences (outer, WT, edit) are provided in the following Primers table. RESSq-PCR was performed in duplicate using cDNA (1-5 μL reverse transcription product per reaction) on an iCycler (Bio-Rad) using SYBR GreenER Super Mix (Life Technologies)

in 25-μL volume reactions containing 0.2 μM of each forward and reverse primer. Cycling conditions were the same as for standard qPCR. Relative RNA editing rates (Relative Edit/WT RNA) were calculated using the following calculation: $2^{-(Ct\ \text{Edit} - Ct\ \text{WT})}$.

High-fidelity PCR and Sanger sequencing analysis

For PCR and targeted Sanger sequencing analysis, 1-2 μL of first-strand cDNA templates were prepared for PCR in 25-50 μL reaction volumes using the high-fidelity KOD Hot Start DNA Polymerase kit according to the manufacturer's instructions (EMD Millipore). "Outer" primers used for sequencing produce predicted amplicons of approximately 150-250 nucleotides in length, and flank each editing site with approximately 50-100 bp on either side of the editing site to facilitate successful sequencing analysis. PCR cycling conditions were as follows: 95°C for 2 minutes, followed by 35 cycles of 95°C for 20 seconds, 62°C for 10 seconds and 70°C for 10 seconds, with a final extension step of 70°C for 30 seconds. Production of amplicons of the predicted size was verified for each outer primer set by DNA gel electrophoresis using 10-20 μL of the reaction mixture separated on 2% agarose gels containing ethidium bromide and visualized under UV light. Then, 15 μL of each reaction was processed within 24 hrs for PCR purification and Sanger sequencing was performed on ABI 3730xl DNA Sequencers (Eton Bioscience, San Diego, CA). Sanger sequencing was carried out using the reverse outer primer used for PCR amplification, so edited loci are identified in the reverse complementary sequence as T/C nucleotides, except in cases where the gene products are transcribed from the reverse strand (e.g. AZIN1). Sequence chromatograms were analyzed using Chromas and peak heights calculated using ImageJ. For RNA editing analysis of sequencing chromatograms,

ratios of edited/WT peaks were calculated using the raw peak amplitude of each sequence trace.

Primers table:

Gene	Forward primer 5'>3'	Reverse primer 5'>3'
ADAR1 **(total)**	TGCTGCTGAATTCAAGTTGG	TCGTTCTCCCCAATCAAGAC
ADAR1 **(p150)**	AACGAAAGCGAAATTGAACC	GGGTGTAGTATCCGCTGAGG
ADAR1 **(p110)**	GACTGAAGGTAGAGAAGGCTACG	TGCACTTCCTCGGGACAC
ADAR2	TGTTCCGTGTGTGTCCAGTT	CGGCAGGTCAGAGTTTTCTC
HPRT1	TCAGGGATTTGAATCATGTTTGTG	CGATGTCAATAGGACTCCAGATG
IRF4	GACATCTCAGACCCGTACAAAG	GAAGGGTAAGGCGTTGTCAT
APOBEC3D **wild type**	GTCCAGGCTGGAATGCAATGTCA	GAGGCTGAAGCAGAAGAATCGCTTAAAC
APOBEC3D **edit**	CTCTGGGATCTCTCTGCCTCCAAATATC	GAGGTTGCAGTGAGTCCAGATGGC
GLI1 **wild type**	GGGGAGGACAGAACTTTGATCCTTACCT	CTGGCTCTTCCTGTAGCCCGCT
GLI1 **edit**	ACTGAGAATGCTGCCATGGATGATG	AAGTCCATATAGGGGTTCAGACCACTGC
AZIN1 **wild type**	CATTCAGCTCAGGAAGAAGACATCT	AATACAAGGAAGATGAGCCTCTGTTTAC
AZIN1 **edit**	ACTGAATGACATCATGTAATAAATGGCT	GAGCTTGATCAAATTGTGGCAG
MDM2 **wild type**	ATAGGACTGAGGTAATTCTGCACAGCA	ATAATGCTTGGAGGACCTCCACATGT
MDM2 **edit**	CTCTGGGATCTCTCTGCCTCCAAATATC	AAGAGATTCTGCTTGGTTGTAGCTGAAG
IL-6	TTCAATGAGGAGACTTGCCTGGTGA	TCTGCACAGCTCTGGCTTGGTTCC
HES1	GATGCTCTGAAGAAAGATAGCTCG	GTGCGCACCTCGGTATTAAC
JAGGED1	TTCGCCTGGCCGAGGTCCTAT	GCCCGTGTTCTGCTTCAGCGT
JAGGED2	CCGGCCCCGCAACGACTTTT	CCTCCCTTGCCAGCCGTAGC

Western blot

A total of 5-10x10^6 cells were harvested in RIPA buffer for total protein extraction. After cell lysis, samples were centrifuged to clear insoluble material. Protein concentrations were determined using a detergent-compatible Bradford assay (Bio-Rad). 20 μg of each sample were loaded onto precast polyacrylamide gels for gel electrophoresis at 100 V. Proteins were transferred to 0.45 μm PVDF membranes at 400 mA for 1 hr. Membranes were blocked for 1 hr at room temperature in 5% nonfat milk in Tris-buffered saline (TBS) containing 0.5% Tween-20 (TBS-T). Primary antibodies (rabbit anti-ADAR1, 1:2500, Abcam; and chicken anti-actin, 1:1000, Abcam) were prepared in 5% bovine serum albumin (BSA) in TBS-T. Membranes were incubated overnight at 4°C with primary antibodies, followed by three 10-minute washes in TBS-T, and secondary antibody incubation (anti-rabbit HRP, 1:5000, Cell Signaling Technology; and anti-chicken HRP, 1:5000, Abcam) in 5% nonfat milk in TBS-T for 1 hr at room temperature. Blots were developed using enhanced chemiluminescence (Femto Detection kit, Promega) on a Chemidoc digital imaging machine.

Flow cytometry analysis

Flow cytometry assays were performed using a BD LSRFortessa Cell Analyzer, BD FACSVerse™ System (BD Biosciences) and MACSQuant (Miltenyi). Data were analyzed using FlowJo (Treestar Inc.) software. For CD138 surface expression on MM cell lines, 1-0.5x10^6 cells were stained with anti-human CD138 APC antibody (BD Biosciences) in PBS+2%FBS+2mM EDTA, while DAPI (1:5000 in PBS) was used for live/dead cell discrimination. For intracellular IL-6 staining, cells were fixed in 4% formaldehyde, permeabilized in 0.5% saponin and stained with anti-human IL-6 APC antibody (eBioscience) or isotype matched control. Single cells derived from mouse tissues were stained with LIVE/DEAD fixable near-IR viability dye (Thermofisher) at 1:1000 in PBS. Samples were then washed and non-specific Fc receptor-mediated antibody binding was blocked by incubation with mouse and human FcR blocking reagent (BD Biosciences). Then samples were stained with anti-human CD138-APC (Miltenyi), CD319-PE (Miltenyi), CD38 PECy7 (BD Biosciences) and CD45 Brilliant Violet 450 (BD Biosciences). All staining were performed at 4℃ in dark. Lastly, samples were washed and fixed with 1% PFA for 10 minutes at 4℃, then acquired by MACSQuant (Miltenyi).

Colony assay formation assay

Lenalidomide treatment was withdrawn from culture for 5-7 days prior colony assay as described[57]. A total of 500 wild type or drug-resistant NCI-H929 cells were plated in methylcellulose (Miltenyi) in 6-well plates. Colonies (more than 40 cells) were scored after 14 days and serial replating assays were performed for an additional 14 days in culture. RT-qPCR on replated cells was performed on RNA extracted from 10 colonies of the same type (fast/slow).

RNA interference

Specific knock-down of Notch ligands Jagged1 and Jagged2 was achieved by transient Stealth Select RNAiTM siRNA expression (Life Technologies). SiRNA sequences were designed according to the Manufacturer's guidelines. HMCLs were plated at $3,5x10^5$ cells/ml, then after 24h Jagged1 and Jagged2 gene expression was simultaneously silenced by shRNA transfection; scrambled shRNAs were used as negative control. Optimal silencing was achieve at 96h (cell were re-transfected at 48h from plating).

Intrahepatic inoculation of tumor cells and tissues collection

New born (1-3 days) Balb/c Rag2-/-γc-/- mice were intrahepatically injected with a 30 gauge Hamilton syringe (Hamilton Company). Each animal received $1\text{-}2x10^6$ TMNCs isolated from primary samples. Animals were weaned at 3 week of age and monitored regularly by heath status assessment; IVIS imaging and peripheral blood screening were regularly performed until signs of disease were observed, including significant loss of weight, limited mobility and presence of palpable tumors. Mice were euthanized by CO_2 inhalation. PB was collected by cardiac puncture immediately after sacrifice. Bones, spleen (SP), liver (LI) and tumors (TU) were collected in ice cold PBS. Bones were flushed in order to isolate BM, while SP and LI were manually dissociated in order to obtain a single cell suspension. TUs were either manually dissociated and incubated with collagenase IV (Sigma), or processed with a Tumor Dissociation kit (Miltenyi) according to the Manufacturer's guidelines.

Transduction of primary PCL-derived TMNC

Prior to transplant TMNCs were transduced with a lentiviral GFP-luciferase (GLF) encoding vector at 100 Multiplicity of Infection (MOI). Cells were plated in U-bottom 96-well plate and incubated with GFL lentivirus for 48h in StemPro complete media (ThermoFisher).

In vivo bioluminescence imaging

Mice were i.p. injected with luciferin (1.5mg/mouse, Caliper Life Science) and anesthetized using isofluorane. Mice were imaged 6-8 minutes after i.p. injection and images were acquired after 1-5 minutes of exposure by Xenogen IVIS-200 (PerkinElmer).

Measurement of serum immunoglobulin light chain levels

Peripheral blood was collected from each mouse by retro-orbital bleeding while animals were anesthetized with isofluorane. 10-50ul of serum were used in enzyme linked immunosorbent assay (Human lambda or kappa ELISA kits, Bethyl Laboratoris Inc.) The assay was carried out according to Manufacturer's guidelines.

Statistical analysis

Data are represented as mean ± SEM of independent experiments performed in duplicates or triplicates. Two-tailed Student's t-test or 1-way ANOVA tests were used to compare the means of normally distributed values.

Results

1. Analysis of ADAR1 expression in MM

1.1 *In silico* correlation of ADAR1 expression with 1q21 copy number alterations

Previous reports in newly-diagnosed MM patients showed that 20-30% of cases harbor copy number amplification at chromosome 1q21, which is associated with more proliferative disease and poor-risk cytogenetic categories. This genomic region includes the CKS1B gene locus, which is located directly adjacent to the ADAR1 gene locus on chromosome 1q21.

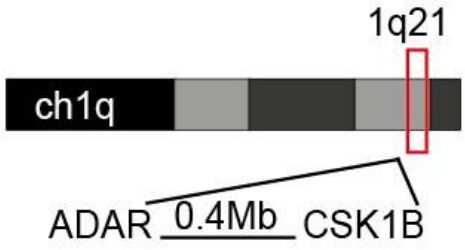

Figure 3.1: Schematic representation of ADAR1 locus on chromosome 1q21 and distance from prognostic factor CKS1B location.

In order to investigate whether ADAR1 gene expression was correlated with 1q21 amplification status, we performed *in silico* analysis of an ADAR1 gene expression dataset from the Multiple Myeloma Genomics Initiative (MMGI) database [27],[149].

We analyzed expression and array comparative genomic hybridization (aCGH) data on CD138-enriched cells derived from a well-characterized cohort of patient samples.

Our analysis revealed an interesting finding: as displayed in Fig.1.2, ADAR1 gene expression levels were increased in primary patient samples corresponding with copy number amplification of the 1q21 locus. Indeed, ADAR1 relative expression was significantly higher in patients with more

than 4 copies of the 1q21 locus compared to normal controls. This was the first evidence that the poorer prognosis associated with 1q21 amplification may be linked to aberrant ADAR1 expression and/or activity.

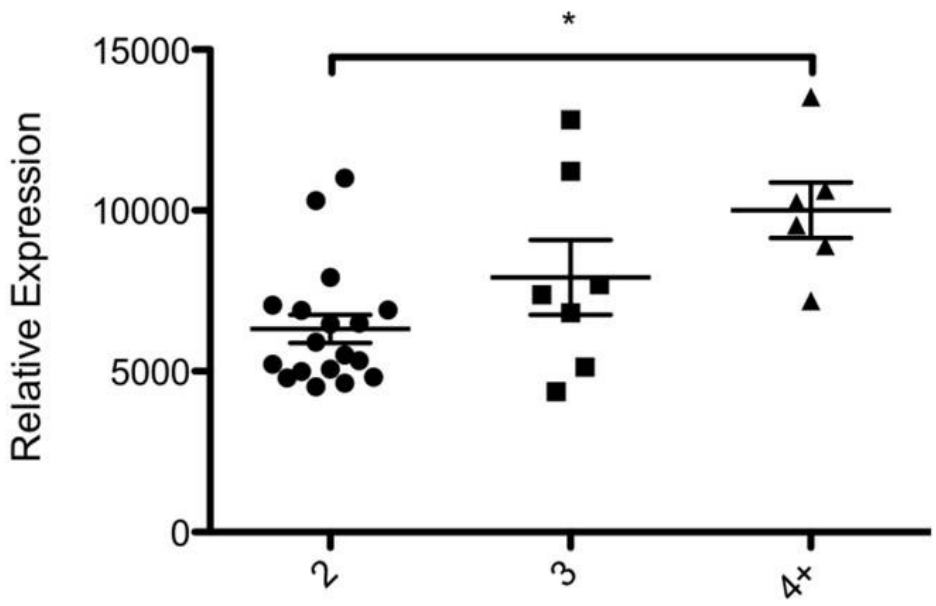

Figure 1.2: ADAR1 expression correlates with CKS1B score. Microarray datasets publicly available through the Multiple Myeloma Genomics Initiative were analyzed in this study. ADAR1 relative expression correlates with copy number amplification of 1q21 CKS1B locus (on the x axis as 2, 3 or >4+ copies) which correlates with poor prognosis; *$p<0.05$ by unpaired, two-tailed Student's t-test.

1.2 Validation of ADAR1 expression in primary MM patient samples

To confirm our findings in a separate set of primary patient samples, we investigated ADAR1 expression in total mononuclear cells (TMNCs) isolated from a collection of primary MM samples (n=11). Patients' disease stage and clinical annotations are shown in Table1. In order to evaluate how ADAR1 expression was modulated in different disease stages, we collected samples from smoldering MM, newly diagnosed, relapsed BM MM and extramedullary PCLs. TMNCs from aged-matched (mean age=60,6 /-16,8 years old) BM (n=3) collected from patients undergoing hip replacement therapy for reasons other than cancer were used as normal healthy controls.

Sample	Age	Gender	Tissue	Diagnosis	Therapy	Light chain	FISH
M1	64	M	BM	Smoldering MM	Untreated	Lambda	Gain ch.5
M2	49	F	BM	Smoldering MM	Untreated	Lambda	Monosomy ch.13; gain ch.5; t(14;16)
M3	77	M	BM	MM newly diagnosed	Supportive care	Kappa	Monosomy ch.13; del17p, t(11;14)
M4	65	M	BM	MM newly diagnosed	Untreated	Lambda	Gain ch.5 ; del17p
M5	71	M	BM	MM	Carfilzomib+DEX	Lambda	Loss 4p16, 17p; gain 5q, 11q, 14q
M6	47	M	BM	MM	CyVD	Kappa	Loss 14q
M7	54	F	BM	MM relapsed	DEX**	Kappa	trisomy ch7 and 9
M8	71	M	BM	MM relapsed	RVD*	Kappa	Normal
M9	70	M	PB	PCL	Untreated-early death	Kappa	NA
M10	73	M	PB	PCL	Supportive care	Lambda	NA
M11	58	F	PB	PCL	Unknown-lost follow up	Kappa	NA

Table 1: Clinical information on primary samples used in this study. Diagnosis was confirmed at the time of the biopsy. DEX, dexamethasone; CyVD, cyclophosphamide-lenalidomide-dexamethasone; RVD, lenalidomide-bortezomib-dexamethasone. *=2 years off therapy at the time of biopsy; **=started dexamethasone, previously on lenalidomide, bortezomib and thalidomide.

As shown in Fig.1.3. MM patients expressed significantly higher levels of ADAR1 compared to age-matched normal controls. In particular, ADAR1 expression was consistently higher in PCL samples while newly diagnosed and relapsed MM samples had variable expression levels. Interestingly, smoldering MM patients had similar ADAR1 expression levels compared to normal controls, suggesting that ADAR1 overexpression may be a later event related to disease progression or emergence of drug-resistance.

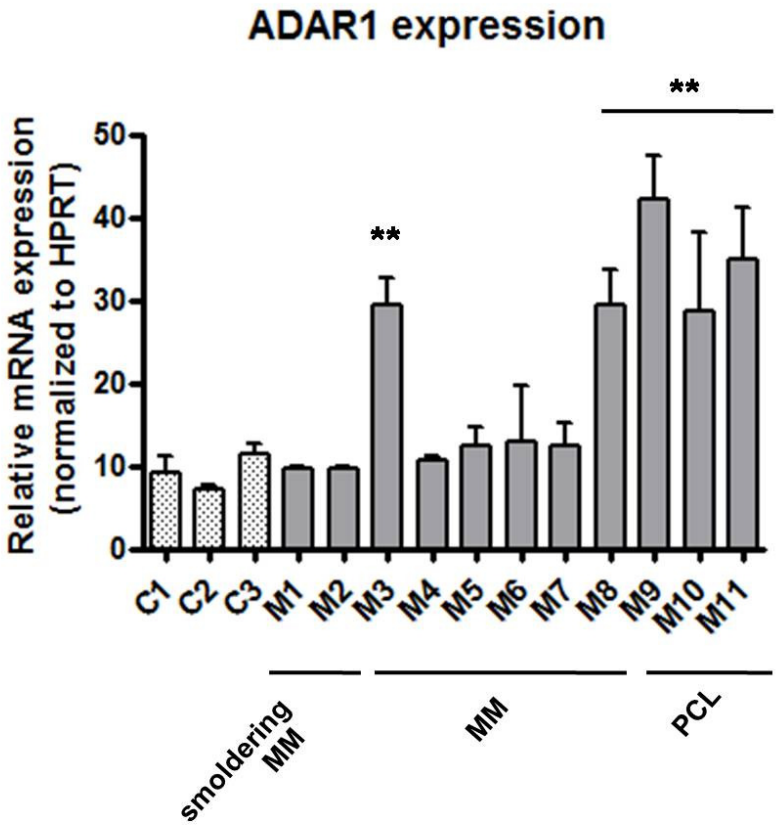

Figure 1.3: ADAR1 expression in primary MM and PCL patient samples. Histograms represent relative ADAR1 mRNA levels assessed in freshly isolated/biobanked TMNC from primary samples (M1-M11) compared to normal controls (C1-C3) of at least three independent qPCR experiments. HPRT gene expression was used as normalization factor. **p<0.01 compared to normal controls by unpaired two-tailed Student's t-test.

As anticipated, ADAR1 exists in two isoforms, the constitutively expressed p110 and the inflammation responsive p150. Considering the central role of pro-inflammatory signals in MM BM, we performed quantitative PCR to measure the relative expression of ADAR1 isoforms.

Among the patients analyzed, expression of ADAR1 isoforms was heterogeneous (Fig.1.4); notably most patients overexpressed both isoforms (M3, M6, M9, M11), compared to healthy controls, thus suggesting that transcriptional activation possibly related to amplification at the 1q21 locus along with microenvironmental inflammatory signals may affect ADAR1 expression in MM.

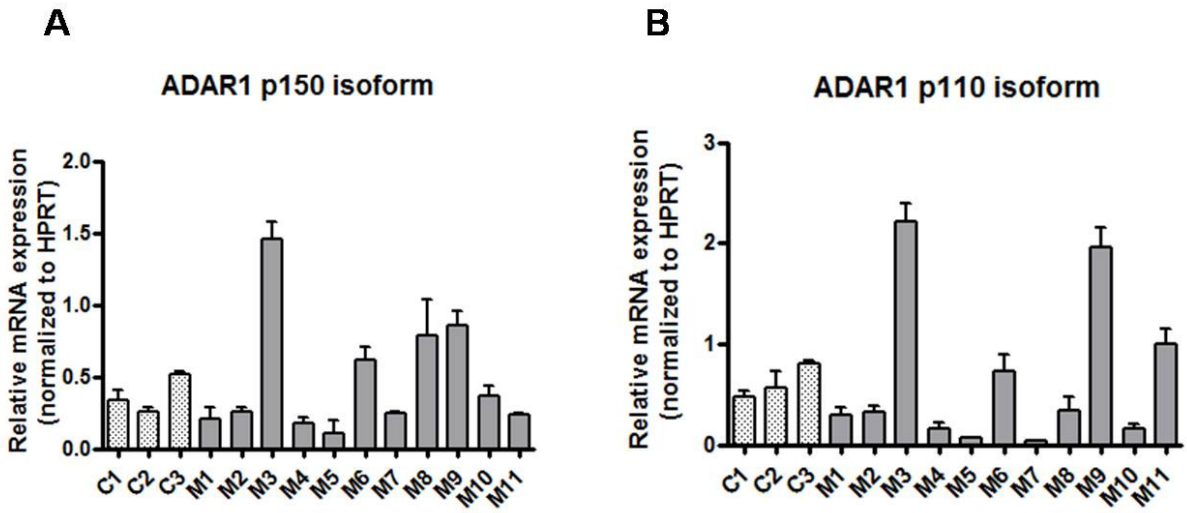

Figure 1.4: Isoform-specificADAR1 expression analysis in primary MM and PCL patients. Histograms represent relative ADAR1 inflammation-responsive p150 (A) and constitutively-expressed p110 (B) mRNA levels in MM and PCL TMNCs compared to HPRT mRNA levels in at least three qPCR experiments.

1.3 Detection of aberrant RNA editing by RESSqPCR

RNA editing is usually detected by traditional Sanger sequencing or by whole-transcriptome sequencing. Both techniques have significant pitfalls: Sanger sequencing is generally affordable but is not sufficiently sensitive to detect rare editing events (rare transcripts *per se* or normally abundant transcripts in rare cell populations), while transcriptome-wide profiling is costly, technically challenging and requires expertise in specialized bioinformatics methods. To overcome a lack of cost-effective, quantitative methods to detect endogenous RNA editing activity, we developed a novel assay, named **R**NA **e**diting **s**ite **s**pecific **q**uantitative real time **PCR** (RESSqPCR), specifically designed to detect RNA editing even in rare transcripts/ rare cell populations[150].

Considering our finding that ADAR1 expression was increased in primary plasma cell neoplasm samples at advanced stages of disease, we sought to determine whether we could detect increased ADAR1 activity in primary MM samples. Therefore, we measured RNA editing in four specific cancer stem cell-associated transcripts: APOBEC3D, GLI1, AZIN1 and MDM2. These transcripts were previously identified by whole-transcriptome sequencing and showed to be more edited in response to increased ADAR1-dependent A-to-I editing during malignant reprogramming and disease progression in chronic myeloid leukemia (CML)[148]

Consistent with increased mRNA levels, MM patients displayed significantly higher levels of edited transcripts compared to age-matched controls (Fig.1.5). Among the four targets, editing rates in APOBEC3D and GLI1 were notably higher than controls, and similar to ADAR1 expression levels, tended to be higher in more advanced stages of disease. Indeed, 100% of patients showed high levels of editing in APOBEC3D mRNA, while 54% (6/11) showed increased editing of GLI1 mRNA. AZIN1 and MDM2 transcripts editing rates were more variable among samples.

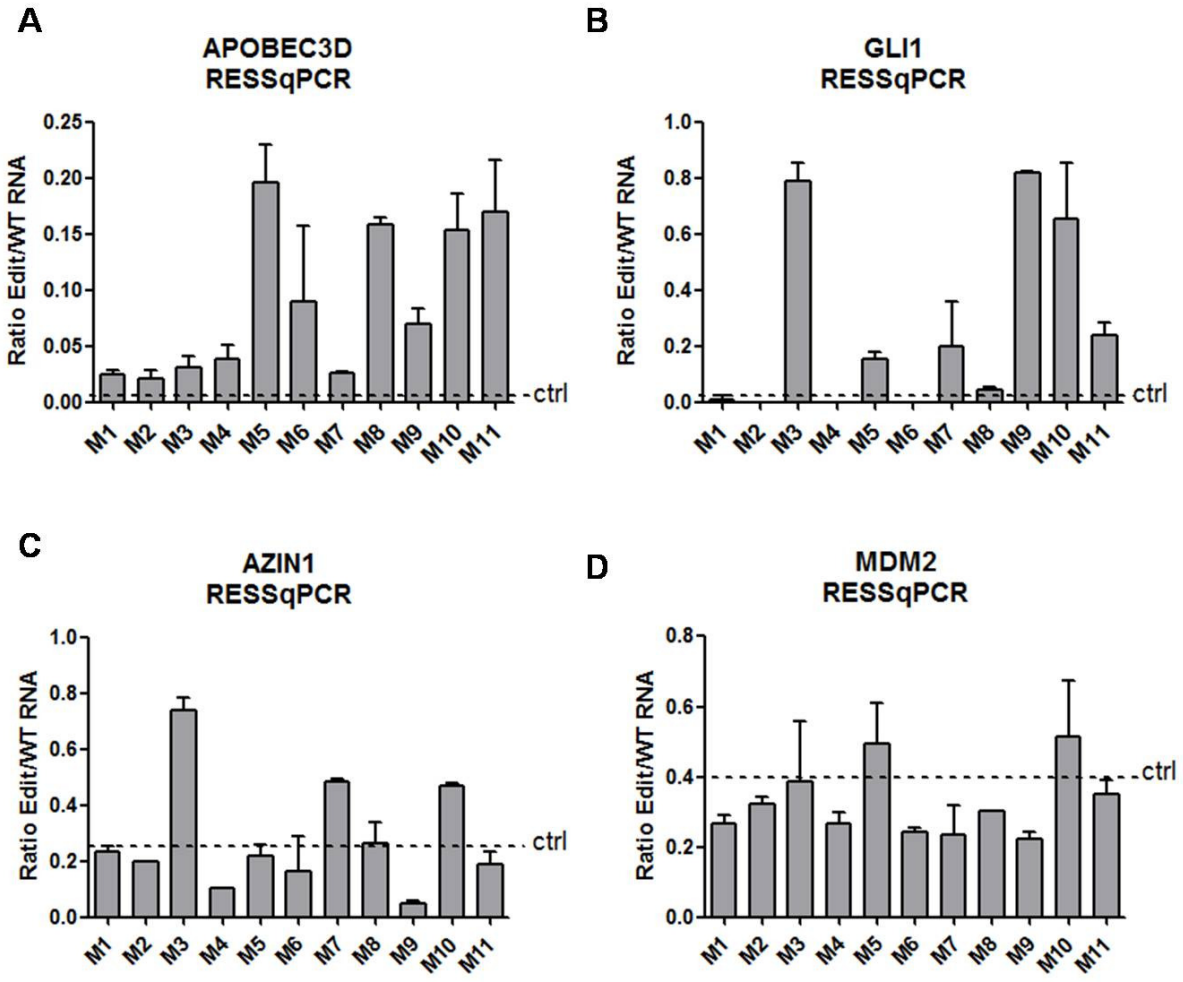

Figure 1.5: RESSqPCR analysis showed increased APOBEC3D AND GLI1 RNA editing in MM and PCL TMNCs. Horizontal dashed lines represent comparative average RNA editing activity normal TMNCs. RESSqPCR analysis was carried out to evaluate relative expression of RNA-edited (G/I) and wild-type transcripts of APOBEC3D (A) GLI1 (B), AZIN1 (C) and MDM2 (D).

We confirmed aberrant RNA editing by Sanger sequencing in the highest ADAR1-expressing PCL samples. Consistent with RESSqPCR results, we detected a double peak in APOBEC3D and GLI1 chromatograms, A/G in GLI1 (editing site on the sense strand) and T/C in APOBEC3D (cDNA antisense strand). Notably, peak height quantification correlated with RESSqPCR ratios of wild-type/edited RNA.

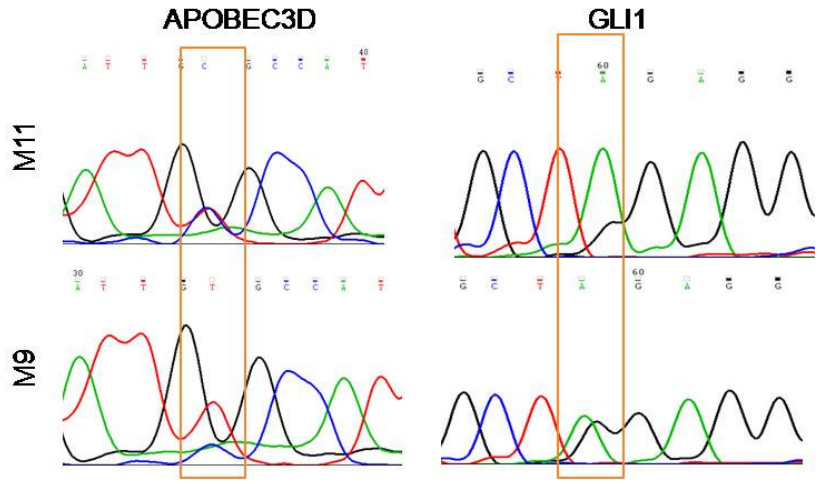

Figure 1.6: Representative chromatograms from Sanger sequencing analysis in high-ADAR1 samples. High-fidelity PCR products were amplified with primers flanking the APOBEC3D or GLI1 editing site and sequenced using a reverse primer (APOBEC3D) or a forward primer (GLI1). Chromatograms shows a dual C (=G in sense strand)/T peak in APOBEC3D cDNA (A) and a dual G/A peak in GLI1 (B).

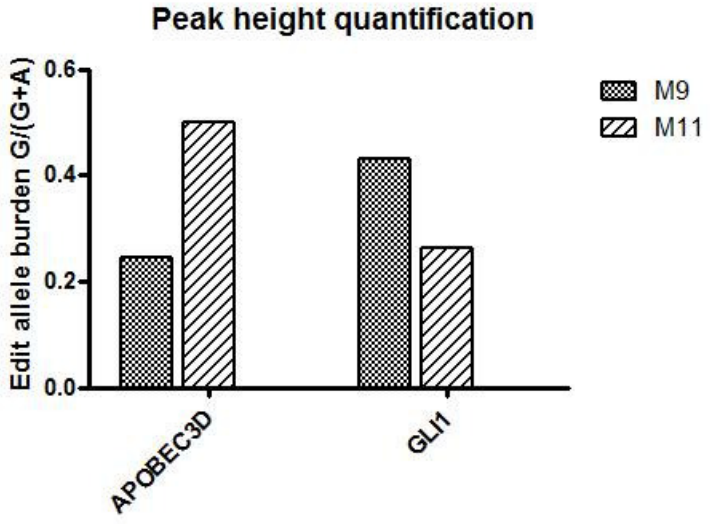

Figure1.7: Quantification of peak height ratios in M9 and M11 PCL samples. Peak height ratios of edit (C/G) versus wild-type (T/A) nucleotides calculated using ImageJ.

2. Continuous IMiD exposure induces ADAR1 expression and activity

Among therapies available for MM, IMiDs are first line treatments used alone or in combination with other agents for relapsed and refractory MM and they have been recently approved for newly diagnosed patients. The ability of this class of drugs to modulate the immune system and pro-inflammatory signaling is dual: for example lenalidomide can downregulate TNFα production in monocytes while induce IFNγ secretion in T cells [47],[49].

We hypothesized that exposure to IMiDs could have cell-intrinsic effects on inflammation-responsive genes such as ADAR1. Therefore, we investigated whether prolonged lenalidomide exposure could directly affect the expression and activity of ADAR1, promoting transcriptome “reprogramming” of tumor cells. In this context, we speculated that aberrant RNA editing could promote tumor cell survival and/or the emergence of drug-resistant malignant clones. Moreover, the combination of a pro-inflammatory BM niche, together with IMiD treatment, could exacerbate the disease, especially in high risk patients harboring copy number amplifications of the ADAR1 gene locus.

2.1 Long-term lenalidomide increases ADAR1 mRNA and protein levels in H929 cells

In order to model the effects of prolonged immunomodulatory therapies in patients, we derived a lenalidomide-resistant NCI-H929 myeloma cell line. Cells were continuously exposed to low dose lenalidomide (1μM) until cell growth was no longer inhibited (data not shown). Then the treatment dose was increased to 10μM in order to develop fully resistant cells [57]. We evaluated total ADAR1 expression and expression ofp150 and p110 isoforms expression by qPCR periodically throughout generation of the drug-resistant cell line.

Prolonged lenalidomide induced a significant increase in ADAR1 expression. Notably, the inflammation-isoform p150 was significantly upregulated in treated cells compared to controls. Continuous lenalidomide treatment selectively affected ADAR1 expression, while ADAR2 levels were not altered (Fig.2.1).

To confirm the efficacy of lenalidomide treatment we assessed the mRNA levels of interferon regulatory factor 4 (IRF4). Consistent with previous reports, long-term lenalidomide exposure induced a downregulation ofIRF4 in treated cells[57]. To determine whether increased ADAR1 mRNA expression coincided with higher protein levels, we investigated ADAR1 protein expression. Western blot analysis revealed that lenalidomide-treated H929 cells showed increased levels of both isoforms p150 and p110 (Fig.2.2), thus suggesting possible drug-dependent mechanism affecting protein stability/degradation of both isoforms.

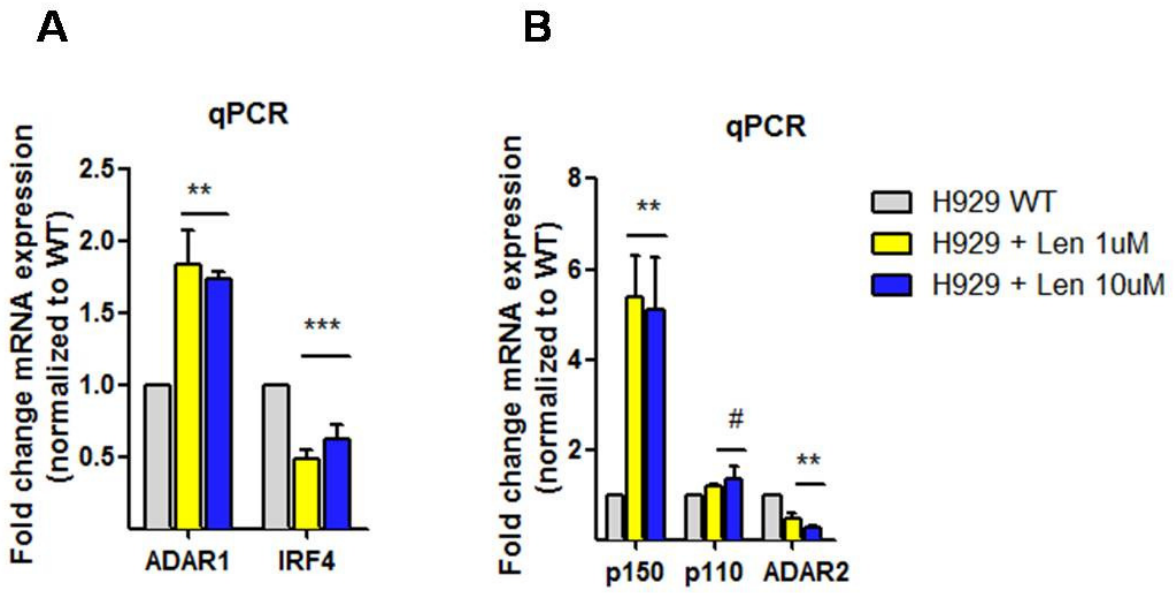

Figure 2.1: qPCR analysis of H929 cells after continuous Lenalidomide (Len) or vehicle (WT) treatment. (A) ADAR1 increased mRNA expression in lenalidomide-treated (1 μM, 5-50 weeks; 10 μM, 5-40 weeks) H929 cells and reduced IRF4 levels in response to treatment. (B) Specific ADAR1 isoform expression and ADAR2 levels in treated H929 versus vehicle (WT).*p<0.05, **p<0.01, # not significant by 1-way ANOVA test.

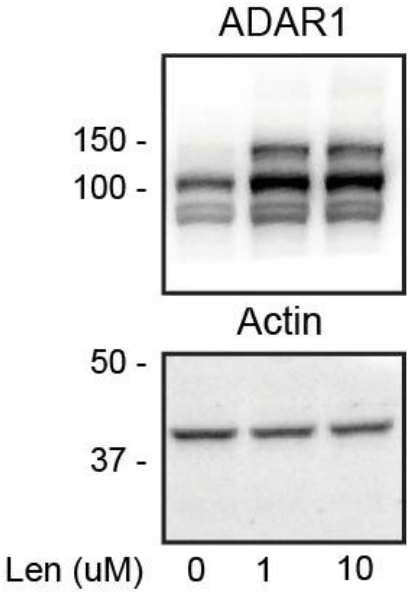

Figure 2.2: Increased protein levels of ADAR1 in H929 after continuous lenalidomide treatment by Western blot analysis. Upper blot: anti-ADAR1 antibody reveals two bands at 150kDa and 110kDa corresponding to isoforms p150 and p110 in lenalidomide-treated cells (1 μM Len, 20 weeks; 10 μM Len, 10 weeks). Bottom blot: anti-actin antibody for normalization.

2.2 Lenalidomide induces aberrant RNA editing in H929 cells

Consistent with increased levels of mRNA and protein, cells expressing high ADAR1 levels showed increased RNA editing by RESSqPCR (Fig.2.3) and Sanger sequencing (Fig.2.4). All four transcripts, APOBEC3D, GLI1, AZIN1 and MDM2 displayed a higher edited/WT ratio in lenalidomide-resistant cells.

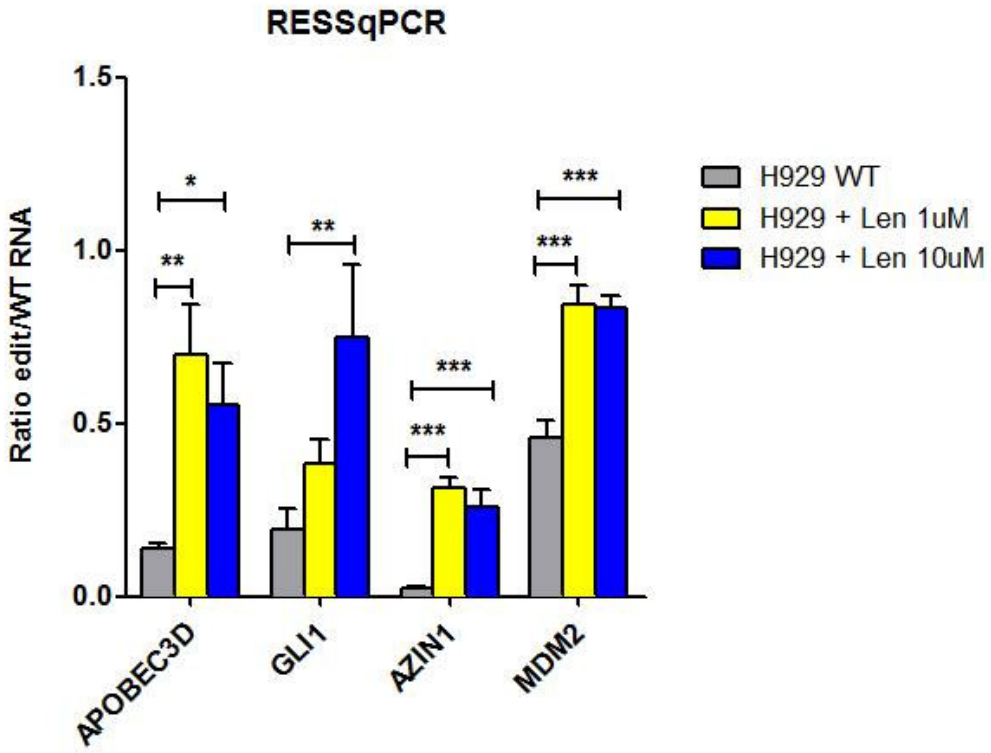

Figure 2.3 Aberrant RNA editing after continuous Len treatment. cDNA derived from lenalidomide-treated cells (1 μM, 5-50 weeks, n=8; 10 μM, 5-40 weeks, n=6) compared with H929 WT at paired passages (n=8) was analyzed by RESSqPCR. *p<0.05, **p<0.01, ***p<0.001 by one-way ANOVA and Dunnett's post test.

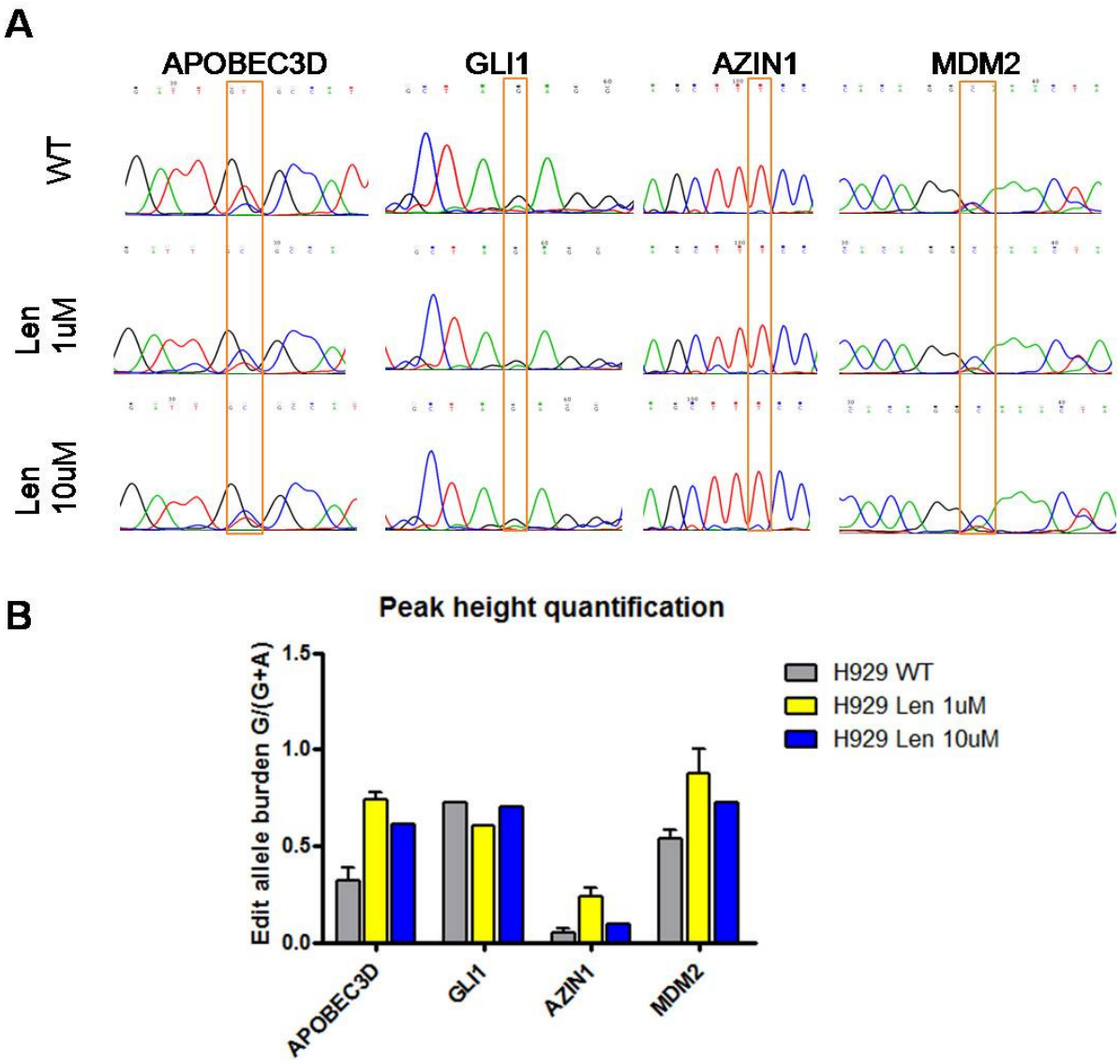

Figure 2.4: Validation of aberrant RNA editing by Sanger sequencing. (A) Representative chromatograms from Sanger sequencing analysis in Len-treated or WT H929. (B) Edit allele burden was measured by peak height quantification as edited/edited+WT.

2.3 ADAR1-overexpressing cells show increased self renewal capacity

To assess the functional effects of lenalidomide-associated aberrant ADAR1 activity, we determined H929 self-renewal and proliferation capacity by colony formation assay. After withdrawal (3-5 days) from IMiD treatment, the low-dose (1 μM) lenalidomide-resistant cell lines formed a significantly higher number of colonies compared to control cells (Fig.2.5).

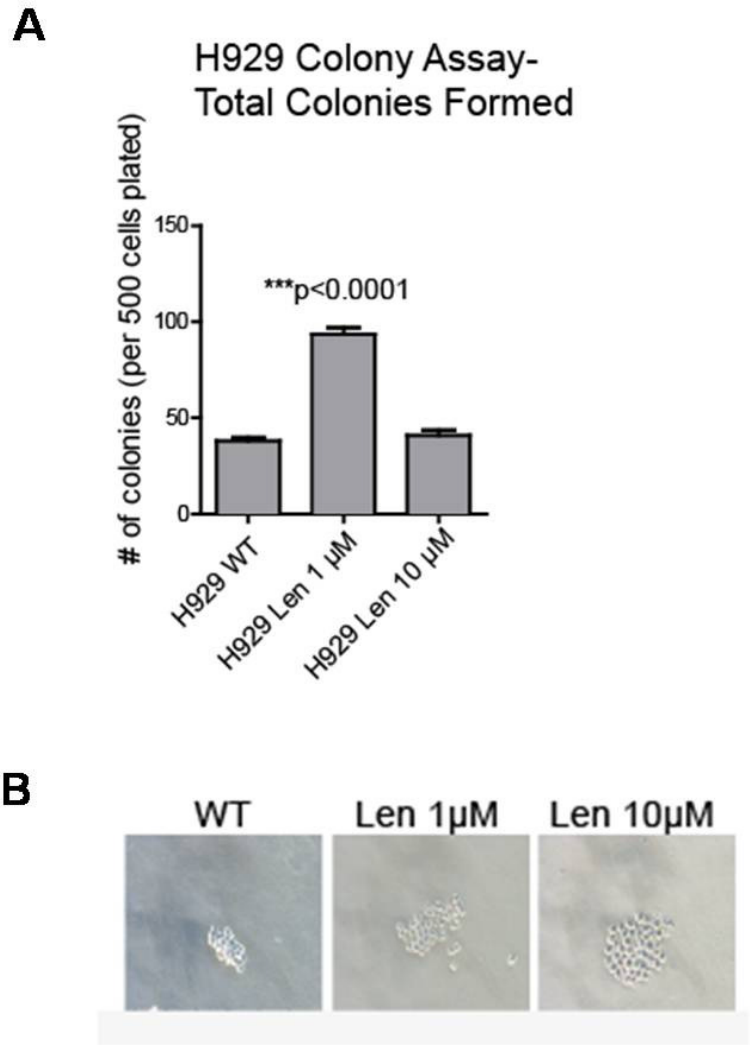

Figure 2.5: Increased colony formation potential of lenalidomide resistant H929. (A) The survival capacity of Len-resistant versus WT-H929 was evaluated by methylcellulose colony formation assay; ***p<0.0001 by unpaired two tailed Student's t test. (B) Representative pictures of colonies after 1 week of culture (20X magnification).

Notably, in serial replating assays, both low and high dose lenalidomide-exposed cells displayed increased self-renewal abilities. Moreover, we could discriminate between “fast” growing colonies, visible after 1 week of re-plating, and “slow” colonies that could be counted after 2 weeks (Fig.2.6). When we assessed ADAR1 expression by qPCR in individual colonies from serial replating assays, we consistently observed that “fast” growing colonies had higher ADAR1 mRNA levels compared to “slow” colonies and controls from the parental cell lines.

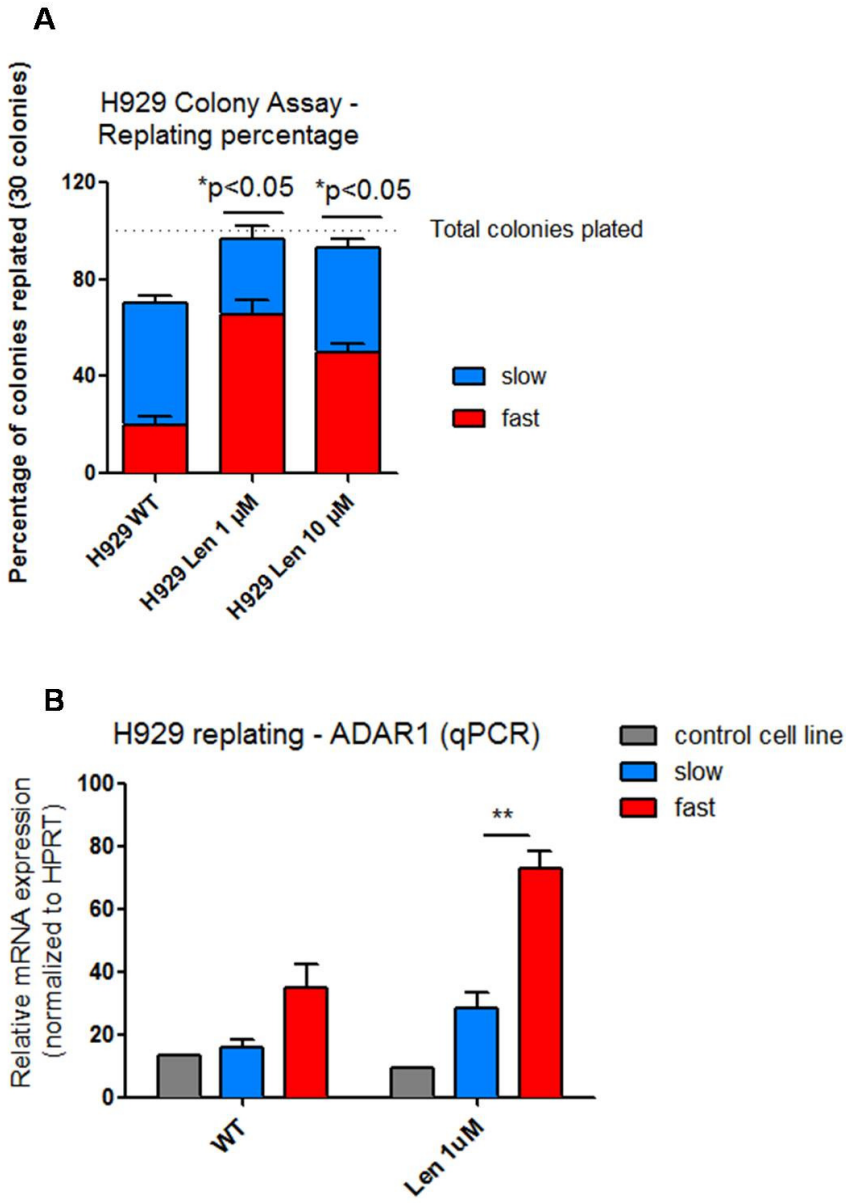

Figure 2.6: Serial replating assay of lenalidomide-resistant H929. (A) Increased replating ability of Len-treated cells was assessed by percentage of replated colonies/colonies plated at day0 (30 colonies). Red represents % of colonies detectable after 1 week of culture, blue represents % colonies grown after 2 weeks. (B) qPCR analysis of ADAR1 expression in "fast" vs "slow" colonies grown after replating in H929 WT or Len 1µM conditions (n=2). Grey columns represent the corresponding mRNA values in parental cell lines. *p<0.05; **p<0.001 by unpaired two tailed Student's t test

2.4 Lenalidomide-resistant cells harbor a CD138dim cancer stem cell-like subpopulation

Therapeutic failure in MM can be caused by several factors, i.e. high risk genetic background, protective microenvironment and drug-resistant dormant cancer stem cells. Cancer stem cells (CSCs) in MM have been a subject of some debate over the last decade, but most of the scientific literature supports the existence of a CSC-like subpopulation bearing a CD138negative/dim immunophenotype[94],[151]. Therefore, to further investigate the stem-like potential of drug-resistant cells, we assessed the cell surface expression of CD138 in H929 WT versus Len-resistant cells by flow cytometry. As shown in Fig.2.7, we observed an increase of CD138dim (stem cells enriched) sub-fraction in cultures exposed to continuous lenalidomide treatment compared to wild type controls.

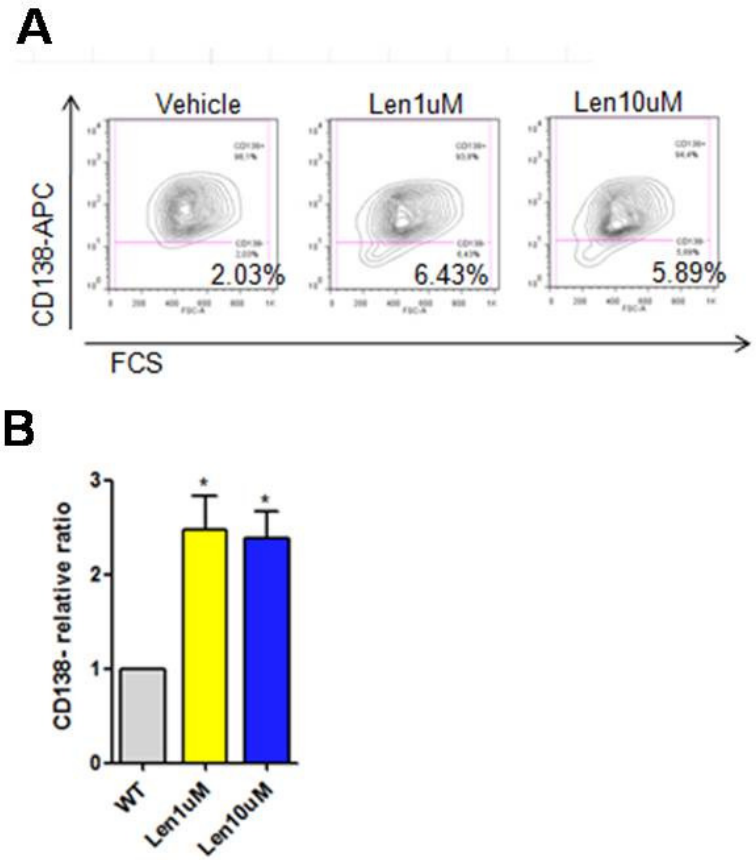

Figure 2.7: Cell surface expression of CD138 after prolonged lenalidomide exposure. (A) Representative density plots of WT or Len-treated H929 displaying a higher fraction of CD138dim subpopulation in Len-H929. (B) Quantification of CD138dim cell percentage from flow cytometry assays. *p<0.05 by unpaired two-tailed Student's t test

3. Bone marrow niche-dependent factors contribute to ADAR1 activation

In the pro-inflammatory microenvironment that characterizes MM BM, tumor cells could be at further risk for deregulated activation of malignant stem cell self-renewal factors such as ADAR1 through cytokine-dependent stimulation, as represented in Figure 3.1.

One fundamental cytokine is MM is IL-6, which promotes cell survival and proliferation and whose levels correlate with disease severity and stage[71],[76],[81],[152]

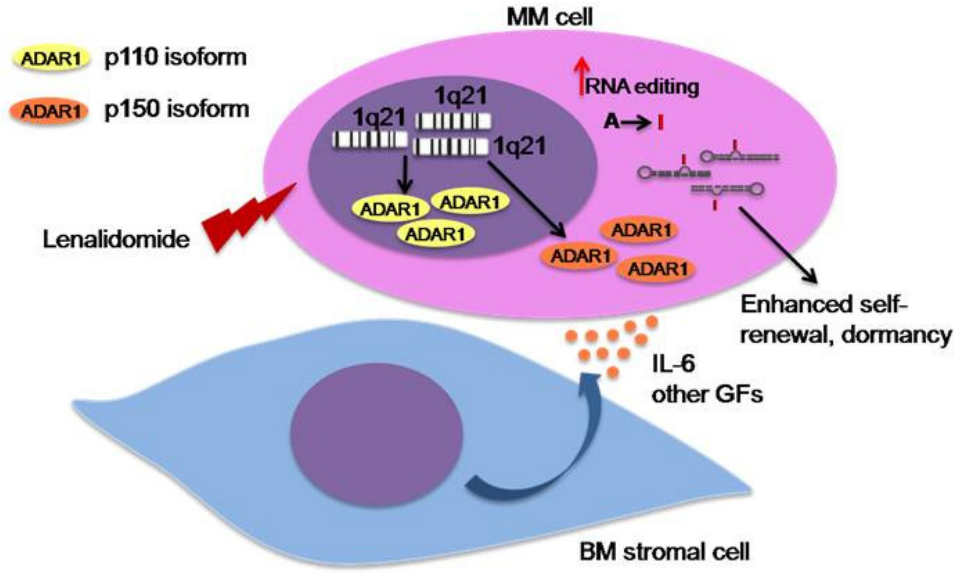

Figure 3.1: Schematic representation of BM-tumor cell interactions triggering ADAR1 expression and activity in MM cells. Patients carrying 1q21 amplification and/or exposed to prolonged immunomodulatory therapies may be at further risk of aberrant transcriptome reprogramming.

3.1 Exogenous IL6 induces ADAR1-dependent RNA editing activity

ADAR1 p150 isoform transcription is under the control of an Interferon Signaling Responsive Element (ISRE) in its promoter. Inflammatory signals, such as IFN or TNFα, trigger a signaling cascade through the JAK/STAT pathway, ultimately culminating in the binding of phosphorylated STAT homo/hetero dimers to ISRE elements, thus promoting downstream target gene transcription. Similarly, IL-6 signaling triggers JAK/STAT pathway activation, and thus it could contribute to inflammation-induced ADAR1 expression. Moreover, a very interesting direct link between IL-6 production and ADAR1 expression has been described in the context of intestinal stem cell maintenance, as inducible-ADAR1 knocked out mice showed progressive intestinal inflammation and increased expression of inflammatory cytokines IL-6, TNFα and IL-1 in the intestinal mucosa[153], suggesting a negative feedback mechanism between ADAR1 and inflammation.

In order to test this hypothesis, H929 wild type cells were stimulated *in vitro* with increasing concentrations of IL-6. Cells were collected at different time points and RNA was isolated to evaluate changes in ADAR1 expression and in RNA editing activity by qPCR and RESSqPCR.
We observed a dose-dependent increase in ADAR1 mRNA expression when cells were exposed to IL-6 for 24h (Fig.3.2A), in both p150 and p110 isoforms (Fig.3.2B-C). Notably, we observed an increase in RNA editing activity after 48h (Fig.3.2D-G). Most CSC-associated sites showed a significantly higher edit/WT RNA ratio, including APOBEC3D, GLI1 and AZIN1.

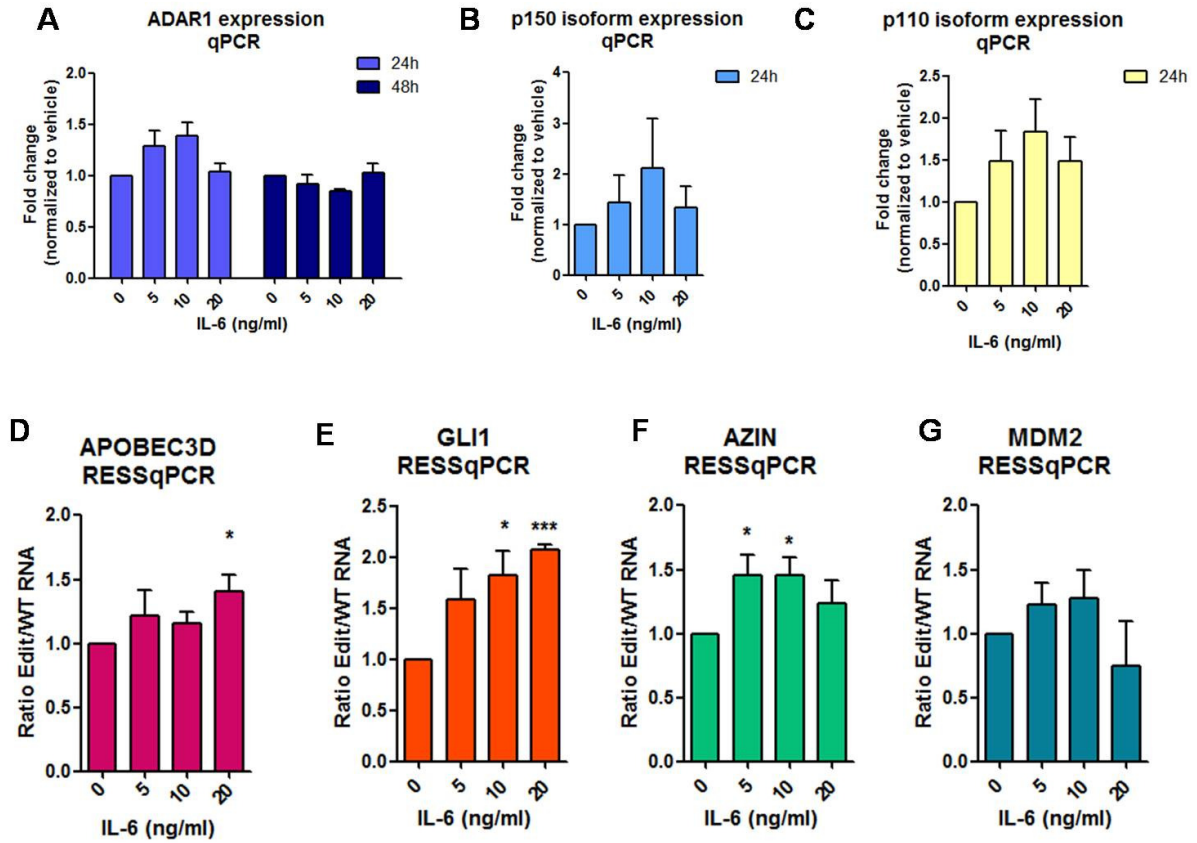

Figure 3.2: IL-6-dependent ADAR1 expression and effects on RNA editing in H929 cells. (A-C) qPCR analysis of total ADAR1 and isoform- specific expression in H929 WT after IL-6 (0-20ng/ml) stimulation at 24-48 hours (n=3). (D-G) Evaluation of RNA editing by RESSqPCR in IL-6-stimulated cells after 48h. *p<0.05, ***p<0.001 compared to vehicle-treated (0 ng/ml IL-6) controls by unpaired two-tailed Student's t test.

3.2 Notch-overexpressing MM cells trigger IL-6 production in BM stromal cells

Plasma-cell derived IL-6 expression in MM is regulated by tumor-stromal interactions. We recently showed that the Notch pathway is a crucial factor promoting MM cell survival, modulating major chemokine pathways such as CXCR4/SDF1[112], osteoclasts/osteoblasts balance[154] and drug-resistance [manuscript under preparation].

Notch is a developmentally conserved pathway that plays a central role in normal and malignant stem cell survival[90],[155]. Tumor cells expressing both Notch ligands and receptors find a protective niche in the BM, where stromal cells also express Notch receptors.

In this environment, MM cells can trigger through overexpressed Notch ligands[106],[109] the transcription of Notch-downstream targets in nearby MM cells and healthy BM cells, acquiring survival advantages and stimulating a tumor-supporting behavior by cells of BM microenvironment.

In order to determine whether BMSCs interactions play a role in pro-inflammatory cues that might drive malignant reprogramming in MM, we investigated the ability of MM cells to induce IL-6 production in BMSC in *in vitro* co-culture models. To facilitate evaluation of IL-6 mRNA expression we co-cultured human myeloma cell lines OPM2 and U266 with NIH3T3 fibroblasts (mouse).

Consistent with previous observations[106], we observed that MM cells overexpressing NOTCH ligands Jagged1 and Jagged2 activate IL-6 production in BMSCs. As shown in Fig.3.3, co-culture of OPM2 and U266 cells with NIH3T3 fibroblasts induced expression of the NOTCH-downstream target gene HES1, as well as IL-6 mRNA expression. Notably, these effects were abolished by double silencing of Jagged1 and Jagged2, achieved through transient siRNA transfection of myeloma cells.

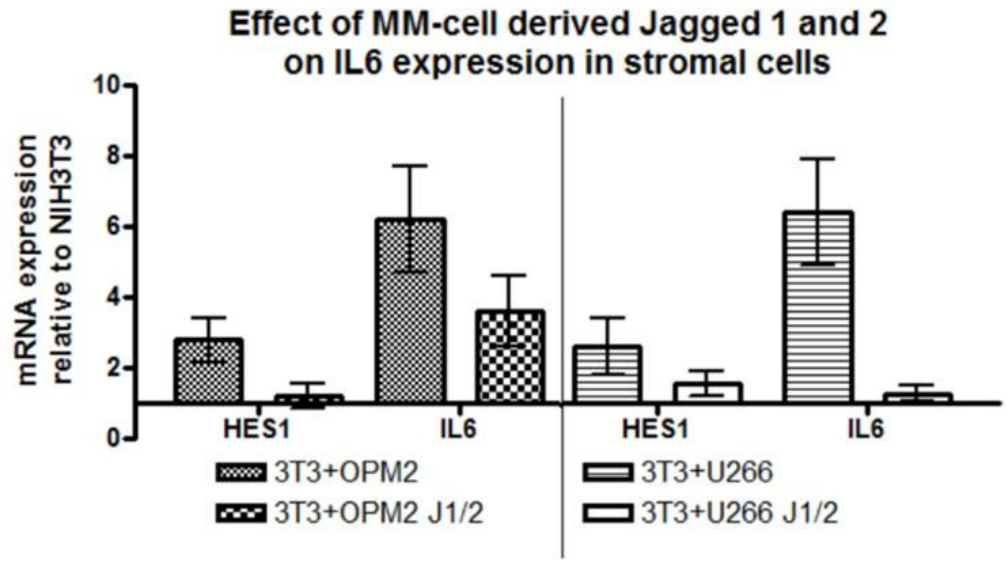

Figure 3.3: NOTCH-dependent BM stromal cell-MM cell interactions. Histograms represent qPCR analysis of human IL-6 and HES1 mRNA expression in 3T3 mouse stromal cells co-cultured with myeloma cells. OPM2 and U266 cells were previously transiently transfected with anti-human Jagged1 and Jagged2 siRNA (or scrambled controls) for 48h, then co-cultured with 3T3 for an additional 48h.

These observations were then confirmed in myeloma-BMSC co-cultures. For co-culture experiments OPM2 or U266 MM cell lines were seeded on a monolayer of human BMSC line previously transduced to express green fluorescent protein (GFP^{+}HS5) to distinguish the two co-cultured cell types. OPM2 or U266 cells induced IL-6 production in HS5 cells as measured by flow cytometry analysis, while double Jagged1 and Jagged2 silencing in MM cells almost completely abrogated this effect (Fig.3.4).

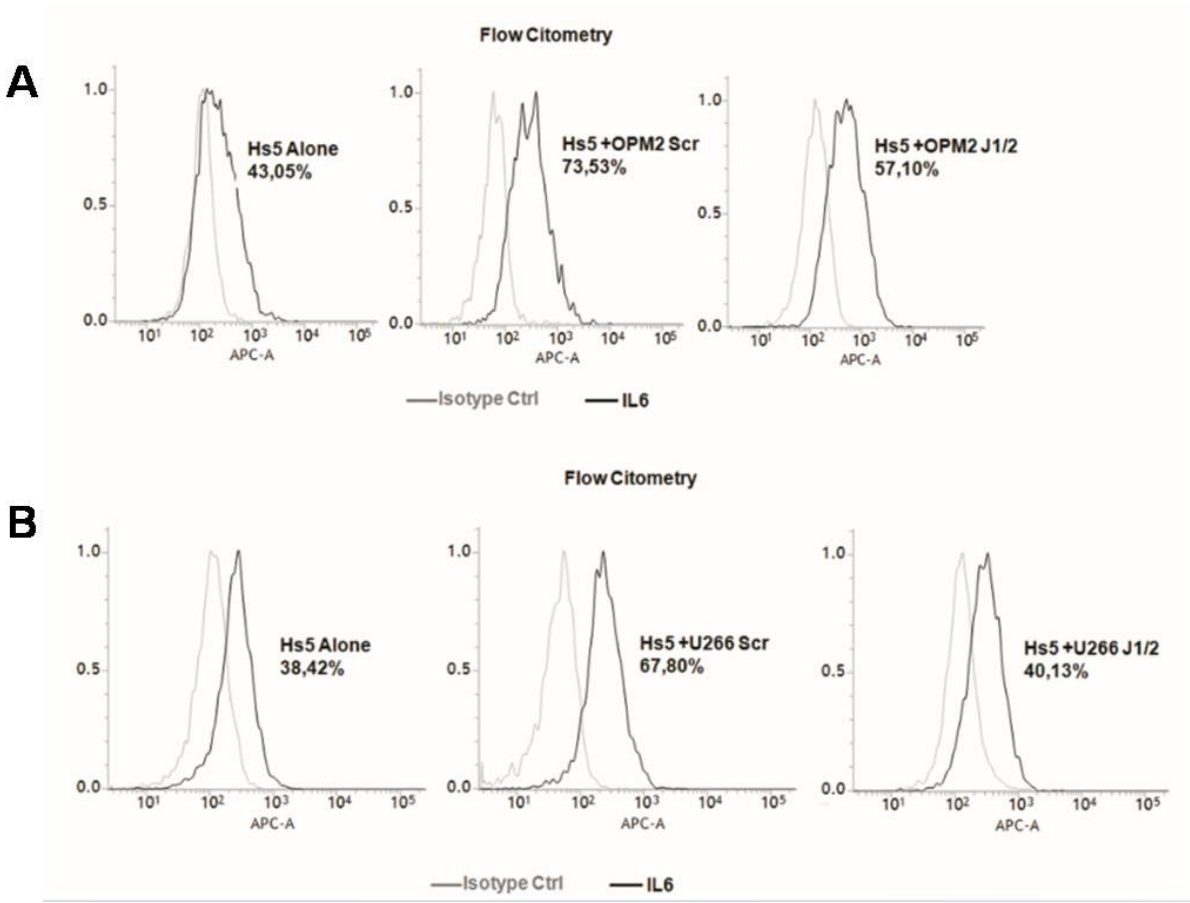

Figure 3.4: MM-induced IL-6 production in BMSCs. Representative histograms of intracellular IL-6 levels measured in GFP+ HS5 cells in single culture or in co-culture with scramble control/ anti-Jagged1 and Jagged2 shRNA transfected OPM2 (A) and U266 cells (B). Anti-IL-6 APC fluorescent signal displayed in black line; isotype-matched control in gray line Histograms are representative of at least 3 experiments with similar results.

4. Establishment of MM in vivo mouse models

Humanized mouse models developed using human cell xenografts or tissue transplants are extremely useful in basic and applied research. Since the early 2000's a series of highly immunodeficient mice has been successfully developed by introducing the mutant IL2 receptor gamma chain gene (IL2Rγ^{null}) into conventional non-obese diabetic severe combined immunodeficient mice (NOD/SCID) or into Balb/c Rag1/2 deficient mice. These highly immunocompromised strains, NSG and RAG2-/-γc-/-, respectively, showed extremely high engraftment rates and differentiation of human cells [156]. A number of different animal models are currently used to study MM, including spontaneous (5T series), transgenic (Vk*myc) and xenograft models.

It is important to emphasize that there are several key limitations and obstacles to the existing *in vivo* models for MM. Most of these models fail to recapitulate complex features of the disease such as tumor homing to the BM, microenvironment-dependence and support for patient-derived primary cell engraftment.

We experienced firsthand some of the current model limitations; indeed, direct intra-femoral injection of CD138-enriched or TMNC from BM MM patients resulted in engraftment of very few patient samples and among those, only low levels of engraftment were detected in highly immunocompromised mice (Rag2-/-γc-/-) (Table 1). Notably, CD138 expression on the cell surface appeared to be inconsistent, thus deeply limiting the ability to trace engrafted human cells by flow cytometry.

Another transplantation strategy we tested was intravenous transplants, which is also limited by the availability of viable primary cells in sufficient numbers for this transplantation method (>10^6 cells per mouse).

Experiment	Tissue	Cell #	Cells transplanted	Engrafted by FACS	Phenotype
1	BM MM	1.x10^6	Total BMNC	0/13	NA
2	BM MM	1.x10^6	CD138+ or CD138-	0/9	NA
3	BM MM	1.x10^6	CD34-/CD138+ or CD34-/CD138-	2/7	CD45+
4	BM MM	1.x10^6	human-enriched cells serial tp from exp.3	0/8	NA
5	BM MM	1.x10^6	Total BMNC	3/10	CD45+/CD319+/CD38+

Table 1: Summary of *in vivo* primary xenografts transplanted by intra-femoral injection. Rag2-/-γc-/- adult (6-8 weeks old) mice were injected directly in the right femur with TMNC or Cd138+/- enriched cells from primary BM MM samples.

Considering our findings that aberrant activation of the malignant reprogramming gene ADAR1 might play a crucial role in MM cell survival, self-renewal and drug resistance, we hypothesized that primary samples expressing high levels of ADAR1 might be more prone to efficient engraftment in immunocompromised mice. Therefore, we aimed to establish novel MM *in vivo* models with high ADAR1 expressing primary samples by intra-hepatic injection in neonatal Rag2-/-γc-/- mice.

Neonatal Rag2-/-γc-/-mice (2-3 days old) lack T, B and NK cells[157] and support hematopoietic human stem cell (HSC) engraftment by direct intrahepatic injection in the liver, without myeloablative regimens. Moreover, human blood-derived cells can efficiently migrate from neonatal (liver) to adult hematopoietic tissues (BM and spleen).

While newborn Rag2-/-γc-/- mice have been extensively used to establish humanized models of HSC-derived malignancies such as chronic myeloid leukemia (CML)[158],[159], no results have been previously reported on engraftment of more terminally differentiated cells, such as malignant plasma cells in MM.

We selected patient-derived samples M9 and M10 (PCLs expressing high ADAR1 levels) to assess PCL engraftment capacity after intrahepatic injection in Rag2-/-γc-/-neonatal mice. We speculated that ADAR1-overexpressing PCL samples would have a high engraftment potential and the ability to circulate in the peripheral blood to reach hematopoietic niches, including the BM, thus recapitulating a critical human myeloma characteristic.

4.1 *In vivo* monitoring of human cell engraftment

In order to monitor human cell engraftment *in vivo*, PCL TMNCs were transduced with a lentiviral GFP-luciferase vector approximately 48 hrs prior to transplant. As displayed in Fig.4.1, patient-specific human immunoglobulin light chains were detected in the serum of the transplanted mice beginning around 8 weeks post-transplantation (post-tp). Additionally, human cell localization was monitored by *in vivo* bioluminescent imaging (IVIS). Fig.4.2 shows a representative image of M10-transplanted animals compared to a naïve control mouse, where luciferase-transduced cells are visible in several tissues, including lower limbs and abdomen. Mice were then sacrificed when symptoms of distress appeared, including loss of weight and presence of palpable tumors.

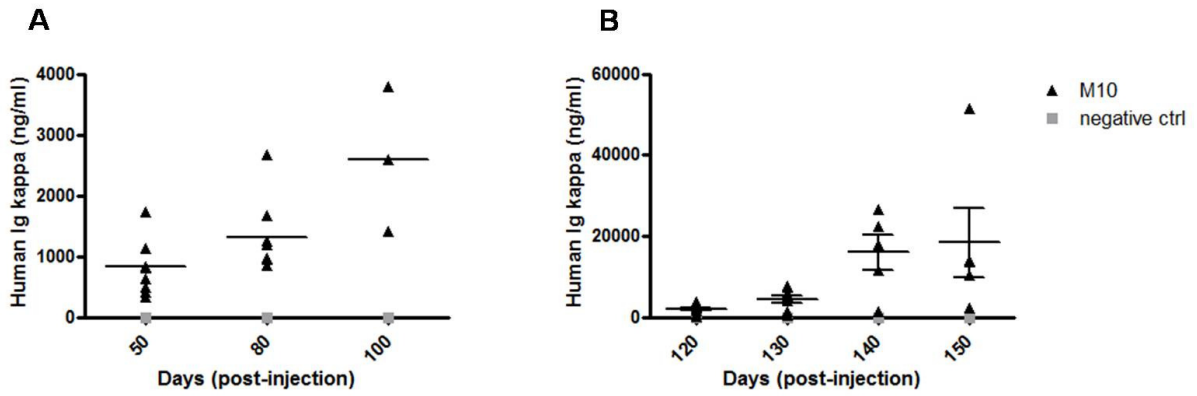

Figure 4.1: Screening of tumor engraftment by detection of human immunoglobulin light chains in mouse serum. ELISA was performed on mouse serum at a minimum of three separate time points post tp. (A) M9-transplanted animals and (B) M10-transplanted animals showed steadily increasing levels of Ig light chains. M9 sample appeared to grow faster (80-100 days post tp.) compared to M10 sample, which required a longer time frame before animals showed sign of tumor burden (120-130 days post tp).

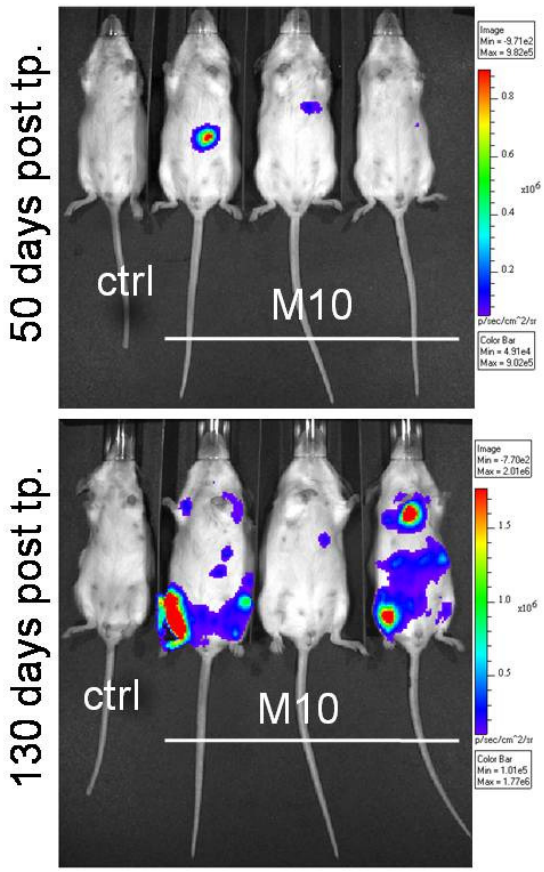

Figure 4.2: Representative images of M10 tumor engraftment by in vivo bioluminescence assay (IVIS). Mice were injected intra-peritoneally (i.p.) with luciferin, and then luciferase signal was acquired by IVIS. In the top panel, animals 50 days post transplant show few or no detectable human cells; while in the bottom panel, animals 130 days post tp show human cell migration throughout the BM and in the abdominal organs.

4.2 Evaluation of malignant plasma cell tissue-specific engraftment

We evaluated primary human cell engraftment by multi-color flow cytometry analysis on different hematopoietic tissues. Our screening panel included CD138, the standard marker for MM plasma cells, along with other malignant plasma cells surface markers, i.e. CD319 and CD38[151],[160]. We also included CD45 in order to discriminate engraftment of other blood-derived human cells.

We observed that Rag2-/-γc-/-mice successfully supported MM primary xenografts: as displayed in Fig.4.3, M9-transplanted animals showed high percentages of human CD138+ cells in the bone marrow (BM) and spleen (SP), with somewhat lower percentages in the peripheral blood (PB) and in the liver (LI, site of injection). Notably, mice developed tumors subcutaneously (ascribable to the needle trajectory), in the abdominal cavity and in the lower limbs that were constituted by CD138+ plasma cells.

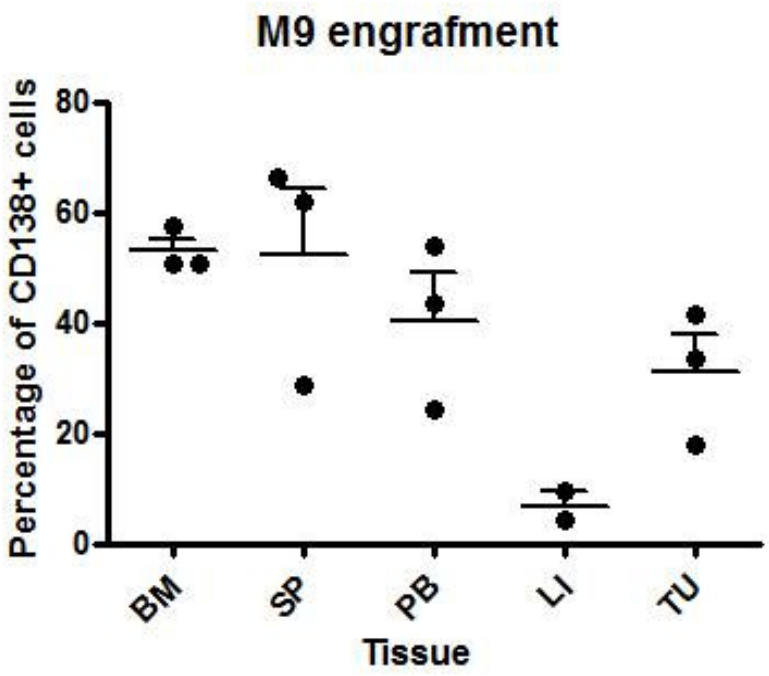

Figure 4.3: Engraftment of M9 sample in Rag2-/-γc-/-mice. Graph shows the percentage of human CD138 positive cells detected out of total live cells in BM), SP, PB, Li and tumors (TU) of individual mice at the end of the experiment (n=3; 105 days post tp). Samples from all tissues were stained for human CD138 and for CD319, CD38 and CD45 (not shown in this panel), acquired on a MACSQuant flow cytometer and analyzed by FlowJo.

M10-transplanted animals consistently showed clear engraftment represented by CD138+ cells detected in the hematopoietic niches of the BM and SP, while no measurable engraftment of human cells was detected in PB or LI (Fig.4.4).

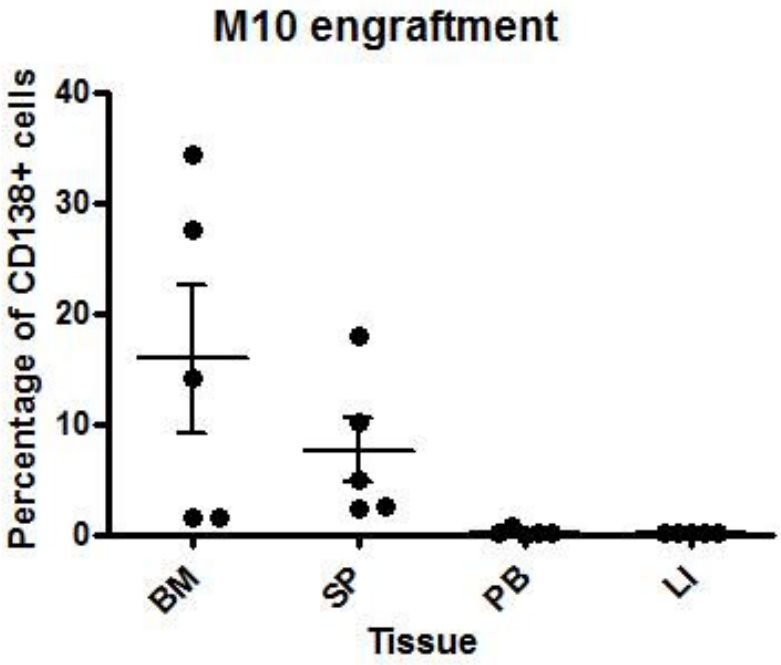

Figure 4.4: Engraftment of M10 sample in Rag2-/-γc-/-mice. Graph shows the percentage of human CD138+cells detected in bone marrow (BM), spleen (SP), peripheral blood (PB), and liver (LI) of individual mice at the end point of the experiment (n=4; 150 days post tp). Samples were stained, acquired and analyzed as previously described for M9-transplanted animals.

4.3 Immunophenotype of MM tumorigenic cells

M9 and M10 PCL samples successfully engrafted in mouse hematopoietic niches, therefore we aimed to better define the immunophenotype of tumorigenic MM cells. Consistently with previous reports, we observed that MM-engrafted cells were CD138+, CD319 (CRACC)+, CD38+ and lacking CD45 surface expression (Fig.4.5). Interestingly, this phenotype was similar in both models, despite variable behavior of the samples in aggressiveness and preference for the vascular and non-hematopoietic niches.

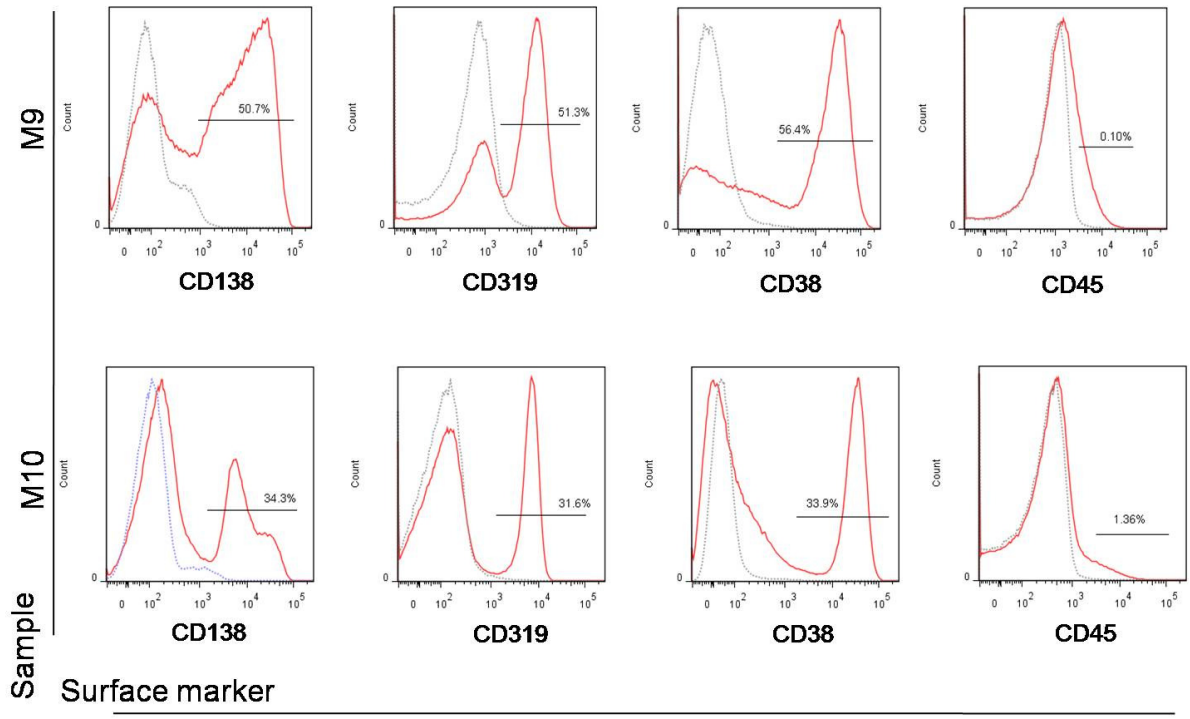

Figure 4.5: Representative flow cytometry analysis of human PCL-derived cells in mouse BM. Histograms show fluorescence intensity of CD138-APC, CD319-PE, CD38- PECy7 and CD45- Brilliant Violet 450 stained samples (red line represents PCL-transplanted mouse; grey dotted line naive control mouse).

4.4 Variability of CD138 expression on MM tumor cell surface

In current practice, MM plasma cells are usually isolated based on CD138 cell surface expression. This marker is generally preferred because of its high plasma cell specificity, as compared with other plasma cell surface markers that are also found on the surface of other cell types, such asCD38 or CD56, for example. Nevertheless, the CD138 antigen has a major drawback in that it disappears/decreases rapidly from the cell surface when the sample is frozen, or even just after a few hours of processing time post-collection[160]. Moreover, in light of the somewhat controversial markers available for MM tumor cancer stem cell identification, especially regarding primary MM xenografts, the stability of CD138 expression on human plasma cells in non-human microenvironments remains unclear.
Overall, this phenomenon reduces sensitivity of immunophenotype-based assays, including fluorescence-activated cell sorting (FACS) and magnetic separation; therefore more robust MM plasma cells markers would facilitate both research and clinical practice in MM. Therefore, using our panel of human-specific plasma cell antibodies, we analyzed the variability of CD138 cell surface expression in engrafted mice tissues compared to plasma cell markers CD38 and CD319.

In M9-transplanted mice, similar proportions of CD138+, CD319+ and CD38+ cells were detected in BM, SP and PB, while there were unexpected differences in tumor cell surface expression. Subcutaneous and abdominal tumors were processed with two protocols, namely A (manual dissociation plus collagenase IV incubation) and B (automated dissociation and Miltenyi enzymatic cocktail incubation).

Notably, cell surface CD138 expression was lower than CD319 or CD38 expression when tumors were dissociated with protocol A, while CD138 completely disappeared after tissues were processed with protocol B. In contrast, both CD319 and CD38 surface expression were consistently stable, regardless from the dissociation protocol applied, with over 90% of cells in the tumors likely being malignant plasma cells.

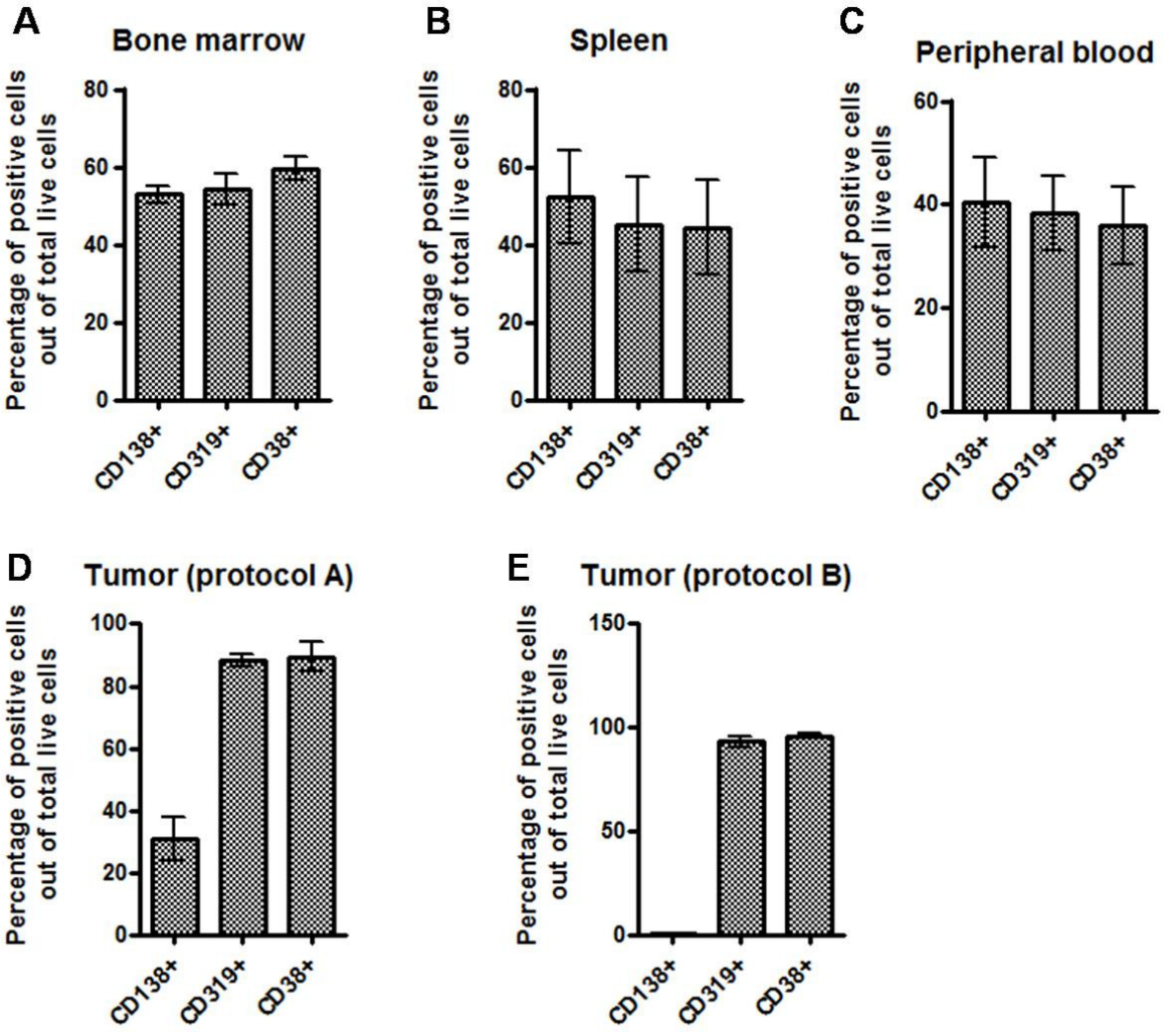

Figure 4.6: Variability of CD138 expression on M9-engrafted tumor cell surface. Graphs show the average percentage of cells positive for human CD138, CD319 and CD38 in M9-transplated mice BM (A); SP (B), PB (C) and tumors (D-E).

M10 transplanted mice showed a similar expression of CD138 compared to CD319 and CD38 in engrafted tissues, as shown in Fig.4.7. This model showed lower overall engraftment rates than M9, and did not display any tumor development.

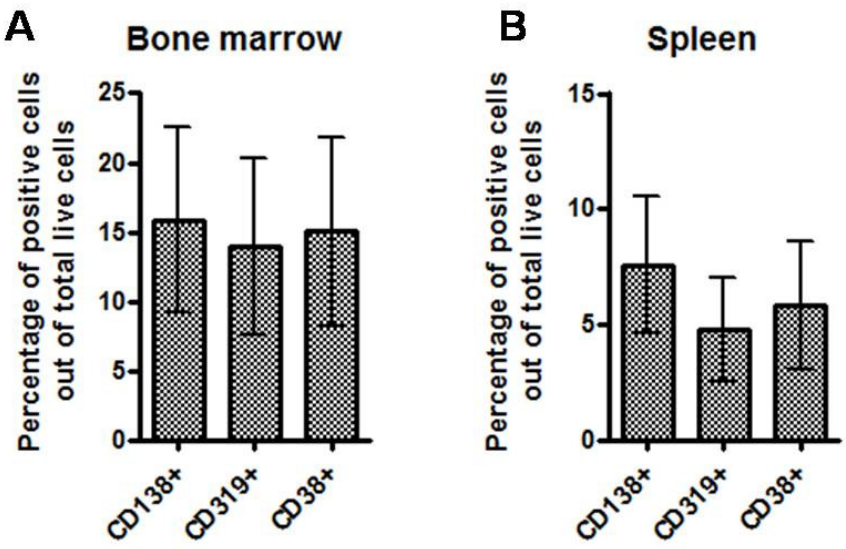

Figure 4.7: Variability of CD138 expression on M10-engrafted tumor cells. Graphs show the average percentage of cells positive for human CD138, CD319 and CD38 in M10-transplated mice BM (A) and SP (B).

Overall these observations highlight how sensitive the CD138 marker is to ablation from MM plasma cell surface, depending on tissue processing and sample handling, thus leading to inconsistent results and underestimation of actual tumor burden. In our hands, manual tumor dissociation followed by incubation with collagenase IV (protocol A) gave the best compromise between cell viability and cell surface marker expression, although CD138 appeared extremely unreliable.

4.5 PCL-derived xenografts are serially transplantable

In order to functionally demonstrate whether the established MM models could serially transplant, thus allowing for future therapeutic treatment studies in a robust MM model, we performed intrahepatic injection in secondary Rag2-/-γc-/-recipients. Single cells obtained from engrafted BM and tumors were pooled together and injected intrahepatically in newborn mice.

As displayed in Fig.4.8, secondary recipient mice successfully recapitulated primary M9-transplanted mice. Indeed, after 80 days from transplant, mice showed signs of distress and presence of palpable tumors.

Once sacrificed, human CD138+/CD319+/CD38+/CD45- cells (Fig.4.8A) were detected in mouse BM, SP and LI in lower percentages, thus reproducing a similar phenotype to primary M9-engrafted samples. Serial transplant recipients developed widespread tumors similar to primary recipients (Fig.4.8B). Given the more rapid development of tumors, the serial transplantation of BM and tumor-derived cells appeared to favor more robust tumor development, which will inform future selection of tissue sources and timeframes for experimental design with these models. As observed in M9-derived tumors in primary recipients, CD138 surface expression in tumor-derived cells from serial transplant recipients was highly inconsistent compared to CD319 and CD38 markers (Fig.4.8C).

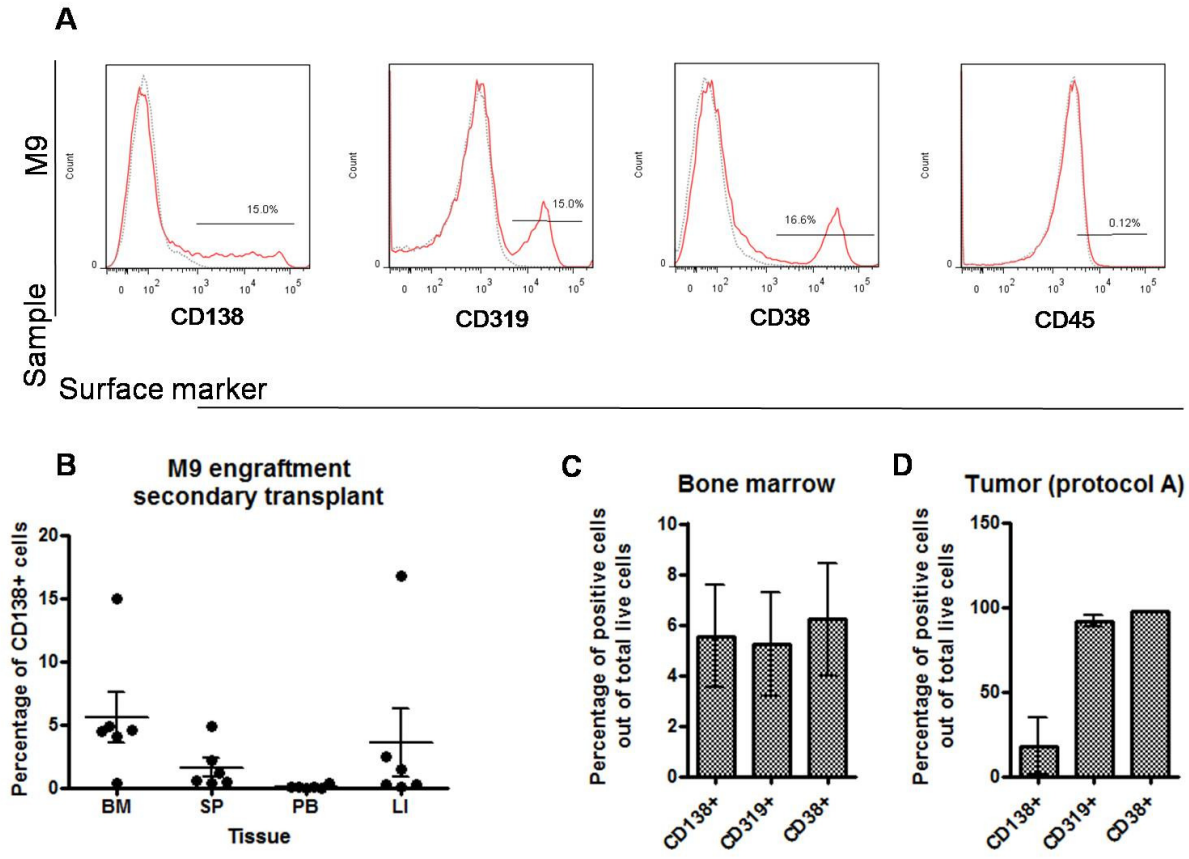

Figure 4.8: Engraftment of M9 sample in secondary recipients. (A) Representative flow cytometry analysis of M9-derived cells in mouse BM (red line serially transplanted mouse; grey dotted line naive control mouse); (B) Percentage of human CD138+ cells detected in BM, SP; PB, LI and tumors of individual mice at the end point of the experiment (n=6; 80 days post tp); (C-D) Average percentage of cells positive for human CD138, CD319 and CD38 in M9-serially transplanted mice BM (C) and tumors (D).

Discussion

Multiple myeloma (MM) is the second most common blood cancer after leukemia, accounting for approximately 10% of hematologic malignancies[7]. In 2014 the American Cancer Society estimated more than 24.000 new cases and 11.000 disease-associated deaths[161]. With a median age at diagnosis of 65 years, this condition affects a significant percentage of the middle-aged and older population. As for other age-related conditions, MM incidence will have to be kept under a close watch. The phenomenon of global aging is changing the demographic composition over the coming decades and it has the potential to significantly impact healthcare systems, research and medical decision making. Despite the introduction of novel therapies and a significant improvement in survival, MM has still no cure. Virtually all patients experience cycles of remission/relapse and/or become unresponsive to treatment. For patients with relapsed or refractory MM (RRMM) many therapeutic options exist but an effective standard of care is still missing. With each successive line of treatment therapeutic options become increasingly limited due to acquisition of drug resistance. Moreover, on each subsequent disease relapse patients experience lower rates of clinical response and shorter progression-free survival (PFS); which is the time between the start of treatment and progression of the disease or death. As more lines of therapy are available, patients with RRMM are living longer. However, as treatment is prolonged, the costs of therapy have become an increasing burden to patients. Autologous stem cell transplant (ASCT) is the current standard of care for most patients who are eligible for transplant, with a 12-month improvement in overall survival compared to non-transplanted patients[162]. The risk of death after ASCT has been declining in the past few years and it is estimated that approximately 5000 ASCT are performed for MM patients in the U.S. annually, with an average cost of $25.000 (adjusted to 2012)[163]. Nevertheless, studies endorsing ASCT predated novel agents; therefore the value of stem cell transplant is currently under

reconsideration in randomized trials that include bortezomib and lenalidomide.

Bortezomib is used as first line therapy and for retreatment in patients who had achieved durable response before relapse. Similarly, lenalidomide treatment in induction and as maintenance therapy has gained widespread use. Lenalidomide-containing regimens are the most expensive in MM therapy: a recent study calculated that the total cost of one year of treatment would range between $126.000-256.000[164]. Although drug costs form a conspicuous portion of treatment cost in MM, myeloma-related healthcare costs are also significantly driven by disease complications, which result in inpatient hospitalizations, hospital readmissions, and medical procedures. Indeed, the same study found that the average length of hospital stay associated with MM was among the longest of the cancers that were evaluated[165]. Therefore, prolonging the duration of remission and/or lengthening PFS remain primary goals of therapy for patients with MM. Thus, it is essential to identify the most effective therapeutic regimens according to patient-specific risk factors.

As in other hematologic malignancies, cytogenetic status is one of the most important prognostic factors in MM. Advances in high-throughput methodologies in genomic analysis greatly helped in investigating genetic abnormalities. Nowadays, in addition to the traditional Durie-Salmon staging criteria and the International Staging System (ISS), MM patients can benefit from a risk-stratification based on recurrent genetic alterations in order to make informed decision about treatment. Importantly, the survival of a particular subgroup of patients with certain cytogenetic abnormalities, collectively called “high-risk” (HR) MM, has remained poor despite aggressive therapy.

According to the International Myeloma Working Group, the term “high-risk” MM should include those patients with at least one of the following features: deletion of 17p, t(4;14), t(14;16), t(14;20) and 1q gains. In particular, 1q21

and del17p were recently described to be associated to a even more aggressive MM risk category, defined as “ultra high risk” (UHR)[166]. UHR patients have an overall survival of less than 12 months (median 5 months), become refractory to therapy after a single induction cycle (30% of cases) and frequently develop secondary plasma cell leukemia (PCL, 14% of cases).

Up to 20% of all myeloma patients may be classified as UHR, and while ISS stage III has been reported to be an effective prognostic indicator, only about 77% of UHR patients would be classified as ISS stage III.

It is well established that the 1q21 amplification contains numerous candidate genes that show amplification or deregulated expression in myeloma, including CKS1B, IL-6R and MCL1[30]. In this study we describe for the first time the correlation between the expression of the Adenosine Deaminase Acting on RNA (ADAR)-1 gene located on 1q21 and copy number amplifications of 1q21 locus itself.

Indeed, our analysis on well-annotated cohorts of patients revealed that copy number amplification of 1q21 correlates with increased mRNA expression of the RNA editases ADAR1. Notably, ADAR1 expression was significantly higher in patients with more than 4 copies of 1q21. These results are in line with Boyd’s observations[26], which revealed that more than 3 copies of 1q21 independently predicted poor survival, with a progression-free survival (PFS) of 17.6 months and a 3-year overall survival (OS) rate of 52%, while ≤3 copies were only marginally associated with PFS and OS.

Our new results suggest a novel relationship between ADAR1 expression and poor prognosis in plasma cell neoplasms, bringing ADAR1 into the spotlight as a new player in myeloma plasma cell clonal evolution and drug resistance.

MM is a genetically complex disease. The basic premise underlying the initiation and progression of myeloma is that multiple mutations in different

pathways deregulate the physiological biology of the plasma cell, thus resulting in the features of myeloma. Many of the genes and pathways mediating this transformation process have been characterized, however, recent sequencing data made it clear that there is no single genetic change underlying this process that can be targeted therapeutically[149].

In addition to the genetic changes, intraclonal heterogeneity of myeloma-initiating cells is emerging as a further level of complexity. In this respect, myeloma-initiating cells could acquire additional “survival advantage” both by genetic and epigenetic events, thus leading to the evolution of this disease.

Indeed, in the last few decades the Darwinian principles of evolution have been applied to cancer: first in 1976, Dr. Peter Nowell pioneered the hypothesis that cancer originates from one founder cell, which progressively accumulates random somatic genetic mutations, thus giving rise to a series of branches of subclonal populations existing in equilibrium[167]. Such subclones compete with each other for the limited microenvironmental resources and are selected according to their fitness to survive.

A growing body of evidence is supporting this model of tumor evolution where several clonal tumor-initiating cells present at diagnosis and therapeutic or niche-dependent selection pressure drives the alternating dominance of these clones over time[168]–[170]. Interestingly, clonal diversity is found to be more prevalent in high-risk MM compared with low-risk disease[168].

The majority of these observations have been made possible by mutation-detection methods such as whole exome sequencing, but still little is known about the role played by epigenetic mechanisms such as RNA editing.

RNA editing provides a post-transcriptional level of genetic regulation that allows for the expression of gene variants while preserving the original gene sequence and product. This phenomenon generates incredible

potential for RNA and protein diversity, that could contribute further survival advantages in selective environments, for instance in the context of the BM niche or under the pressure of chemotherapy.

In the present study we examined ADAR1 gene expression in MM and PCL-derived mononuclear cells. We showed that ADAR1 was significantly overexpressed in PCL, while its levels in smoldering MM were not significantly different from normal controls. Since deregulated RNA editing can result in transcriptome “recoding”, this could contribute significant genetic diversity in plasma cell neoplasms, eventually resulting in the generation of dominant clones with a more aggressive transcriptional profile. It is believed that CKS1B amplification is associated with progression to PCL[171], however, the gain of chromosome band 1q21 has been commonly determined by fluorescence in situ hybridization (FISH), using a bacterial artificial clone (180kb) carrying the CKS1B gene[29],[172]. Hence, 1q21 amplification has been linked to CKS1B overexpression, but whether this gene is solely responsible for 1q21 prognostic value is arguable: as described by Avet-Loiseau and colleagues, 1q gains can in fact involve a more extended region, up to the 1q23.3 chromosomal band[173]. As a result of copy number amplifications of the ADAR1 gene locus on chromosome 1q, HR MM patients would be at risk for more rapid clonal evolution through transcriptome recoding. Interestingly, ADAR1 appeared to be significantly increased also in a relapsed MM patient (M8) previously exposed to immunomodulatory treatment (lenalidomide), driving us to hypothesize those agents could provide the selective pressure inducing inflammation-responsive ADAR1 isoform expression, as supported by higher levels of ADAR1 isoform p150 in the same sample.

ADAR1 levels were also increased in a newly diagnosed MM patient (M3) without previous treatment. In this sample both ADAR1 pro-inflammatory p150 and constitutive p110 isoforms were overexpressed. FISH analysis on this patient’s BM biopsy revealed the presence of a cyclin D1-IgH

(CCND1/IGH) gene fusion, resulting from translocation (11;14) in CD138-enriched plasma cells. While this translocation is not considered an adverse prognostic factor when found in MM BM, it is very common in PCL[23],[174]. Unfortunately, we were not able to determine 1q21 copy number variations in our set of primary samples as diagnostic assays at the time of sample collection did not include this probe. However, future studies will clarify whether ADAR1 overexpression could be predicted by 1q amplification and/or by recurrent translocations in PCL, such as t(11;14). Furthermore, we demonstrated that ADAR1 overexpression was associated with increased RNA editing by a novel RNA editing detection assay[150], namely RESSqPCR, and validated our findings by Sanger sequencing.

Identification of a MM-specific RNA editing “fingerprint” would be highly valuable to tracking its evolution within the course of the disease and in response to treatment.

In this work we assessed RNA editing in four transcripts previously associated with ADAR1-induced malignant transformation in other cancers including CML[148],[145]: apolipoprotein B mRNA editing enzyme, catalytic polypeptide-like 3D (APOBEC3D), Glioma- associated oncogene 1 (GLI1), antizyme inhibitor 1 (AZIN1) and murine double minute 2 E3 ubiquitin protein ligase (MDM2).

In keeping with increased ADAR1 expression, analysis of endogenous RNA editing levels in primary patient samples revealed abnormal RNA editing patterns. In particular, APOBEC3D transcripts were highly edited across all MM and PCL samples compared to controls, which virtually lacked any detectable editing at this locus. In addition, PCL and newly diagnosed MM samples showed elevated editing in GLI1 transcript, while editing in AZIN1 and MDM2 sites were heterogeneous among samples. The potential implications of an increase in edited transcripts for these genes appears worthy of note as all four genes have been previously associated with cancer progression.

Interestingly, next-generation sequencing analyses have revealed an important role for genome editing by APOBEC3 family members. For example, a mutational signature associated with APOBEC3 (A3) has been identified several cancers, such as HER2-amplified breast cancer and human papilloma virus (HPV)-associated head and neck squamous carcinoma [175]–[177]. Notably, a study of B cell-derived chronic lymphocytic leukemia (CLL) reported that an A3-like mutation signature was found within CLL samples that had undergone somatic hypermutation (SHM) but not in samples that had not, whereas the expression of A3 proteins was unchanged[178]. In light of these observations, it is reasonable to hypothesize a role for other APOBEC3 family members with genome-editing capacity such as APOBEC3D in post-SHM plasma cell-derived malignancies as MM as potential driver of further tumor clonal variation, and the functional impact of RNA editing in this DNA-modifying gene product is under further examination.

GLI1 is a zinc finger transcription factor downstream of Hedgehog (Hh) signaling, a highly conserved pathway essential for embryonic development and adult tissue homeostasis. Aberrant activation of Hh signaling has been reported in both solid and hematologic tumors, such as cancers of the pancreas, prostate, lungin and B-cell lymphoma. Moreover, several groups identified its contribution in MM survival by inhibition of chemotherapy-induced apoptosis. Notably, bothCD138+[179],[180] and CD138-[181] cell populations were described to be major producers and secretors of Hh ligands Sonic hedgehog (SHH), thus inducing Hh pathway activation by autocrine signaling. Mechanistic studies showed that sonic hedgehog (SHH) signaling activated the SHH/GLI1/BCL-2 axis, leading to the inhibition of myeloma cell apoptosis[180]. The edited GLI1 has been shown to have a higher capacity to activate its transcriptional targets and to be less susceptible to inhibition by the negative regulator of Hh signaling, suppressor of fused (SUFU)[182]. As a result, an increase of edited GLI1

could support the prolonged activation of Hh signaling in both MM bulk tumor and cancer stem cells.

AZIN1 hyper-editing provided one of the early clues about the functional impact of RNA editing in cancerogenesis as Chen and colleagues proved that AZIN1 editing results in a single amino acid substitution that confers a “gain of function” phenotype, where the edited form results in increased protein stability and promotes cell proliferation in hepatocellular carcinoma (HCC)[145]. As for MDM2, the editing site in located in the 3’ UTR instead that in the coding region. Therefore, rather than a “gain of function” effect, increased editing would likely result in a change in microRNA binding site. MDM2 is an E3 ubiquitin ligase responsible for the ubiquitination and degradation of p53, therefore editing in the 3’ UTR may hamper the ability of microRNAs to bind to MDM2, leading to a “lack of inhibition” effect by which cells could inactivate p53 in the process of transformation.

Overall these findings led us to infer that both genetic (1q21 amplification) and environmental (inflammation, IMiDs) factors can modulate ADAR1 expression. Moreover, ADAR1 overexpression is associated with aberrant RNA editing in key pro-tumoral transcripts. The functional consequences of A-to-I editing are have not been fully elucidated for all of the specific transcripts we identified, however studies are under way to provide further insights into the mechanisms of ADAR1-associated aberrant editing of APOBEC3D, GLI1, AZIN1 and MDM2.

In a parallel series of experiments, we investigated the ability of lenalidomide, an immunomodulatory agent, to modulate ADAR1 expression and activity in MM. For this purpose, we developed lenalidomide-resistant NCI-H929 cells, a HMCL harboring 4 copies of the 1q21 locus. We observed that continuous exposure to lenalidomide significantly increased ADAR1 mRNA and protein level, thus sustaining abnormal RNA editing of APOBEC3D, GLI1, AZIN1 and MDM2. Remarkably, only ADAR1 levels

were modulated, while ADAR2 expression was very low in wild type cells and was not increased by continuous lenalidomide treatment.

Notably, ADAR1-enriched cells harbored increased self-renewal and serial replating potential *in vitro*. These results are consistent with previous findings from our collaborators, where Jiang and colleagues demonstrated that ADAR1 is an essential self-renewal factor in CML progenitor cells and that disease progression from chronic to blast crisis phase is associated with increased A-to-I RNA editing[148].

Consistent with the reported role for ADAR1 in malignant reprogramming leading to generation of leukemia stem cells in advanced stages of CML, we demonstrated that prolonged exposure to lenalidomide led to an increase in the percentage of stem-like CD138dim cells in H929. Our findings are consistent with Matsui and colleagues' work, who described how CD138dim/- subpopulation have been showed to display increased clonogenic growth compared to CD138+ when exposed to drugs, including lenalidomide and dexamethasone[94]. In addition to cell-intrinsic changes, microenvironmental cues could contribute to clonal evolution and drug-resistance. To address this aspect, we investigated whether pro-inflammatory signals from the MM BM microenvironment, namely IL-6, could modulate ADAR1 expression levels. Indeed, we observed that aberrant RNA editing in H929 cells was induced by exogenous IL-6 exposure. Recently, we and others demonstrated that IL-6 is produced by BM stromal cells upon contact with malignant plasma cells and that its levels are modulated by the Notch signaling pathway. In fact, IL-6 secretion by BMSCs is inhibited when Notch signaling is antagonized by Jagged 1 and Jagged2 silencing in MM cells. These observations led to the identification of important key factors tuning ADAR1 expression and consequently RNA editing. In order to further translate these findings *in vivo* we developed primary xenografts in Rag2-/-γc-/- mice. To our knowledge this is the first time that a successful primary PCL xenograft by intrahepatic

injection is described. We showed that high-ADAR1 PCL samples successfully engrafted in primary and secondary Rag2-/-γc-/- recipients and demonstrated tropism towards hematopoietic tissues. Human CD138+/CD319+/CD38+ plasma cells engrafted the liver in neonatal animals and migrated to bone marrow and spleen in adult recipients. We believe these models could be further employed to investigate therapeutic approaches for drug resistance plasma cell neoplasms, such as treatment strategies targeting ADAR1 and aberrant RNA editing, in order to provide specific therapeutic approaches for HR and advanced MM patients.

Conclusions

MM is a disease that affects elderly people. As it is estimated that by 2029 more than 20% of the total U.S. population will be over the age of 65[183], increased demand for healthcare and long-term care for the aging population will be a major challenge for healthcare professionals. Myeloma accounts for a small percentage of all cancers (1%) but the associated costs over the course of the disease are disproportionately high compared to other cancers that invade the bone marrow niche[164]. In recent years the Darwinian evolution model proved valid for tumor initiation and progression. In fact, the presence of clonal heterogeneity at diagnosis and in response to selective pressure represents a novel paradigm in myeloma with profound therapeutic implications. RNA editing is an epigenetic mechanism with the potential to generate vast RNA and protein diversity of key cancer-regulatory and stem cell-associated gene products. These molecular alterations can provide further survival advantages to malignant cells including tumor-initiating populations in selective environments, for instance in the context of the BM niche or under the pressure of chemotherapy. In this work we showed that ADAR1, located on the high-risk associated- 1q21 locus is highly expressed in late stage PCL patient samples, and that aberrant RNA editing occurs in cancer stem cell-associated transcripts APOBEC3D and GLI1. Moreover, we showed that environmental factors such as immunomodulatory treatment (lenalidomide) or BM niche soluble factors (IL-6) can support ADAR1-induced aberrant RNA editing and that lenalidomide-sustained ADAR1 overexpression promotes self-renewal and a cancer stem cell-like phenotype in MM cells. Together, ADAR1-dependent transcriptome recoding could eventually lead to further malignant clonal diversity and disease progression in MM. Therefore, a NOTCH/IL-6/ADAR1 axis, together with ADAR1 editing substrates, represents novel targets for diagnostic and therapeutic development in MM and PCL.

BIBLIOGRAPHY

1. **Rajkumar SV**. Multiple myeloma: 2012 update on diagnosis, risk-stratification, and management. *Am J Hematol*. 2012; **87**(1):78–88.

2. **Palumbo A, Anderson K**. Multiple myeloma. *N. Engl. J. Med*. 2011; **364**(11):1046–60.

3. **Kyle R a, Rajkumar SV**. Multiple myeloma. *N. Engl. J. Med.* 2004; **351**(18):1860–73.

4. **Landgren O, Weiss BM**. Patterns of monoclonal gammopathy of undetermined significance and multiple myeloma in various ethnic/racial groups: support for genetic factors in pathogenesis. *Leuk. Off. J. Leuk. Soc. Am. Leuk. Res. Fund, U.K*. 2009; **23**(10):1691–7.

5. **Kyle R a, Remstein ED, Therneau TM, *et al.*** Clinical course and prognosis of smoldering (asymptomatic) multiple myeloma. *N. Engl. J. Med.* 2007; **356**(25):2582–90.

6. **Donk N Van De**. How I treat plasma cell leukemia. *Blood*. 2012; **120**(12):2376–2389.

7. **Rajkumar SV**. Multiple myeloma: 2013 update on diagnosis, risk-stratification, and management. *Am. J. Hematol.* 2013; **88**(3):226–35.

8. **Kyle R a, Gertz M a, Witzig TE, *et al.*** Review of 1027 patients with newly diagnosed multiple myeloma. *Mayo Clin. Proc.* 2003; **78**(January):21–33.

9. **Greipp PR, San Miguel J, Durie BGM, *et al.*** International staging system for multiple myeloma. *J. Clin. Oncol.* 2005; **23**(15):3412–20.

10. **Kumar SK, Mikhael JR, Buadi FK, *et al.*** Management of newly diagnosed symptomatic multiple myeloma: updated Mayo Stratification of Myeloma and Risk-Adapted Therapy (mSMART) consensus guidelines. *Mayo Clin. Proc.* 2009; **84**(12):1095–110.

11. **Kumar SK, Rajkumar SV, Dispenzieri A, *et al.*** Improved survival in multiple myeloma and the impact of novel therapies. *Blood*. 2008; **111**(5):2516–20.

12. **Hallek M, Bergsagel PL, Anderson KC**. Multiple myeloma: increasing evidence for a multistep transformation process. *Blood*. 1998; **91**(1):3–21.

13. **O'Connor B, Gleeson MW, Noelle RJ, Erickson LD**. The rise and fall of long-lived humoral immunity: terminal differentiation of plasma cells in health and disease. *Immunol Rev*. 2003; **194**:61–76.

14. **Witzig TE, Timm M, Larson D, Therneau T, Greipp PR**. Measurement of apoptosis and proliferation of bone marrow plasma cells in patients with plasma cell proliferative disorders. *Br. J. Haematol.* 1999; **104**(1):131–137.

15. **Hose D, Rème T, Hielscher T, *et al.*** Proliferation is a central independent prognostic factor and target for personalized and risk-adapted treatment in multiple myeloma. *Haematologica*. 2011; **96**(1):87–95.

16. **Morgan GJ, Walker B a., Davies FE**. The genetic architecture of multiple myeloma. *Nat. Rev. Cancer*. 2012; **12**(5):335–348.

17. **Zhou Y, Barlogie B, Shaughnessy JD**. The molecular characterization and clinical management of multiple myeloma in the post-genome era. *Leukemia*. 2009; **23**(11):1941–56.

18. **Bergsagel PL, Kuehl WM**. Chromosome translocations in multiple myeloma. *Oncogene*. 2001; **20**:5611–5622.

19. **Kuehl WM, Bergsagel PL**. Multiple myeloma: evolving genetic events and host interactions. *Nat. Rev. Cancer*. 2002; **2**(3):175–87.

20. **Bergsagel PL, Kuehl WM, Zhan F, *et al.*** Cyclin D dysregulation: An early and unifying pathogenic event in multiple myeloma. *Blood*. 2005; **106**(1):296–303.

21. **González D, van der Burg M, García-Sanz R, *et al.*** Immunoglobulin gene rearrangements and the pathogenesis of multiple myeloma. *Blood*. 2007; **110**(9):3112–21.

22. **Bergsagel PL, Kuehl WM**. Molecular pathogenesis and a consequent classification of multiple myeloma. *J. Clin. Oncol.* 2005; **23**(26):6333–6338.

23. **Avet-Loiseau H, Gerson F, Magrangeas F, *et al.*** Rearrangements of the c-myc oncogene are present in 15% of primary human multiple myeloma tumors. *Blood*. 2001; **98**(10):3082–3086.

24. **Van Wier S, Braggio E, Baker A, *et al.*** Hypodiploid multiple myeloma is characterized by more aggressive molecular markers than non-hyperdiploid multiple myeloma. *Haematologica*. 2013; **98**(10):1586–1592.

25. **Chng WJ, Dispenzieri a, Chim C-S, *et al.*** IMWG consensus on risk stratification in multiple myeloma. *Leukemia*. 2014; **28**(2):269–77.

26. **Boyd KD, Ross FM, Chiecchio L, *et al.*** A novel prognostic model in myeloma based on co-segregating adverse FISH lesions and the ISS: analysis of patients treated in the MRC Myeloma IX trial. 2012; **26**(2):349–355.

27. **Carrasco DR, Tonon G, Huang Y, *et al.*** High-resolution genomic profiles define distinct clinico-pathogenetic subgroups of multiple myeloma patients. *Cancer Cell*. 2006; **9**(4):313–25.

28. **Hanamura I, Stewart JP, Huang Y, *et al.*** Frequent gain of chromosome band 1q21 in plasma-cell dyscrasias detected by fluorescence in situ hybridization : incidence increases from MGUS to relapsed myeloma and is related to prognosis and disease progression following tandem stem-cell transplantati. *Blood*. 2006; **108**(5):1724–1732.

29. **Fonseca R, Van Wier S a, Chng WJ, *et al.*** Prognostic value of chromosome 1q21 gain by fluorescent in situ hybridization and increase CKS1B expression in myeloma. *Leukemia*. 2006; **20**(11):2034–40.

30. **Sawyer JR, Tian E, Heuck CJ, *et al.*** Jumping translocations of 1q12 in multiple myeloma: a novel mechanism for deletion of 17p in cytogenetically defined high-risk disease. *Blood*. 2014.

31. **Nemec P, Zemanova Z, Greslikova H, *et al.*** Gain of 1q21 is an unfavorable genetic prognostic factor for multiple myeloma patients treated with high-dose chemotherapy. *Biol. Blood Marrow Transplant.* 2010; **16**(4):548–54.

32. **Wu L, Grigoryan A V, Li Y, *et al.*** Specific Small Molecule Inhibitors of Skp2-Mediated p27 Degradation. *Chem Biol*. 2012; **19**(12):1515–1524.

33. **Pellat-Deceunynck C, Barillé S, Puthier D, *et al.*** Adhesion molecules on human myeloma cells: significant changes in expression related to malignancy, tumor spreading, and immortalization. *Cancer Res.* 1995; **55**:3647–3653.

34. **Chang H, Jiang N, Jiang H, *et al.*** CKS1B nuclear expression is inversely correlated with p27 klp1 expression and is predictive of an adverse survival in patients with multiple myeloma. *Haematologica*. 2010; **95**(9):1542–1547.

35. **Inoue J, Otsuki T, Hirasawa A, *et al.*** Overexpression of PDZK1 within the 1q12-q22 amplicon is likely to be associated with drug-resistance phenotype in multiple myeloma. *Am. J. Pathol.* 2004; **165**(1):71–81.

36. **Sawyer JR, Tian E, Thomas E, *et al.*** Evidence for a Novel Mechanism for Gene Amplification in Multiple Myeloma: 1q12 Pericentromeric Heterochromatin Mediates Breakage-Fusion-Bridge Cycles of a 1q12~23 Amplicon. *Br J Heamatol*. 2009; **147**(4):484–494.

37. **Bergsagel PL, Mateos MV, Gutierrez NC, Rajkumar SV, San Miguel JF**. Improving overall survival and overcoming adverse prognosis in the treatment of cytogenetically high-risk multiple myeloma. *Blood*. 2013; **121**(6):884–892.

38. **Haessler J, Shaughnessy JD, Zhan F, *et al.*** Benefit of complete response in multiple myeloma limited to high-risk subgroup identified by gene expression profiling. *Clin. Cancer Res.* 2007; **13**(23):7073–7079.

39. **Anderson KC, Kyle R a., Dalton WS, *et al.*** Multiple Myeloma: New Insights and Therapeutic Approaches. *Hematology Am. Soc. Hematol. Educ. Program*. 2000:147–165.

40. **Bladé J, de Larrea CF, Rosiñol L**. Incorporating monoclonal antibodies into the therapy of multiple myeloma. *J. Clin. Oncol.* 2012; **30**(16):1904–6.

41. **Rajkumar SV**. Multiple myeloma: 2014 Update on diagnosis, risk-stratification, and management. *Am. J. Hematol.* 2014; **89**(10):999–1009.

42. **Greenstein S, Ghias K, Krett NL, Rosen ST**. Mechanisms of glucocorticoid-mediated apoptosis in hematological malignancies. *Clin. Cancer Res.* 2002; **8**(6):1681–1694.

43. **Palumbo a, Dimopoulos M, San Miguel J, *et al.*** Lenalidomide in combination with dexamethasone for the treatment of relapsed\ror refractory multiple myeloma. *Blood rev*. 2008; **In press**(1):129–136.

44. **Hardin J, MacLeod S, Grigorieva I, *et al.*** Interleukin-6 prevents dexamethasone-induced myeloma cell death. *Blood*. 1994; **84**(9):3063–3070.

45. **Hideshima T, Richardson PG, Anderson KC**. Mechanism of Action of Proteasome Inhibitors and Deacetylase Inhibitors and the Biological Basis

of Synergy in Multiple Myeloma. *Mol. Cancer Ther.* 2011; **10**(11):2034–2042.

46. **Fenaux P, Giagounidis A, Selleslag D, *et al.*** A randomized phase 3 study of lenalidomide versus placebo in RBC transfusion-dependent patients with Low- / Intermediate-1-risk myelodysplastic syndromes with del5q. *Blood*. 2013; **118**(14):3765–3776.

47. **Sampaio EP, Sarno EN, Galilly R, Cohn Z a, Kaplan G**. Thalidomide selectively inhibits tumor necrosis factor alpha production by stimulated human monocytes. *J. Exp. Med.* 1991; **173**(3):699–703.

48. **D'Amato RJ, Loughnan MS, Flynn E, Folkman J**. Thalidomide is an inhibitor of angiogenesis. *Proc. Natl. Acad. Sci. U. S. A.* 1994; **91**(9):4082–4085.

49. **Haslett BP a J, Corral LG, Albert M**. Thalidomide Costimulates Primary Human T Lymphocytes, Preferentially Inducing Proliferation, Cytokine Production, and Cytotoxic Responses in the CD8. *J. Exp. Med.* 1998; **187**(11):6–13.

50. **Quach H, Ritchie D, Stewart a K, *et al.*** Mechanism of action of immunomodulatory drugs (IMiDS) in multiple myeloma. *Leuk. Off. J. Leuk. Soc. Am. Leuk. Res. Fund, U.K*. 2010; **24**(1):22–32. Available at: http://dx.doi.org/10.1038/leu.2009.236.

51. **Davies FE, Raje N, Hideshima T, Al E**. Thalidomide and immunomodulatory derivatives augment natural killer cell cytotoicity in multiple myeloma. *Blood*. 2001; **98**(1):210–216.

52. **Fujii S, Shimizu K, Steinman RM, Dhodapkar M V**. Detection and activation of human Valpha24+ natural killer T cells using alpha-galactosyl ceramide-pulsed dendritic cells. *J. Immunol. Methods*. 2003; **272**(1-2):147–159.

53. **Wu L, Adams M, Carter T, *et al.*** Lenalidomide enhances natural killer cell and monocyte-mediated antibody-dependent cellular cytotoxicity of rituximab-treated CD20+ tumor cells. *Clin. Cancer Res.* 2008; **14**(14):4650–4657.

54. **Corral LG, Kaplan G**. Immunomodulation by thalidomide and thalidomide analogues. *Ann. Rheum. Dis.* 1999; **58 Suppl 1**(Suppl I):I107–I113.

55. **Gupta D, Treon SP, Shima Y, *et al.*** Adherence of multiple myeloma cells to bone marrow stromal cells upregulates vascular endothelial growth factor secretion: therapeutic applications. *Leuk. Off. J. Leuk. Soc. Am. Leuk. Res. Fund, U.K*. 2001; **15**(12):1950–1961.

56. **Shaffer A, Emre N, Lamy L, Ngo V**. IRF4 addiction in multiple myeloma. *Nature*. 2008; **454**(7201):226–231..

57. **Lopez-Girona A, Heintel D, Zhang L-H, *et al.*** Lenalidomide downregulates the cell survival factor, interferon regulatory factor-4, providing a potential mechanistic link for predicting response. *Br. J. Haematol.* 2011; **154**(3):325–36.

58. **Ito T, Ando H, Suzuki T, *et al.*** Identification of a primary target of thalidomide teratogenicity. *Science*. 2010; **327**(5971):1345–1350.

59. **Lopez-Girona a, Mendy D, Ito T, *et al.*** Cereblon is a direct protein target for immunomodulatory and antiproliferative activities of lenalidomide and pomalidomide. *Leukemia*. 2012; **26**(11):2326–35.

60. **Thakurta A, Gandhi a K, Waldman MF, *et al.*** Absence of mutations in cereblon (CRBN) and DNA damage-binding protein 1 (DDB1) genes and significance for IMiD therapy. *Leukemia*. 2013:1–3.

61. **Schuster SR, Kortuem KM, Zhu YX, *et al.*** The clinical significance of cereblon expression in multiple myeloma. *Leuk. Res.* 2014; **38**(1):23–8.

62. **Lu G, Middleton RE, Sun H, *et al.*** The myeloma drug lenalidomide promotes the cereblon-dependent destruction of Ikaros proteins. *Science*. 2014; **343**(January):305–9.

63. **Krönke J, Udeshi N, Narla A, Grauman P**. Lenalidomide causes selective degradation of IKZF1 and IKZF3 in multiple myeloma cells. *Science (80-.).* 2014; **343**(6168):301–305.

64. **Yang B, Yu R, Chi X, Lu X**. Lenalidomide treatment for multiple myeloma: systematic review and meta-analysis of randomized controlled trials. *PLoS One*. 2013; **8**(5):e64354.

65. **Kumar SK, Lee JH, Lahuerta JJ, *et al.*** Risk of progression and survival in multiple myeloma relapsing after therapy with IMiDs and bortezomib: A multicenter international myeloma working group study. *Leuk. Off. J. Leuk. Soc. Am. Leuk. Res. Fund, U.K*. 2011; (May 2011):149–157.

66. **Di Pauli F, Berger T, Reindl M**. Monoclonal antibodies in the treatment of multiple sclerosis. *Curr. Med. Chem.* 2009; **16**(36):4858–4868.

67. **Kaufman JL, Fabre C, Lonial S, Richardson PG**. Histone deacetylase inhibitors in multiple myeloma: rationale and evidence for their use in combination therapy. *Clin. Lymphoma. Myeloma Leuk.* 2013; **13**(4):370–6.

68. **Hideshima T, Anderson KC**. Molecular mechanisms of novel therapeutic approaches for multiple myeloma. *Nat. Rev. Cancer*. 2002; **2**(12):927–37.

69. **Roodman GD**. New potential targets for treating myeloma bone disease. *Clin. Cancer Res.* 2006; **12**(20 Pt 2):6270s–6273s.

70. **Ribatti D, Nico B, Vacca a**. Importance of the bone marrow microenvironment in inducing the angiogenic response in multiple myeloma. *Oncogene*. 2006; **25**(31):4257–66.

71. **Chauhan D, Uchiyama H, Akbarali Y, *et al.*** Multiple myeloma cell adhesion-induced interleukin-6 expression in bone marrow stromal cells involves activation of NF-kappa B. *Blood*. 1996; **87**(3):1104–12.

72. **Podar K, Tai YT, Davies FE, *et al.*** Vascular endothelial growth factor triggers signaling cascades mediating multiple myeloma cell growth and migration. *Blood*. 2001; **98**(2):428–35.

73. **Hideshima T, Chauhan D, Hayashi T, *et al.*** The Biological Sequelae of Stromal Cell-derived Factor-1 α in Multiple Myeloma. *Mol. Cancer Ther.* 2002; **1**:539–544.

74. **Mitsiades CS, Mitsiades NS, McMullan CJ, *et al.*** Inhibition of the insulin-like growth factor receptor-1 tyrosine kinase activity as a therapeutic strategy for multiple myeloma, other hematologic malignancies, and solid tumors. *Cancer Cell*. 2004; **5**(3):221–30.

75. **Blank U, Karlsson G, Karlsson S, Dc W**. Signaling pathways governing stem-cell fate Review article Signaling pathways governing stem-cell fate. 2013; **111**(2):492–503.

76. **Barillé S, Collette M, Bataille R, Amiot M**. Myeloma cells upregulate interleukin-6 secretion in osteoblastic cells through cell-to-cell contact but downregulate osteocalcin. *Blood*. 1995; **86**(8):3151–9.

77. **Dankbar B, Padró T, Leo R, *et al.*** Vascular endothelial growth factor and interleukin-6 in paracrine tumor-stromal cell interactions in multiple myeloma Vascular endothelial growth factor and interleukin-6 in paracrine tumor-stromal cell interactions in multiple myeloma. *Blood*. 2000; (95):2630–2636.

78. **Ferlin M, Noraz N, Hertogh C, *et al.*** Insulin-like growth factor induces the survival and proliferation of myeloma cells through an interleukin-6-independent transduction pathway. *Br. J. Haematol.* 2000; **111**(2):626–34.

79. **Alsayed Y, Ngo H, Runnels J, *et al.*** Mechanisms of regulation of CXCR4/SDF-1 (CXCL12)-dependent migration and homing in multiple myeloma. *Blood*. 2007; **109**(7):2708–17.

80. **Urashima M, Ogata a, Chauhan D, *et al.*** Interleukin-6 promotes multiple myeloma cell growth via phosphorylation of retinoblastoma protein. *Blood*. 1996; **88**(6):2219–2227.

81. **Hitzler JK, Martinez-Valdez H, Bergsagel DB, Minden MD, Messner H a**. Role of interleukin-6 in the proliferation of human multiple myeloma cell lines OCI-My 1 to 7 established from patients with advanced stage of the disease. *Blood*. 1991; **78**(8):1996–2004.

82. **Abe M, Hiura K, Wilde J, *et al.*** Osteoclasts enhance myeloma cell growth and survival via cell-cell contact: A vicious cycle between bone destruction and myeloma expansion. *Blood*. 2004; **104**(8):2484–2491.

83. **Tanaka Y, Abe M, Hiasa M, *et al.*** Myeloma cell-osteoclast interaction enhances angiogenesis together with bone resorption: A role for vascular endothelial cell growth factor and osteopontin. *Clin. Cancer Res.* 2007; **13**(3):816–823.

84. **Hideshima T, Chauhan D, Schlossman R, Richardson P, Anderson KC**. The role of tumor necrosis factor alpha in the pathophysiology of human multiple myeloma: therapeutic applications. *Oncogene*. 2001; **20**(33):4519–27.

85. **Kuhn DJ, Berkova Z, Jones RJ, *et al.*** Targeting the insulin-like growth factor-1 receptor to overcome bortezomib resistance in preclinical models of multiple myeloma. 2012; **120**(16):3260–3270.

86. **Damiano JS, Cress a E, Hazlehurst L a, Shtil a a, Dalton WS**. Cell adhesion mediated drug resistance (CAM-DR): role of integrins and

resistance to apoptosis in human myeloma cell lines. *Blood*. 1999; **93**(5):1658–1667.

87. **Hazlehurst LA, Damiano JS, Buyuksal I, Pledger WJ, Dalton WS**. Adhesion to fibrobronectin via b1 integrins regulates p27 kip1 levels and contributes to cell adhesion mediated drug resistance (CAM-DR). *Oncogene*. 2000; (19).

88. **Hazlehurst L a, Dalton WS**. Mechanisms associated with cell adhesion mediated drug resistance (CAM-DR) in hematopoietic malignancies. *Cancer Metastasis Rev.* 2001; **20**(1-2):43–50.

89. **Neri P, Ren L, Azab AK, *et al.*** Integrin {beta}7-mediated regulation of multiple myeloma cell adhesion, migration, and invasion. *Blood*. 2011; **117**(23):6202–13.

90. **Chiron D, Maïga S, Descamps G, *et al.*** Critical role of the NOTCH ligand JAG2 in self-renewal of myeloma cells. *Blood Cells. Mol. Dis.* 2012; **48**(4):247–53.

91. **Kim D, Park CY, Medeiros BC, Weissman IL**. CD19-CD45 low/-CD38 high/CD138+ plasma cells enrich for human tumorigenic myeloma cells. *Leukemia*. 2012; **26**(12):2530–7.

92. **Van Valckenborgh E, Matsui W, Agarwal P, *et al.*** Tumor-initiating capacity of CD138- and CD138+ tumor cells in the 5T33 multiple myeloma model. *Leukemia*. 2012; **26**(6):1436–1439.

93. **Matsui W, Huff CA, Wang Q, *et al.*** Characterization of clonogenic multiple myeloma cells. *Blood*. 2004; **103**(6):2332–6.

94. **Matsui W, Wang Q, Barber JP, *et al.*** Clonogenic multiple myeloma progenitors, stem cell properties, and drug resistance. *Cancer Res.* 2008; **68**(1):190–197.

95. **Kirshner J, Thulien KJ, Martin LD, *et al.*** A unique three-dimensional model for evaluating the impact of therapy on multiple myeloma. 2008; **112**(7):2935–2945.

96. **Pilarski LM, Baigorri E, Mant MJ, *et al.*** Multiple Myeloma Includes Phenotypically Defined Subsets of Clonotypic CD20+ B Cells that Persist During Treatment with Rituximab. *Clin. Med. Oncol.* 2008; **2**:275–287.

97. **Hosen N, Matsuoka Y, Kishida S, *et al.*** CD138-negative clonogenic cells are plasma cells but not B cells in some multiple myeloma patients. *Leukemia*. 2012; **26**(9):2135–2141.

98. **Blank U, Karlsson G, Karlsson S**. Signaling pathways governing stem-cell fate. *Blood*. 2008; **111**(2):492–503.

99. **Mirandola L, Comi P, Cobos E, *et al.*** Notch-ing from T-cell to B-cell lymphoid malignancies. *Cancer Lett.* 2011; **308**(1):1–13.

100. **Colombo M, Mirandola L, Platonova N, *et al.*** Notch-directed microenvironment reprogramming in myeloma: a single path to multiple outcomes. *Leuk. Off. J. Leuk. Soc. Am. Leuk. Res. Fund, U.K*. 2013; (November 2012):1–10.

101. **Mumm JS, Kopan R**. Notch signaling: from the outside in. *Dev. Biol.* 2000; **228**(2):151–65.

102. **Beel AJ, Sanders CR**. Substrate Specificity of γ-Secretase and Other Intramembrane Proteases. *Cell Mol Life Sci*. 2008; **65**(9):1311–1334.

103. **Osborne B a, Minter LM**. Notch signalling during peripheral T-cell activation and differentiation. *Nat. Rev. Immunol.* 2007; **7**(1):64–75.

104. **Le Borgne R**. Regulation of Notch signalling by endocytosis and endosomal sorting. *Curr. Opin. Cell Biol.* 2006; **18**(2):213–22.

105. **Fryer CJ, White JB, Jones K a**. Mastermind recruits CycC:CDK8 to phosphorylate the Notch ICD and coordinate activation with turnover. *Mol. Cell*. 2004; **16**(4):509–20.

106. **Houde C, Li Y, Song L, *et al.*** Overexpression of the NOTCH ligand JAG2 in malignant plasma cells from multiple myeloma patients and cell lines. *Blood*. 2004; **104**(12):3697–704.

107. **Ghoshal P, Nganga AJ, Moran-Giuati J, *et al.*** Loss of the SMRT/NCoR2 corepressor correlates with JAG2 overexpression in multiple myeloma. *Cancer Res.* 2009; **69**(10):4380–7.

108. **Jundt F, Anagnostopoulos I, Förster R, *et al.*** Activated Notch1 signaling promotes tumor cell proliferation and survival in Hodgkin and anaplastic large cell lymphoma Activated Notch1 signaling promotes tumor cell proliferation and survival in Hodgkin and anaplastic large cell lymphoma. *Blood*. 2002:3398–3403.

109. **Jundt F, Pröbsting KS, Anagnostopoulos I, *et al.*** Jagged1-induced Notch signaling drives proliferation of multiple myeloma cells. *Blood*. 2004; **103**(9):3511–5.

110. **Xu D, Hu J, De Bruyne E, *et al.*** Dll1/Notch activation contributes to bortezomib resistance by upregulating CYP1A1 in multiple myeloma. *Biochem. Biophys. Res. Commun.* 2012; **428**(4):518–24.

111. **Hodkinson PS, Elliott P a., Lad Y, *et al.*** Mammalian NOTCH-1 Activates beta1 Integrins via the Small GTPase R-Ras. *J. Biol. Chem.* 2007; **282**(39):28991–29001.

112. **Mirandola L, Apicella L, Colombo M, *et al.*** Anti-Notch treatment prevents multiple myeloma cells localization to the bone marrow via the chemokine system CXCR4/SDF-1. *Leuk. Off. J. Leuk. Soc. Am. Leuk. Res. Fund, U.K*. 2013; (November 2012).

113. **Nefedova Y, Cheng P, Alsina M, Dalton WS, Gabrilovich DI**. Involvement of Notch-1 signaling in bone marrow stroma-mediated de novo drug resistance of myeloma and other malignant lymphoid cell lines. *Blood*. 2004; **103**(9):3503–10.

114. **Nefedova Y, Sullivan DM, Bolick SC, Dalton WS, Gabrilovich DI**. Inhibition of Notch signaling induces apoptosis of myeloma cells and enhances sensitivity to chemotherapy. *Blood*. 2008; **111**(4):2220–9.

115. **Zanotti S, Smerdel-Ramoya A, Stadmeyer L, *et al.*** Notch inhibits osteoblast differentiation and causes osteopenia. *Endocrinology*. 2008; **149**(8):3890–9.

116. **Gott JM, Emeson RB**. Functions and Mechanisms of RNA Editing. *Annu. Rev. Genet.* 2000; **34**:499–531.

117. **Smith HC**. A guide to RNA editing. *RNA*. 1997; **3**:1105–1123.

118. **Farajollahi S, Maas S**. Molecular diversity through RNA editing: a balancing act. *Trends Genet.* 2010; **26**(5):221–230.

119. **Maas S**. *Posttranscriptional recoding by RNA editing*. 1st ed. Elsevier Inc.; 2012.

120. **Li JB, Levanon EY, Yoon J-K**. Genome-Wide Identifcation of Human RNA Editing Sited by Parallel DNA Capturing and Sequencing. *Science (80-.).* 2009; **324**.

121. **Kim DDY, Kim TTY, Walsh T, *et al.*** Widespread RNA Editing of Embedded Alu Elements in the Human Transcriptome Widespread RNA Editing of Embedded Alu Elements in the Human Transcriptome. 2004:1719–1725.

122. **Athanasiadis A, Rich A, Maas S**. Widespread A-to-I RNA editing of Alu-containing mRNAs in the human transcriptome. *PLoS Biol.* 2004; **2**(12).

123. **Maas S, Rich A, Nishikura K**. A-to-I RNA editing: recent news and residual mysteries. *J. Biol. Chem.* 2003; **278**(3):1391–4.

124. **Zhang Z, Carmichael GG**. The fate of dsRNA in the Nucleus: A p54nrb-containing complex mediates the nuclear retention of promiscuously A-to-I edited RNAs. *Cell*. 2001; **106**(4):465–475.

125. **Chen L, Carmichael GG**. Altered nuclear retention of mRNAs containing inverted repeats in human embryonic stem cells: Functional role of a nuclear noncoding RNA. *Mol. Cell.* 2009; **35**(4):467–478.

126. **Hundley H a, Krauchuk A a, Bass BL**. C. elegans and H. sapiens mRNAs with edited 3' UTRs are present on polysomes. *RNA*. 2008; **14**(10):2050–2060.

127. **Zipeto MA, Jiang Q, Melese E, Jamieson CHM**. RNA rewriting, recoding, and rewiring in human disease. *Trends Mol. Med.* 2015:1–11.

128. **Yang W, Chendrimada TP, Wang Q, Higuchi M, Peter H**. Modulation of microRNA processing and expression through RNA editing by ADAR deaminases. *Nat Struct Mol Biol*. 2006; **13**(1):13–21.

129. **Kawahara Y, Megraw M, Kreider E, *et al.*** Frequency and fate of microRNA editing in human brain. *Nucleic Acids Res.* 2008; **36**(16):5270–5280.

130. **Wagnert RW, Smitht JE, Coopermant BS, Nishikurat K**. double-stranded RNA unwinding activity. *Proc. Natl. Acad. Sci.* 1989; **86**(April):2647–2651.

131. **Ryter JM, Schultz SC**. Molecular basis of double-stranded RNA-protein interactions: Structure of a dsRNA-binding domain complexed with dsRNA. *EMBO J.* 1998; **17**(24):7505–7513.

132. **Valente L, Nishikura K**. RNA binding-independent dimerization of adenosine deaminases acting on RNA and dominant negative effects of

nonfunctional subunits on dimer functions. *J. Biol. Chem.* 2007; **282**(22):16054–16061.

133. **Kim U, Wang Y, Sanford T, Zeng Y, Nishikura K**. Molecular cloning of cDNA for double-stranded RNA adenosine deaminase, a candidate enzyme for nuclear RNA editing. *Proc Natl Acad Sci U S A*. 1994; **91**(24):11457–11461.

134. **Lai F, Drakas R, Nishikura K**. Mutagenic analysis of double-stranded RNA adenosine deaminase, a candidate enzyme for RNA editing of glutamate-gated ion channel transcripts. *J. Biol. Chem.* 1995; **270**(29):17098–17105.

135. **Macbeth MR, Schubert HL, VanDemark AP, *et al.*** Inositol Hexakisphosphate Is Bound in the ADAR2 Core and Required for RNA Editing. *Science (80-.).* 2005; **309**(5740):1534–1539.

136. **Herbert a, Alfken J, Kim YG, *et al.*** A Z-DNA binding domain present in the human editing enzyme, double-stranded RNA adenosine deaminase. *Proc. Natl. Acad. Sci. U. S. A.* 1997; **94**(16):8421–8426.

137. **George CX, Wagner M V., Samuel CE**. Expression of interferon-inducible RNA adenosine deaminase ADAR1 during pathogen infection and mouse embryo development involves tissue-selective promoter utilization and alternative splicing. *J. Biol. Chem.* 2005; **280**(15):15020–15028.

138. **Patterson JB, Samuel CE**. Expression and regulation by interferon of a double-stranded-RNA-specific adenosine deaminase from human cells: evidence for two forms of the deaminase. *Mol. Cell. Biol.* 1995; **15**(10):5376–5388.

139. **Weier HU, George CX, Greulich KM, Samuel CE**. The interferon-inducible, double-stranded RNA-specific adenosine deaminase gene (DSRAD) maps to human chromosome 1q21.1-21.2. *Genomics*. 1995; **30**(2):372–375.

140. **Fritz J, Strehblow A, Taschner A, *et al.*** RNA-regulated interaction of transportin-1 and exportin-5 with the double-stranded RNA-binding domain regulates nucleocytoplasmic shuttling of ADAR1. *Mol. Cell. Biol.* 2009; **29**(6):1487–1497.

141. **Herbert a, Rich a**. The role of binding domains for dsRNA and Z-DNA in the in vivo editing of minimal substrates by ADAR1. *Proc. Natl. Acad. Sci. U. S. A.* 2001; **98**(21):12132–12137.

142. **Meltzer M, Long K, Nie Y, *et al.*** The RNA Editor Gene Adar1 is Induced in Myoblasts by Inflammatory Ligands and Buffers Stress Response. *Clin. Transalational Sci.* 2010; **3**(3):73–80.

143. **Maas S, Patt S, Schrey M, Rich a**. Underediting of glutamate receptor GluR-B mRNA in malignant gliomas. *Proc. Natl. Acad. Sci. U. S. A.* 2001; **98**(25):14687–14692.

144. **Cenci C, Barzotti R, Galeano F, *et al.*** Down-regulation of RNA editing in pediatric astrocytomas: ADAR2 editing activity inhibits cell migration and proliferation. *J. Biol. Chem.* 2008; **283**(11):7251–7260.

145. **Chen L, Li C, LIn CH, *et al.*** Recoding RNA editing of antizyme inhibitor 1 predisposes to hepatocellular carcinoma. *Nat. Med.* 2013; **29**(6):997–1003.

146. **Qin YR, Qiao JJ, Chan THM, *et al.*** Adenosine-to-inosine RNA editing mediated by adars in esophageal squamous cell carcinoma. *Cancer Res.* 2014; **74**(3):840–851.

147. **Beghini a, Ripamonti CB, Peterlongo P, *et al.*** RNA hyperediting and alternative splicing of hematopoietic cell phosphatase (PTPN6) gene in acute myeloid leukemia. *Hum. Mol. Genet.* 2000; **9**(15):2297–2304.

148. **Jiang Q, Crews L a, Barrett CL, *et al.*** ADAR1 promotes malignant progenitor reprogramming in chronic myeloid leukemia. *Proc. Natl. Acad. Sci. U. S. A.* 2013; **110**(3):1041–6.

149. **Chapman M a, Lawrence MS, Keats JJ, *et al.*** Initial genome sequencing and analysis of multiple myeloma. *Nature*. 2011; **471**(7339):467–72.

150. **Crews L a, Jiang Q, Zipeto M a, *et al.*** An RNA editing fingerprint of cancer stem cell reprogramming. *J. Transl. Med.* 2015; **13**:1–12.

151. **Chaidos A, Barnes CP, Cowan G, *et al.*** Clinical drug resistance linked to interconvertible phenotypic and functional states of tumor-propagating cells in multiple myeloma. *Blood*. 2013; **121**(2):318–28.

152. **Bataille R, Jourdan M, Zhang XG, Klein B**. Serum levels of interleukin 6, a potent myeloma cell growth factor, as a reflect of disease severity in plasma cell dyscrasias. *J. Clin. Invest.* 1989; **84**(6):2008–11.

153. **Qiu W, Wang X, Buchanan M, *et al.*** ADAR1 is essential for intestinal homeostasis and stem cell maintenance. *Cell Death Dis.* 2013; **4**(4):e599.

154. **Colombo M, Thummler K, Mirandola L, *et al.*** Notch signaling drives multiple myeloma induced osteoclastogenesis. *Oncotarget*. 2014; **5**(21).

155. **Xu D, Hu J, Xu S, *et al.*** Dll1/Notch activation accelerates multiple myeloma disease development by promoting CD138+ MM-cell proliferation. *Leukemia*. 2012; **26**(6):1402–5.

156. **Ito R, Takahashi T, Katano I, Ito M**. Current advances in humanized mouse models. *Cell. Mol. Immunol.* 2012; **9**(3):208–214.

157. **Traggiai E, Chicha L, Mazzucchelli L, *et al.*** Development of a human adaptive immune system in cord blood cell-transplanted mice. *Science*. 2004; **304**(5667):104–107.

158. **Goff DJ, Recart AC, Sadarangani A, *et al.*** A Pan-BCL2 inhibitor renders bone-marrow-resident human leukemia stem cells sensitive to tyrosine kinase inhibition. *Cell Stem Cell*. 2013; **12**(3):316–28.

159. **Ma W, Gutierrez A, Goff DJ, *et al.*** NOTCH1 signaling promotes human T-cell acute lymphoblastic leukemia initiating cell regeneration in supportive niches. *PLoS One*. 2012; **7**(6):e39725.

160. **Frigyesi I, Adolfsson J, Ali M, *et al.*** Robust isolation of malignant plasma cells in multiple myeloma. *Blood*. 2014; **123**(9):1336–1340.

161. **American Cancer Society**. Cancer Facts & Figures 2014. *Am. Cancer Soc.* 2014.

162. **Gwertz MA, Dingli D**. How we manage autologous stem cell transplantation for patients with multiple myeloma. *Blood*. 2014; **124**(6):882–890.

163. **Pandya C, Hashmi S, Khera N, *et al.*** Cost-effectiveness analysis of early vs. late autologous stem cell transplantation in multiple myeloma. *Clin. Transplant.* 2014; **28**(10):1084–1091.

164. **Roy A, Kish JK, Bloudek L, *et al.*** Estimating the Costs of Therapy in Patients with Relapsed and/or Refractory Multiple Myeloma: A Model Framework. *Am. Heal. Drug Benefits | www.AHDBonline.com Am Heal. Drug Benefits*. 2015; **2048**(44):204–215.

165. **Price R, Stranges E, Elixhauser A**. Cancer hospitalizations for adults, 2009. *Stat. Briefs. Agency Healthc. Res. Qual.* 2012; **61**(4):1–11.

166. **Zhuang J, Da Y, Li H, *et al.*** Cytogenetic and clinical risk factors for assessment of ultra high-risk multiple myeloma. *Leuk. Res.* 2014; **38**(2):188–93.

167. **Bianchi G, Ghobrial IM**. Biological and Clinical Implications of Clonal Heterogeneity and Clonal Evolution in Multiple Myeloma. *Curr Cancer Ther Rev*. 2014; **29**(6):997–1003.

168. **Keats JJ, Chesi M, Egan JB, *et al.*** Clonal competition with alternating dominance in multiple myeloma. *Blood*. 2012; **120**(5):1067–1077.

169. **Walker B a, Wardell CP, Melchor L, *et al.*** Intraclonal heterogeneity and distinct molecular mechanisms characterize the development of t (4 ; 14) and t (11 ; 14) myeloma. *Blood*. 2012; **120**(5):1077–1086.

170. **Bolli N, Avet-Loiseau H, Wedge DC, *et al.*** Heterogeneity of genomic evolution and mutational profiles in multiple myeloma. *Nat. Commun.* 2014; **5**:2997.

171. **Chang H, Yeung J, Xu W, Ning Y, Patterson B**. Significant increase of CKS1B amplification from monoclonal gammopathy of undetermined significance to multiple myeloma and plasma cell leukaemia as demonstrated by interphase fluorescence in situ hybridisation. *Br. J. Haematol.* 2006; **134**(6):613–615.

172. **Hanamura I, Stewart JP, Huang Y, *et al.*** Frequent gain of chromosome band 1q21 in plasma-cell dyscrasias detected by fluorescence in situ hybridization: Incidence increases from MGUS to relapsed myeloma and is related to prognosis and disease progression following tandem stem-cell transplantatio. *Blood*. 2006; **108**(5):1724–1732.

173. **Avet-Loiseau H, Li C, Magrangeas F, *et al.*** Prognostic significance of copy-number alterations in multiple myeloma. *J. Clin. Oncol.* 2009; **27**(27):4585–90.

174. **Chiecchio L, Dagrada GP, White HE, *et al.*** Frequent Upregulation of MYC in Plasma Cell Leukemia. *Genes. Chromosomes Cancer*. 2009; **48**:624–636.

175. **Roberts S a, Lawrence MS, Klimczak LJ, *et al.*** An APOBEC cytidine deaminase mutagenesis pattern is widespread in human cancers. *Nat. Genet.* 2013; **45**(9):970–6.

176. **Henderson S, Chakravarthy A, Su X, Boshoff C, Fenton TR**. APOBEC-Mediated Cytosine Deamination Links PIK3CA Helical Domain Mutations to Human Papillomavirus-Driven Tumor Development. *Cell Rep.* 2014; **7**(6):1833–1841.

177. **Roberts S a., Gordenin D a.** Hypermutation in human cancer genomes: footprints and mechanisms. *Nat. Rev. Cancer*. 2014; **14**(12):786–800.

178. **Rebhandl S, Huemer M, Gassner FJ, *et al.*** APOBEC3 signature mutations in chronic lymphocytic leukemia. *Leukemia*. 2014; **28**(9):1929–1932.

179. **Blotta S, Jakubikova J, Calimeri T, *et al.*** Canonical and non canonical Hedgehog pathway in the pathogenesis of multiple myeloma. *Blood*. 2012; **120**(25):1–4.

180. **Liu Z, Xu J, He J, *et al.*** A critical role of autocrine sonic hedgehog signaling in human CD138+ myeloma cell survival and drug resistance. *Blood*. 2014; **124**(13):2061–2072.

181. **Peacock CD, Wang Q, Gesell GS, *et al.*** Hedgehog signaling maintains a tumor stem cell compartment in multiple myeloma. *Proc Natl Acad Sci U S A*. 2007; **104**(10):4048–4053.

182. **Shimokawa T, Rahman MF-U, Tostar U, *et al.*** RNA editing of the GLI1 transcription factor modulates the output of Hedgehog signaling. *RNA Biol.* 2013; **10**(February):321–33.

183. **Colby SL, Ortman JM**. The Baby Boom Cohort in the United States : 2012 to 2060. 2014:16.

SCIENTIFIC PRODUCTION AND FUNDING

"An RNA editing fingerprint of cancer stem cell reprogramming" L.A. Crews, Q. Jiang, M.A Zipeto, **E. Lazzari**, A.C. Court, S.Ali, C.L. Barrett, K.A. Frazer, C.H.M. Jamieson. *Journal of Translational Medicine,* 2015.

"PI3K/AKT signaling inhibits NOTCH1 lysosome-mediated degradation". Platonova N. Manzo T., Mirandola L., Colombo M., Calzavera E., Vigolo E., Cermisoni G.C., De Simone D., Garavelli S., Cecchinato V., **Lazzari E**., Neri A., Chiaramonte R. *Genes Chromosomes Cancer* 2015.

"**Notch signaling drives multiple myeloma induced osteoclastogenesis"** M. Colombo, K. Thummler, L. Mirandola, S. Garavelli, K. Todoerti, L. Apicella, **E. Lazzari**, M. Lancellotti, N. Platonova, M. Akbar, M. Chiriva-Internati, R.Soutar, A. Neri, C.S. Goodyear and R. Chiaramonte. *Oncotarget*, 2014.

"**Notch activation increases interleukin-6 expression in multiple myeloma niche**" Colombo M., Galletti S., Bulfamante G., Falleni M., Tosi D., Todoerti K., **Lazzari E**., Crew L., Jamieson C, Garavelli S., Platonova N. , Neri A., Chiaramonte R. (Manuscript in preparation).

"**ADAR1 drives disease progression and aberrant RNA editing in multiple myeloma**". L.A. Crews*, **E. Lazzari***, C. Wu, H. Leu, S. Ali, M. Minden, R. Chiaramonte and C.H. Jamieson. (Manuscript in preparation).

"Bone marrow-mediated drug resistance is promoted by Jagged-induced Notch pathway in multiple myeloma" E.Lazzari, S.Garavelli, M. Colombo, L.A. Crews, A. Paoli, N. Platonova, S. Galletti, K.Todoerti, C.H. Jamieson, A. Neri, R. Chiaramonte. (Manuscript in preparation).

"Tracking human myeloma cell therapeutic resistance using a novel diagnostic assay for detection of RNA editing biomarkers of cancer stem cell generation" E. Lazzari, L.A. Crews, C. Wu, M.A. Zipeto, H. Leu, S. Ali, R. Chiaramonte and C.H.M. Jamieson. *Translational Oncology Symposium*, La Jolla, February 2015 (poster).

"Bone marrow-mediated drug resistance is promoted by Jagged-induced Notch pathway in multiple myeloma" S. Garavelli, **E. Lazzari**, M. Colombo, A. Paoli, N. Platonova, S. Galletti, K.Todoerti, A. Neri, R. Chiaramonte. *20th Congress of European Hematology Association*, Vienna, June 2015 (poster).

This work has been supported by the Italian Ministry of Education, University and Research (MIUR) doctoral fellowship (2013-2015), by the Multiple Myeloma Research Grant (2014-2015) and the National Cancer Institute Provocative Question Grant 1R21 CA189705-01A1 (2015-2018).

ACKNOWLEDGEMENTS

I would like to dedicate my warmest thanks to my mentors, Dr. Raffaella Chiaramonte, who took me under her wing as PhD student at the Doctoral School of Molecular Medicine, University of Milan, and Dr. Catriona Jamieson, who welcomed me in her group as Visiting Student at University of California, San Diego. I am deeply thankful for the opportunities they gave me and for being such passionate, perseverant and confident mentors. Thanks to Dr. Leslie Crews, who has been an amazing guide, friend and foodie pal. She is one of the brightest and most supportive people I know, always able to find the silver lining, which meant a lot to me. Countless thanks to all my lab mates, Michela, Silvia, Serena, Marialuigia, Daria, Natalia and Leonardo from Chiaramonte's lab and to the San Diego gang, Heather, Tina, Marianna, Cayla, Frida, Fay, Karina, Gabriel, Shawn and Wen from the Jamieson's lab. They have been an incomparable source of scientific support and thoughtful suggestions, but more importantly I want to thank them for all the laughs, the conversations and the billion coffees we shared, it was great working with all of them.

RINGRAZIAMENTI

Vorrei ringraziare mia madre, Rosanna Pagani, e mio padre, Valerio Lazzari, per avermi supportata e talvolta sopportata durante questo percorso. Vorrei dedicare mille grazie anche a Concetta Frisenna e Valter Dallari, per avermi accolta e fatta sentire in famiglia in un battito di ciglia.
Un grazie più speciale degli altri a Simone Dallari, per essere la persona che mi sprona ad esserne una migliore. Grazie per ogni giorno insieme.